Mutagenesis studies of L-carnitine dehydrogenase for development of biomolecule measurement tool

生体分子測定ツールの創製に向けたカルニチン脱水素酵素のタンパク質工学的研究

A DISSERTATION

By

MOHAMED MUTASIM ELTAYEB ELEBEID

Submitted to the United Graduate School of Agricultural Sciences, Tottori University in Partial Fulfillment of the Requirements for the Degree of Doctor of Philosophy in Bio-resources Sciences

2014

DEDICATION

I would like to dedicate this humble thesis to:

My beloved wife Sara, my sweet daughter Aula and my lovely son Omer

My family: *Mutasim, Balalh, Sulafa, Magdi, Abdellhah, Sana, Fatima, and Farooq*

For their generous love and support

ACKNOWLEDGEMENT

First and foremost, I would like to praise and thank ALLAH, the almighty Merciful, who has granted countless blessing, knowledge, and people's help, so that I have been finally able to accomplish the thesis.

My sincere gratitude goes to my academic advisor Dr. Jiro Arima wholeheartedly, who supervised my research and always provided his insight and valuable comments to guide me marvelously through the study. Dr. Arima advised me at every step of my doctoral study. He has spent much time helping me to identify and to check every single element in order to make sure that it was rational. I would never have been able to finish my PhD study without his generous support and understanding.

My profound respect and sincere appreciation goes to my Ph.D. co-supervisor Professor Nobuhiro Mori, Faculty of Agriculture, Tottori University for thesis generous support, inspiration, discussion and encouragement through research and prepare the thesis..

Also my deep respect and sincere appreciation to my Ph.D. co-supervisor Professor Dr. Yoshihiro Sawa, Department of Life Science and Biotechnology, Shimane University, for his delicate supervising, and his valuable comment on the progress of this study.

My deepest thanks and appreciation offer to my former supervisor Prof. Elfadil Elfadl Babiker for his constant advising and remarkable comments.

I would like to express my sincere gratitude to Dr. Isam Ali Mohamed Ahmed, visiting Associate Professor at the Arid Land Research Center, Tottori University for his constant advice and discussion through research and prepare the thesis.

I wish to express my thanks to Prof. Kip A. Kates Faculty of Regional Sciences, Tottori University for his editorial help in manuscript and his valuable comments.

My personal acknowledge goes to Dr. Mohammed Abd Elbasit Mohammed, National Center for Research, Sudan for his generous help and encouragement during the period of my study.

My thanks and appreciation goes to staff member of International Affairs Division Center, United Graduate School of Agricultural Sciences, Tottori University for their unlimited help and support through my study and personal life.

I would like to thank the entire members of my lab previous and current, especially Fujimitsu, Isoda, Sato, and Irikawa. I received a lot of help from them both in my research and personal life.

I gratefully acknowledge the financial support provided by Government of Japan, Ministry of Education, Culture, Sports, Science, and Technology (MEXT) for my PhD study in Japan; and also I would like to thank University of Khartoum, Sudan for giving me the chance for further study in Japan.

This thesis is dedicated to my family; my father and my mother for their help, encourage, love, Patience, prayers, understandings and supports.

Last but not the least; I wish to express my sincere gratitude to my beloved wife, Sara Ahmed, for her support, encourage and help for prepare the thesis and manuscripts. She would not settle for less than the finished work. If it was not for her, I would not have been able to finish. This work belongs to her as much as it does to me.

Mohamed,,,

TABLE OF CONTENTS

LIST OF FIGURES

LIST OF TABLES

LIST OF ABBREVIATIONS

L-Car	L-Carnitine
CDH	L-Carnitine dehydrogenase
Xt-CDH	L-Carnitine dehydrogenase from *Xanthomonas translucens*
Rs-CDH	L-Carnitine dehydrogenase from *Rhizobium* sp.
LB	Luria-Bertani medium
IPTG	Isopropyl-ß-tiogalactopyranoside
KBP	Potassium phosphate buffer
2-ME	2-mercaptoethanol
HAD	3-hydroxyacyl-CoA dehydrogenase
h-HAD	Human 3-hydroxyacyl-CoA dehydrogenase
EDTA	Ethylenediaminetetraacetic acid
kDa	Kilo dalton
SDS–PAGE	Sodium dodecyl sulphate polyacrylamide gel electrophoresis
PDB	Protein data bank
MBP	Maltose binding protein

CHAPTER ONE

GENERAL INTRODUCTION

1.1 INTRODUCTION

Carnitine is a quaternary ammonium compound discovered in muscle tissue approximately 108 years ago (Gulewitsch and Krimberg, 1905) and subsequently identified as 3-hydroxy-4-N,N,N-trimethylaminobutyric acid, a water soluble quaternary amine, around 20 years later (Tomita and Sendju, 1927). Initially, Carnitine identified as an essential nutritional factor required for the growth of the meal worm larvae (*Tenebrio molitor*), which one year later was given the name vitamin B_T, means biological B complex group of vitamins for the Tenebrio meal worm (Fraenlel and Friedman, 1957; Fraenkel et al., 1948; Williams, 1994). Carnitine is a white, highly water-soluble powder and is a substance with good thermostability (up to 200 °C). It has very low toxicity with a LD 50 in rodents of 9 g/kg body weight. In aqueous solution carnitine, being a zwitterion, is freely soluble in water as its ionisable groups (COO- and $N^+(CH_3)_3$) are over 90 % dissociated at a physiological pH (~7.4) due to their pK values. The C-atom of the β-hydroxyl group is optically active due to its four different ligands and occurs in two isomeric forms, the D-form and the L-form. Of the two, L-form is encountered in the body and found to be biologically active, but the D-form can also exert effects in the body. It interacts with various transport proteins which carry L-carnitine (L-Car) from the plasma into the cells and competitively inhibits L-carnitine acyltransferases (Cerretelli and Marconi, 1990; Meier, 1987). Furthermore, D-carnitine used to deplete tissue L-Car level partially (Paulson and Shug, 1981). However, the third form of carnitine, DL-carnitine is toxic and has no beneficial effects. In prokaryotic cells, L-Car serves either as a nutrient, such as a carbon and

nitrogen source (Kleber, 1997), or as an osmoprotectant (Jung et al., 1990; Robert et al., 2000). This function was different to what was observing for L-Car in eukaryotes. In eukaryotic cells, it serves exclusively as a carrier of acyl moieties through various subcellular compartments (Ramsay and Arduini, 1993). It has an important role in the transport of activated long-chain fatty acids across the inner mitochondrial membrane (Bieber, 1988; McGarry and Brown, 1997). Furthermore, it is involved in the transfer of the products of peroxisomal β-oxidation, including acetyl-CoA, to the mitochondria for oxidation to CO_2 and H_2O in the Krebs cycle (Jakobs and Wanders, 1995; Verhoeven et al., 1998).

As essential biological substance, L-Car is present in most, if not all, animal species, and in several micro-organisms and plants (Schwabedissen-Gerbling and Gerhard, 1995; Panter and Mudd, 1969; Ramsay et al., 2001; Kendler, 1986). In general, L-Car is low in foods of plant origin and high in animal foods (Rebouche, 1992). Animal tissues contain relatively high amounts of L-Car, varying between 0.2 and 6 μmol g^{-1}, with the highest concentrations in heart and skeletal muscle (Bremer, 1983). In humans, approximately 75% of body L-Car sources comes from the diet and 25% from *de novo* biosynthesis (Tein et al., 1996). L-Car is synthesized ultimately from the amino acids lysine and methionine (Fig. 1.1) (Steiber et al., 2004). Lysine provides the carbon backbone of L-Car and the 4-N-methyl groups originate from methionine (Horne et al., 1973). Firstly, 6-N-trimethyl lysine is formed by N-methylation of lysine. In this process S-adenosyl-methionine acts as a donor of methyl groups. Trimethyl lysine is initially bound to the protein, which may be found in myosin for example. It is released in lysosomes through proteolysis. Then 6-N-trimethyl lysine is converted into 3-hydroxy-6-N-trimethyl lysine by hydroxylation of the C_3 of 6-N-trimethyl lysine. This reaction requires the participation of vitamin C (R ebouche, 1991; Dunn et al., 1984;

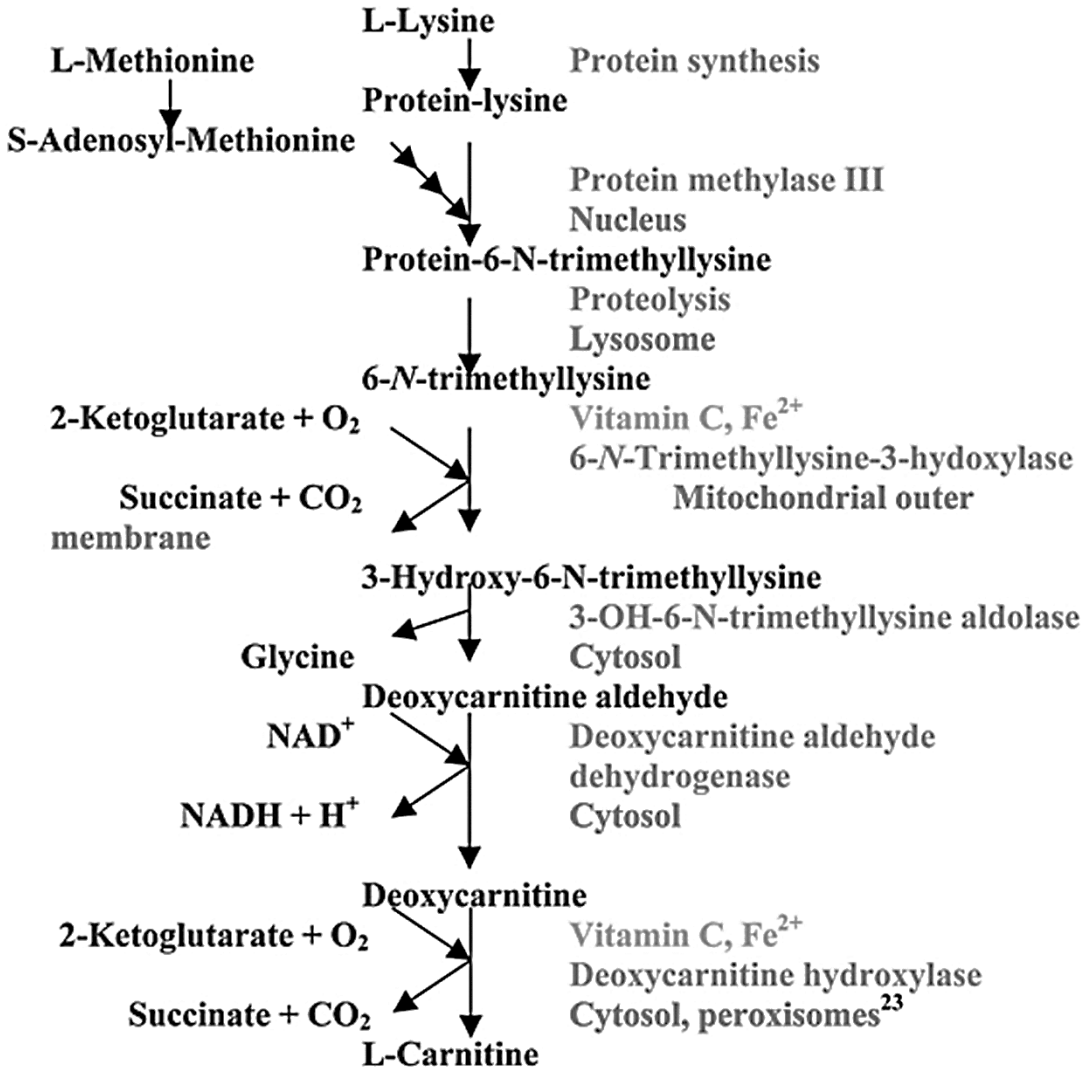

Fig. 1.1 Pathway of L-carnitine biosynthesis (Scholte et al., 1987; Paul, 1992; Vaz, 2002)

Nelson et al., 1981; Vaz et al., 2001) and bivalent iron (Fe^{2+}). Following cleavage of a C2-body, the third reaction product (γ-trimethyl-aminobutyraldehyde) is formed. It is also called deoxy L-carnitine aldehyde. The formation of this intermediate requires the presence of vitamin B6. Oxidation of the aldehyde to the carboxyl group results γ-

butyrobetaine, which consider as the immediate precursor of L-Car. Oxidation of deoxy L-carnitine finally leads to the formation of L-Car (Bremer, 1983; Rebouche and Engel, 1980; Englard, 1979; Hulse et al., 1978; Sachan and Hoppel, 1980). Data from animal studies showed that L-Car is synthesized in the liver but stored in skeletal (Mitchell, 1978).

1.2 BIOLOGICAL ROLE OF L-CARNITINE

Fatty acid ß-oxidation pathway is very important in cellular energy homeostasis, particularly during fasting or when the energy demand is increased (during exercise or stress). Before long-chain fatty acids can be metabolized by the mitochondrial β-oxidation system, they must be transported into the mitochondrial matrix. In fact, the quaternary ammonium compound, L-Car plays an essential role in fatty acid metabolism (Olson, 1966). Whereas medium and short-chain fatty acids enter the mitochondrial matrix, where β-oxidation takes place, as free acids, long-chain acyl-CoAs must first be converted into their corresponding carnitine-esters in order to cross the inner mitochondrial membrane (Bremer, 1983; McGarry and Brown, 1997; Ramsay et al., 2001; Bieber, 1988), which termed as “carnitine shuttle”. In particular, fatty acid containing more than fourteen carbon atoms needs L-Car transport; they constitute either dietary fatty acids or fatty acids released from adipose tissues in response to hormone sensitive triacylglycerol lipase action (David et al., 2005). However, long-chain fatty acids are firstly activated outside the mitochondria by one of the several long-chain acyl-CoA synthetases (Fig. 1.2) (Watkins, 1997). Acyl-CoA can pass the outer mitochondrial membrane, while it cannot cross the inner mitochondrial membrane. Therefore, Acyl-CoAs must first be trans-esterified to L-Car (Acyl-carnitine

complex) by Carnitine Palmitoyl Transferase I, in the inner side of the mitochondrial outer membrane (Price et al., 2002; Murthy et al., 1987; Fiona et al., 1997; Van der Leij et al., 1999). Consequently, the resulting acyl-carnitines are transported through the mitochondrial inner membrane in the presence of Carnitine/Acyl-Carnitine Transporter (Dayanand et al., 2011). Finally, Carnitine Palmitoyl Transferase II reconverts the acyl-carnitines into their CoA-esters (Acyl-CoAs) plus L-Car. Thereafter, the acyl-CoAs can enter the β-oxidation pathway. L-Car is transported back into the cytosol either as free carnitine to import another acyl-group or it can be converted into a new acyl-carnitine by Carnitine Palmitoyl Transferase II or Carnitine Acetyl Transferase or can be exported from the mitochondrial matrix, out of the cell (McGarry and Brown, 1997; Ramsay et al., 2001). By this way, it assists in maintaining of the acyl-CoA and CoA ratio. Consequently, modulation of toxic effects of poorly metabolized acyl groups by excreting them as carnitine esters. Through this mechanism of reversible acylation, L-Car is able to modulate the intracellular concentrations of free CoA and acyl-CoA (Duran et al., 1990; Rebouche, 1996).

In addition, a huge number of reports publicized that L-Car has other beneficial effects in the biological system. In 1973, Casillas demonstrated that spermatozoa accumulate L-Car in mammalian epididymis, which is closely related with the development of fertilizing capacity by spermatozoa. Such studies demonstrated a positive correlation between L-Car and male fertility (Chiu Ming et al., 2004; Agrawal and said, 2004; Zhou et al., 2007). Moreover, L-Car has been proposed as a protective agent against exposure of ionizing radiation in the body organs and consequently its side effects such as fatigue, nausea, hair loss, skin irritation, anemia, infertility, cardiovascular disease, cognitive impairment and even the development of secondary cancers.

It is known that L-Car has beneficial effects on sickle-cell (Ronca et al., 1994), thalassaemic (Palmieri et al., 1994) and chronic renal failure anemia (Golper et al., 2003). In addition, oral or intravenous L-Car therapy results in an increase in haematocrit, mean reticulocyte count, haemoglobin levels, erythrocyte count and survival time, and a significant decrease in erythropoietin requirement in hemodialysis patients. L-carnitine stabilizes cellular membranes, prolongs their lives and raises red blood cell osmotic resistance (Nikolaos et al., 2000; Matsumoto et al., 2001). L-Car has potentially beneficial effects on athletic performance, obesity, ergogenic aid, diabetes (Youn, 2008), hemodialysis (Calo et al., 2012; Veselá et al., 2001), and male infertility (Zhou et al., 2007). Moreover, L-Car deficiency is associated with various clinical problems such as hyperammonemia, cardiovascular diseases, and muscle weakness (Peter et al., 2012).

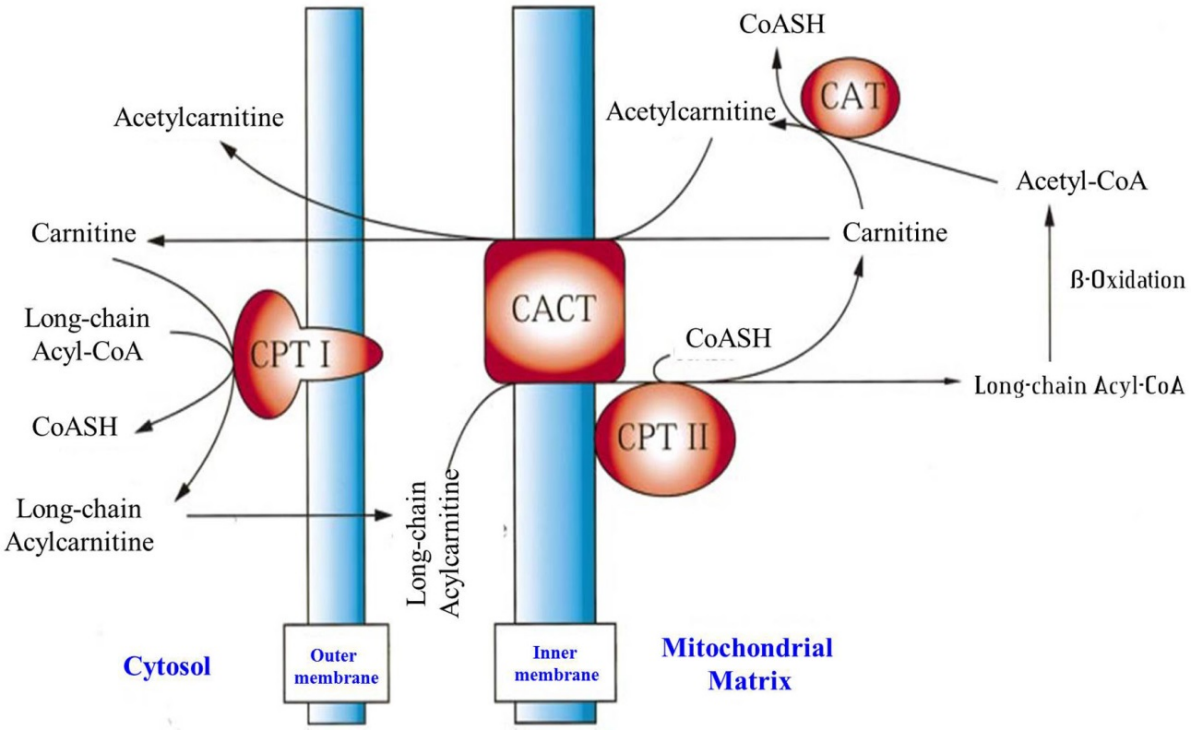

Fig. 1.2 Function of carnitine in the transport of mitochondrial long-chain fatty acid oxidation and regulation of the intramitochondrial acyl-CoA/CoA ratio (Vazi and Wanders, 2002).

Whereas; CPT I is carnitine palmitoyltransferase I, CPT II is carnitine palmitoyltransferase II, CAT is carnitine acetyltransferase, CACT is carnitine-acylcarnitine translocase.

1.3 L-CARNITINE DEFICIENCY SYMPTOMS

Human carnitine primary deficiency is caused by mutations in the gene coding for the plasma membrane carnitine transporter OCTN2. As a result, dietary carnitine is taken up poorly and urinary carnitine is not reabsorbed by the kidney which leads to severely decreased levels of carnitine in plasma and tissues (Tein, 2003; Magoulas and El-Hattab, 2012). Intracellular carnitine deficiency impairs the entry of long-chain fatty acids into the mitochondrial matrix. Consequently, long-chain fatty acids are not available for beta-oxidation and energy production, and the production of ketone bodies (which are used by the brain) is also impaired. In the infancy or early childhood, carnitine primary deficiency can include severe brain dysfunction, a weakened and enlarged heart, confusion, vomiting, muscle weakness, and low blood sugar (hypoglycemia). Furthermore, people who have any of the organic acidemias, mitochondrial disorders, severe liver disease, and/or renal tubular dysfunction may be at risk of developing secondary carnitine deficiency (Stanley, 2004; Shimizu et al., 1994; Shug et al., 1978; Spagnoli et al., 1982; Rizzon et al., 1989; Suzuki et al., 1982; Regitz et al., 1990).

In secondary carnitine deficiency, which is caused by other metabolic disorders (eg, fatty acid oxidation disorders and organic acidemias) (Rinaldo and Matern, 2002; Chace et al., 2001; Abdenur et al., 1998; Santer et al., 2003), carnitine depletion may be secondary to the formation of acylcarnitine adducts and the inhibition of carnitine transport in renal cells by acylcarnitines. In disorders of fatty acid oxidation, excessive lipid accumulation occurs in muscle, heart, and liver, with cardiac and skeletal myopathy and hepatomegaly. Long-chain acylcarnitines are also toxic and may have an arrhythmogenic effect, causing sudden cardiac death (Ogier de Baulny and Saudubray, 2002).

1.4 L-CARNITINE MEASUREMENT

Measurements of free and total carnitine in plasma are important in the diagnosis and clinical management of patients with carnitine deficiency syndromes and certain inborn errors of metabolism (Pons and Vivo, 1995). Initially, concentration of L-Car in various tissues have been previously determined such as bioassay procedures dependent upon the growth requirement of *Tenebrio molitor* for vitamin B_T (Fraenkel, 1954; Fraenkel and Friedman, 1957), a bioassay dependent upon the response of frog rectus to carnitine derivatives (Strack et al., 1960), methods based upon the complexing of quaternary compounds with bromophenol blue, and chromatographic separation, with subsequent conversion of the compound to its periodide derivative (Friedman, 1958; Mehlman and Wolf, 1962; Christianson et al., 1963). These methods lack specificity and precision. In last part, all reactive quaternary compounds other than carnitine must either be removed prior to colorimetric determination or be corrected through various procedures.

A few years later, a spectrophotometric method has been developed based on the colorimetric assay of reaction between carnitine and acetyl-CoA catalysis by carnitine acetyl transferase (Marquis and Fritz, 1964). In this method, CoA formulated interacts 5,5'-dithiobis-2-nitrobenzoic acid (DTNB). However, the highest cost of acetyl-CoA and CoA plus the long procedure for enzyme preparation are impaired method development. In addition to carnitine acetyltransferase, several enzymatic assays for L-Car have been reported (de Sousa et al., 1990; Bremen and Vienna, 1990; Schopp and Schafer, 1985; Mcgan-j and Daniel, 1976; Cederblad and Lindstedt, 1972; Aurich and Kleber, 1968; Pearson et al., 1974; Parvin and Pande, 1977); these include a radiochemical method with carnitine acetyltransferase (EC 2.3.1.7), radioisotopic

determination (Demarquoy et al., 2004), and spectrophotometric methods involving L-carnitine dehydrogenase (CDH) (EC 1.1.1.108) (Takahashi et al., 1994; Matsumoto et al., 1990). In CDH method, L-Car assessment is based on the monitoring the increase of NADH reading at 340 nm.

In recent past, several analytical methods have been established such as HPLC (Minkler and Hoppel, 1993; Minkler et al., 1987; 1995; McEntyre et al., 2004; Lever et al., 1992), tandem mass spectrometry (Vernez et al., 2003; Sanchez-Hernandez et al., 2010). However, many of these methods such as radioenzymatic and tandem mass spectrometry that is often not available in clinical laboratories. As a result, a spectrophotometric analysis of L-Car using CDH has been proposed as the most sensitive, specific, rapid and low-capital equipment cost would facilitate L-Car determination in the clinical laboratories as well as in research.

1.5 BACTERIAL METABOLISM OF L-CARNITINE

Three different approaches have been developed by prokaryotes to metabolite L-Car (Fig 1.3) (Kleber, 1997). In the first degradation pathway, strains of *Acinetobacter calcoaceticus* and *Serratia marcescens* are able to cleaved L-Car into trimethylamine and malic acid. The enzymes involved in this conversion are not yet recognized. By this means, the above mentioned bacterial species are capable of assimilating the carbon-chain of 3-hydroxy-4-(trimethylammonio) butyric acid betaine, whereas trimethylamine is not metabolically used by these strains and remains unchanged. Strains of *Escherichia coli*, *Salmonella typhimurium*, *Proteus mirabilis*, and *Proteus vulgaris*, which belong to the enterobacteriaceae family, are able to convert L-Car into γ-butyrobetaine via crotonobetaine, with the help of several proteins as carbon and

nitrogen sources under anaerobic conditions (Seim et al., 1982). Their genes are grouped in, which are called CaiTABCDE-operon designated as CaiA, CaiB, and CaiD (Eichler et al., 1994; Elssner et al., 2001; Jung et al., 2002). Initially, L-carnitinyl-CoA converts into crotonobetainyl-CoA via reversible reaction catalysis by enoyl-CoA hydratase (CaiD). Then the γ-butyrobetaine is formulated with the assistant of CaiA and CaiB (Preusser et al., 1999; Stenmark et al., 2004).

In contrast to what was observed in the above mentioned bacterial strains, several species of bacteria have been reported to grow aerobically on L-Car as sole source of carbon and nitrogen, namely *Agrobacterium* sp. (Hanschmann et al., 1996; Setyahadi et al., 1998), *Alcaligenes* sp. (Houriyou et al., 1993), *Pseudomonas putida*, *P. aeruginosa* (Goulas, 1988; Aurich et al., 1968), *Xanthomonas translucens*, *Rhizobium* sp. (Mori et al., 1988a; 1994), *Burkholderia cepacia*, *Pseudomonas spp*. (Grimont et al., 1996), and *Sinorhizobium meliloti* (Goldmann et al., 1991). Of them, seven species oxidize the β-hydroxyl group of L-Car with concomitant formation of 3-Dehydrocarnitine by NAD^+ dependent CDH. In addition to L-Car, CDH could be also induced by D-carnitine, γ-butyrobetaine, crotonobetaine (Hanschmann et al., 1994), and D,L-carnitine (Ehricht 1995). However, 3-dehydrocarnitine formed by the CDH could be degraded to glycinebetaine by using unidentified enzymes in the presence of NAD^+, ATP, and CoA as cofactors (Lindstedt et al., 1967). Recently, Wargo and co-workers (2009) investigated metabolic pathway of L-Car in *Pseudomonas aeruginosa*. They predicted an enzyme namely 3-ketoacid CoA-transferase, which hypothesized to be involved in the first step of deacetylation of 3-dehydrocarnitine. Like L-Car, several *Agrobacterium* species also can grow on the D-carnitine medium as the sole source of carbon and nitrogen. In such bacterial species, the oxidation of D-carnitine catalyzes by an NAD^+ dependent D-carnitine dehydrogenase (EC.1.1.1.254), which has been purified and

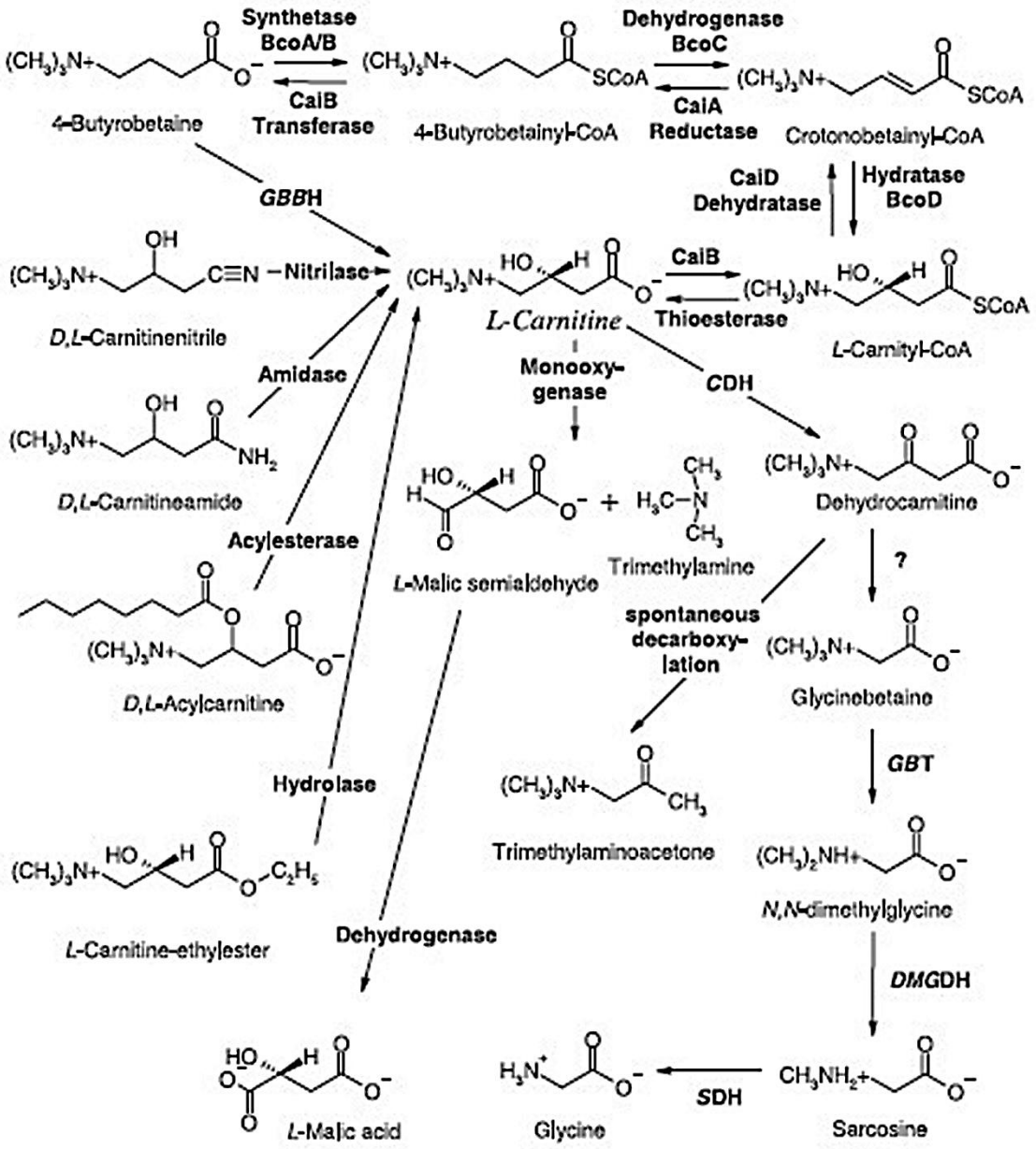

Fig. 1.3 Bacterial L-carnitine metabolisms

Whereas: Bco, butyrobetaine-L-carnitine operon; Cai, L-carnitine-butyrobetaine operon; CoA, coenzyme A, DMGDH, dimethylglycine-dehydrogenase; GBBH, gamma butyrobetaine hydroxylase; GBT, glycinebetaine-transmethylase; CDH, L-carnitine dehydrogenase; SDH, sarcosine dehydrogenase (Uanschou et al., 2005).

biochemically characterized by Hanschmann and Kleber (1997) and Setyahadi et al (1997). However, *Acinetobacter calcoaceticus* 69/V is able to metabolize D-carnitine only in the presence of a supplementary carbon source like L-Car, DL- carnitine in the incubation medium but no growth was observed with D-carnitine as sole source of carbon (Kleber et al., 1977). The utilization of these compounds and the growth of the organisms are correlated with the stoichiometric formation of trimethylamine.

Moreover, D-carnitine effectively supports the growth of *A. calcoaceticus.* The utilization of carnitine resulted in stoichiometric formation of trimethylamine and equivalent loss of the carboxyl-labelled carbon backbone from the growth medium. Therefore, D-carnitine does not induce the initial enzyme of carnitine degradation in *A. calcoaceticus* (Miura-Fraboni and Englard, 1983)

1.6 L-CARNITINE DEHYDROGENASE

CDH is an oxidoreductase enzyme that acts upon an alcohol functional group (C-OH). CDH catalyzes the oxidative reaction of L-Car to 3-dehydrocarnitine with the contaminant reduction of NAD^+ to NADH (Fig 1.4). It has been isolated from the bacterium of *Pseudomonas aeruginosa*, *Alcaligenes* sp., *Pseudomonas putida, Xanthomonas translucens, Rhizobium* sp., and *Agrobacterium* sp. (Houriyou et al., 1993; Aurich et al., 1968; Mori et al., 1988a; Mori et al., 1994; Goulas, 1988; Hanschmann et al., 1996). CDHs are homodimer proteins with native molecular weight range from 60 to 114 kDa, with highly specific to the L-Car and NAD^+. The enzymes are not reacting with $NADP^+$ or other L-Car analogs such as D-carnitine. As shown in Table 1.1, the specific activities of CDHs for oxidation reaction were range from 0.35 – 200 μmol min^{-1} mg^{-1}, which are lower than that of reduction reaction of investigated

enzymes. Furthermore, CDHs have an optimum pH of the oxidation reaction of 9.0 to 9.5. In contrast to that the optimum pH of the reduction reaction varies from 5.5 to 8.0. The differences between the K_m-values for the substrates of the reduction reaction for all CDHs are much slighter (0.54 – 1.71 mM) than that of the oxidation reaction. There clearly exist much larger differences in the K_m-values of the substrates of the oxidation reaction. Most of the CDHs have a K_m-value for L-Car of about 1.1–10 mM. However, CDH from *Agrobacterium* sp. exhibits two K_m values for L-Car, consequently, CDH from this species is unstable and may has different form for substrate binding during catalysis mechanism.

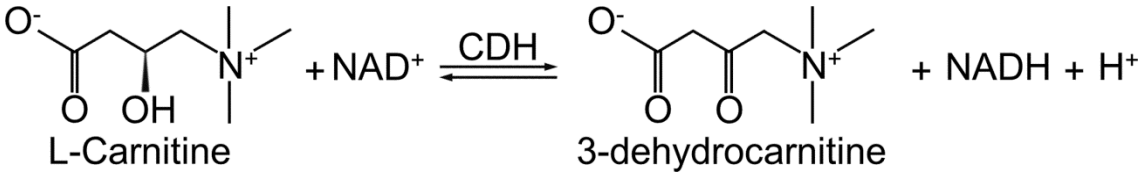

Fig. 1.4 Reaction catalysis by L-carnitine dehydrogenase

To my current knowledge, the whole sequence of CDH has been identified in *Xanthomonas translucens* (Xt-CDH) (Mori et al., 1988b), *Rhizobium* sp. (Rs-CDH) (Arima et al., 2010), *Alcaligenes* sp. (Houriyou et al., 1993), and *Pseudomonas aeruginosa* (Wargo et al., 2009). Of them, two CDHs (Xt-CDH and Rs-CDH) have been detected, purified, cloned, and overexpressed in the laboratory of Microbial Biotechnology, Tottori University, Tottori, Japan. The primary structures of CDHs

exhibit high identity to that of 3-hydroxyacyl-CoA dehydrogenase (HAD) (EC 1.1.1.35) (Uanschou et al., 2005). Hydroxyacyl-CoA dehydrogenases of two types exist in the microorganism: one has an extra sequence in the C-terminal region with a molecular mass of approximately 54 kDa. The second group does not have extra sequence (Molecular mass of approximately 34 kDa). The difference in the molecular mass between Xt-CDH (37 kDa) and Rs-CDH (50 kDa) (Table 1.1) is considered to be attributed to the presence of extra C-terminal region in Rs-CDH (496 amino acids) compared to that of Xt-CDH (321 amino acids). Deletion of this extra tail, in a previous study (Arima et al., 2010), did not altered protein properties.

Table 1.1 Molecular and kinetic properties of L-carnitine dehydrogenase from different bacterial species

Properties	***Rhizobium* sp.**	***Agrobacterium* sp.**	***Pseudomonas putida***	***Pseudomonas aeruginosa***	***Alcaligenes* sp.**	***Xanthomonas translucens***
Native MW (kDa)	110	114	60	n.d.	51	74
Subunit MW (kDa)	50	57	32	n.d.	n.d.	37
subunits	2	2	2	n.d.	n.d.	2
IEP	5.5	5.2-5.4	4.7	n.d.	5.3	n.d.
K_m (mM)						
L-carnitine	1.1	0.29/6.1	6.25	8.9	9.3	10
NAD^+	0.1	0.018/0.042	0.2	0.16	0.14	0.25
3-dehydrocarnitine	0.54	0.72	1.1	1.3	n.d.	1.71
NADH	0.019	0.032	0.013	0.022	n.d.	0.04
pH optimum						
Oxidation	9.5	9.5	9.0	9.0 – 9.5	9.0	9.5
Reduction	6.5-8.0	5.6 – 6.5	7.0	7.0	n.d.	6.5
Temperature (ºC)						
Optimum	40	45	30	n.d.	50	n.d.
Stability	38	n.d.	n.d.	35	n.d.	45

n.d. Not determined

1.7 DESCRIPTIVE, RATIONAL AND AIMS OF THE STUDY

While CDH, as a rapid and low-cost tool for measurement of biologically essential compound L-Car, have been isolated and purified from several bacterial species, precious little information is available on the structure-function of this superior enzyme. To date, four CDHs gene have been explored revealing 47% homology percent to each other. Furthermore, their primary structure belong the oxideoreductase family, which include several well investigated enzymes. Taking the information in our own hand, a more complete understanding of the catalytic mechanism would be gained through investigation of the interactions between bound substrates and key amino acid residues they contact. In the current study, site-directed mutagenesis was employed in two separate studies to scrutinize the roles of 56 residues in the catalytic function and substrate affinity of Xt-CDH and Rs-CDH.

To approaches these studies, the first question that must be inquired is “what residues do you mutate?” and then “What do you mutate them to?” In the first study (Chapter 2) of this project, the residues of Ala137, Tyr140, Ala185, Val187, Gly188, Ser220, and Phe221 in Rs-CDH were mutated to their corresponding residues in Xt-CDH (Gly140, Phe143, Gly188, Ile190, Ala190, Gly223, and Ala224) due to their involvement in the active site of Xt-CDH and Rs-CDH and their position near to the bound substrate (L-Car). In particular, structural data of Xt-CDH and Rs-CDH homology models based on the crystal structure of human-HAD (h-HAD) revealed that only seven residues are different between the residues composing the putative active site of CDHs. A part of this study was directed to examine the role of phenyl ring of the aromatic residues Phe143 in Xt-CDH and Tyr140 of Rs-CDH in the catalytic function and substrate binding.

In the second study (Chapter 3), a total of 42 residues (Glu93, Ser117, Thr119, Ser120, His133, Arg136, His141, Asn144, Tyr147, Glu153, Met177, Lys184, Glu185, Phe189, Asp192, Arg193, Glu196, Trp199, Arg200, Glu201, Asp217, Arg221, Arg227, Trp228, Met231, Phe234, Thr236, Trp237, Met246, Arg247, His248, Phe249, Gln252, Phe253, Trp261, Thr262, Gln284, Ser189, Glu294, Arg295, Arg297, and Asp298) in Xt-CDH were examined because of highly degree of conservation among CDHs and bacterial HADs enzymes. In order to study the roles of these residues on catalytic function and substrate affinity as well as to minimize disruption of protein structure, the residues were mutated to Alanine. Based on the kinetic data of Alanine mutants and homology model of Xt-CDH, regions and specific residues that are important for catalysis and for the recognition of the substrate in Xt-CDH are classified.

CHAPTER 2

SITE-DIRECTED MUTAGENESIS OF L-CARNITINE BINDING SITE: INSIGHT INTO THE ROLE OF F143 OF Xt-CDH AND Y140 IN Rs-CDH

2.1 INTRODUCTION

The oxidoreductase CDH has been proposed as a superior tool for measurement of biologically essential compound L-Car (3-hydroxy-4-trimethylaminobutyrate). Actually, without L-Car the body cannot metabolize long chain fatty acids and therefore decreasing available energy for biological functions (Bremer, 1983).

To date, CDH has been found in various microbes (Aurich et al., 1968; Goulas, 1988; Mori et al., 1988a; Houriyou et al., 1993; Mori et al., 1994; Hanschmann et al., 1996; Wargo et al., 2009). Of those, we have two CDHs from *Xanthomonas translucens* (Xt-CDH) (Mori et al., 1988a) and *Rhizobium* sp. (Rs-CDH) (Mori et al., 1994). Xt-CDH has lower molecular weight (MW) (37 kDa) and lower affinity (K_m 10 mM) towards L-Car than Rs-CDH (MW 50 kDa and K_m 1.0 mM for L-Car). As reported previously, the higher MW for Rs-CDH results from the presence of an extra C-terminal tail. However, the deletion of this extra tail (162 amino acids) demonstrated that it has no effect on substrate affinity (Armia et al., 2010). The primary structure of Rs-CDH and Xt-CDH exhibited high identity with that of 3-hydroxyacyl-CoA dehydrogenases, which includes several known crystal structure enzymes. Stable and high substrate affinity CDH is necessary to obtain precise results in L-Car measurement, but the structure–function relation of CDH remains largely unknown.

The residues composing the active site must have some roles in catalytic activity or substrate binding. Therefore, we speculate that some residues, which differ in the active sites between Xt-CDH and Rs-CDH, are responsible for the substrate affinity variation. We used the protein primary structure alignment of Xt-CDH and Rs-CDH with the structural information of the human heart 3-hydroxyacyl-CoA dehydrogenase (PDB: 1F0Y) (h-HAD) (Barycki et al., 2000) for the prediction of the residues associated to the catalytic activity or affinity to the substrate. In the structure of h-HAD, several residues surround the acetoacetyl moiety of the substrate. Of them, seven residues namely Lue157, Phe160, Gly204, Ile206, Val207, Gly239, and Ala240 were selected. These residues matched Gly140, Phe143, Gly188, Ile190, Ala191, Gly223, and Ala224 of Xt-CDH, which correspond to Ala137, Tyr140, Ala185, Val187, Gly188, Ser220, and Phe221 in Rs-CDH.

For this Chapter, The selected residues of Xt-CDH were replaced with that of Rs-CDH at the corresponding position and *vice versa*. Four single mutation and four double mutation were conducted investigate the substrate affinity of both dehydrogenases as influenced by mutagenesis. As expected, the induced mutation depicted different influence on dehydrogenation ability of either enzyme. Therefore, we further modified the residue Phe143 of Xt-CDH, which produced the highest alteration in substrate affinity and its corresponding Tyr140 of Rs-CDH. Based on the comparative kinetic study, the mechanism of the substrate recognition of the CDHs is discussed.

2.2 MATERIALS AND METHODS

2.2.1 Materials

2.2.1.1 Bacterial strains, plasmids, substrates and cofactors

Plasmids pMal-RsCDH and pMal-Xt-CDH (pMal-c2 vector with the CDH genes inserted into the *BamH*I–*Hind*III gap) (Arima et al., 2010) were used for expression of the wild-type enzymes and as a template of site-directed mutagenesis. *Escherichia coli* JM109 which was collected from Takara Bio Inc. (Shiga, Japan) was used as the host strain for general cloning procedures and for gene expression. The substrate L-Car was purchased from Hamari Chemicals, Ltd., Yonezawa, Japan. NAD^+ was purchased from Oriental Yeast Co. Ltd., Tokyo, Japan.

2.2.1.2 PCR reagents

Oligonucleotide primers for site directed mutagenesis were synthesized at Operon Biotechnologies (Tokyo, Japan) and were suspended in nuclease-free Tris-EDTA buffer upon receipt as a 100 μmol/ml stock solution. A working solution of each primer was 5 μmol/ml. The sequences of the pairs of oligonucleotides synthesized for the mutagenesis are presented in Table 2.1 and 2.2. The universal primers (pMal-c2 forward, pMal-c2 reverse, and M13 forward) used for sequencing are presented in Table 2.3. Pwo polymerase was purchased from Roche Applied Science (USA). Agaroses used for gel-electrophoresis of DNA fragment were collected from BMA (Rockland, ME, USA) or Takara Bio Inc. (Shiga, Japan). Loading quick λ/StyI and loading quick λ/HindIII were purchased from Toyobo, Japan. A DNA staining reagent, SYBR Gold was collected from life technologies (USA). Econo Spin™ IIa spin column was purchased from INA OPTIKA (Nagano, Japan). BigDye Terminator Cycle

Sequencing Ready Reaction kit ver 3.1 was from Applied Biosystems (Foster City, CA). The dye terminators, deoxynucleoside triphosphates, AmpliTaq DNA Polymerase, FS, rTth pyrophosphatase, magnesium chloride, and buffer were premixed into a single tube of Ready Reaction Mix and were ready to use. Restriction enzymes, Taq polymerase and DNA sample loading dye were from New England Biolabs (Massachusetts, USA), Takara Bio Inc. (Shiga, Japan), and Toyobo (Osaka, Japan).

2.2.1.3 Culture, purification, and polyacrylamide gel electrophoresis

Bacto trypton, agar and yeast extract were purchased from Difco (Lawrence, USA). Ampicillin and Isopropyl-ß-tiogalactopyranoside (IPTG) were purchase from Wako Pure Chemical Ind. Ltd. (Osaka, Japan). Amylose resin and Color Plus pre-stained protein marker for SDS–PAGE were from New England Biolabs Inc. (Massachusetts, USA). Enzyme samples were prepared for loading by mixing with an equal volume of 2x EzApply sample buffer (Atto, Tokyo, Japan). For proteins staining Coomasie brilliant blue R250 were collected from Wako Pure Chemical Ind. Ltd. were used.

2.2.1.4 Other reagents

All other chemicals and materials were of the highest purity grade were supplied from Wako Pure Chemical Ind. Ltd. (Osaka, Japan) and used without further processing.

Table 2.1 Primers used for site-directed mutagenesis of Xt-CDH and Rs-CDH

Primer name	DNA sequence
Xt-G140A-F	5’ AGCGCTGCGTGGTC**GCG**CACCCTTTCAAC 3’
Xt-G140A-R	5’ GTTGAAAGGGTG**CGC**GACCACGCAGCGCT 3’
Xt-F143Y-F	5’ TCGGCCACCCT**TAC**AACCCGGTGTAC 3’
Xt-F143Y-R	5’ GTACACCGGGTT**GTA**AGGGTGGCCGA 3’
Xt-G188A-F	5’ AAGGAAGTCCCC**GCC**TTCATCGCCGAT 3’
Xt-G188A-R	5’ ATCGGCGATGAA**GGC**GGGGACTTCCTT 3’
Xt-I190V/A191G-F	5’ AAGTCCCCGGCTTC**GTCGGC**GATCGTCTGCTC 3’
Xt-I190V/A191G-R	5’ GAGCAGACGATC**GCCGAC**GAAGCCGGGGACTT 3’
Xt-G223S/A224F-F	5’ ACGCGATCCGCTTC**TCCTTC**GGCCTGCGCTGGT 3’
Xt-G223S/A224F-R	5’ ACCAGCGCAGGCC**GAAGGA**GAAGCGGATCGCGT 3’
Rs-A137G-F	5’AGCGCATGTTCGTG**GGC**CATCCCTACAACC 3’
Rs-A137G-R	5’GGTTGTAGGGATG**GCC**CACGAACATGCGCT 3’
Rs-Y140F-F	5’ TTCGTGGCGCATCCC**TTC**AACCCCGTCTAC 3’
Rs-Y140F-R	5’ GTAGACGGGGTT**GAA**GGGATGCGCCACGAA 3’
Rs-A185G-F	5’ AAGGAGATCGAG**GGC**TTCGTCGGCGAC 3’
Rs-A185G-R	5’ GTCGCCGACGAA**GCC**CTCGATCTCCTT 3’
Rs-V187I/G188A-F	5’ AGATCGAGGCCTTC**ATCGCC**GACCGCCTGCT 3’
Rs-V187I/G188A-R	5’ AGCAGGCGGTC**GGCGAT**GAAGGCCTCGATCT 3’
Rs-S220G/F221A-F	5’ AACGTCATGCGTTAT**GGCGCC**GGCATGCGCTGGG3’
Rs-S220G/F221A-R	5’ CCCAGCGCATGCC**GGCGCC**ATAACGCATGACGTT3’

Bold letters denote the codon of mutated residues.

Table 2.2 Primers used for mutation of Xt-F143 and Rs-Y140

Primer name	**DNA sequence**
Rs-Y140W-F	5’ TTCGTGGCGCATCCC**TGG**AACCCCGTCTAC 3’
Rs-Y140W-R	5’ GTAGACGGGGTT**CCA**GGGATGCGCCACGAA 3’
Rs-Y140A-F	5’ TTCGTGGCGCATCCC**GCG**AACCCCGTCTAC 3’
Rs-Y140A-R	5’ GTAGACGGGGTT**CGC**GGGATGCGCCACGAA 3’
Rs-Y140G-F	5’ TTCGTGGCGCATCCC**GGC**AACCCCGTCTAC 3’
Rs-Y140G-R	5’ GTAGACGGGGTT**GCC**GGGATGCGCCACGAA 3’
Rs-Y140S-F	5’ TTCGTGGCGCATCCC**AGC**AACCCCGTCTAC 3’
Rs-Y140S-R	5’ GTAGACGGGGTT**GCT**GGGATGCGCCACGAA 3’
Rs-Y140C-F	5’ TTCGTGGCGCATCCC**TGC**AACCCCGTCTAC 3’
Rs-Y140C-R	5’ GTAGACGGGGTT**GCA**GGGATGCGCCACGAA 3’
Rs-Y140N-F	5’ TTCGTGGCGCATCCC**AAT**AACCCCGTCTAC 3’
Rs-Y140N-R	5’ GTAGACGGGGTT**ATT**GGGATGCGCCACGAA 3’
Rs-Y140K-F	5’ TTCGTGGCGCATCCC**AAA**AACCCCGTCTAC 3’
Rs-Y140K-R	5’ GTAGACGGGGTT**TTT**GGGATGCGCCACGA 3’
Rs-Y140H-F	5’ TTCGTGGCGCATCCC**CAT**AACCCCGTCTAC 3’
Rs-Y140H-R	5’ GTAGACGGGGTT**ATG**GGGATGCGCCACGAA 3’
Rs-Y140D-F	5’ TTCGTGGCGCATCCC**GAT**AACCCCGTCTAC 3’
Rs-Y140D-R	5’ GTAGACGGGGTT**ATC**GGGATGCGCCACGAA 3’
Xt-F143W-F	5’ TGGTCGGCCACCCT**TGG**AACCCGGTGTAC 3’
Xt-F143W-R	5’ GTACACCGGGTT**CCA**AGGGTGGCCGACCA 3’
Xt-F143A-F	5’ TGGTCGGCCACCCT**GCG**AACCCGGTGTAC 3’
Xt-F143A-R	5’ GTACACCGGGTT**CGC**AGGGTGGCCGACCA 3’
Xt-F143G-F	5’ TGGTCGGCCACCCT**GGC**AACCCGGTGTAC 3’
Xt-F143G-R	5’ GTACACCGGGTT**GCC**AGGGTGGCCGACCA 3’
Xt-F143S-F	5’ TGGTCGGCCACCCT**AGC**AACCCGGTGTAC 3’
Xt-F143S-R	5’ GTACACCGGGTT**GCT**AGGGTGGCCGACCA 3’
Xt-F143C-F	5’ TGGTCGGCCACCCT**TGC**AACCCGGTGTAC 3’
Xt-F143C-R	5’ GTACACCGGGTT**GCA**AGGGTGGCCGACCA 3’

Table 2.2 (Continue)

Primer name	DNA sequence
Xt-F143N-F	5’ TGGTCGGCCACCCT**AAT**AACCCGGTGTAC 3’
Xt-F143N-R	5’ GTACACCGGGTT**ATT**AGGGTGGCCGACCA 3’
Xt-F143K-F	5’ TGGTCGGCCACCCT**AAA**AACCCGGTGTAC 3’
Xt-F143K-R	5’ GTACACCGGGTT**TTT**AGGGTGGCCGACCA 3’
Xt-F143H-F	5’ TGGTCGGCCACCCT**CAT**AACCCGGTGTAC 3’
Xt-F143H-R	5’ GTACACCGGGTT**ATG**AGGGTGGCCGACCA 3’
Xt-F143D-F	5’ TGGTCGGCCACCCT**GAT**AACCCGGTGTAC 3’
Xt-F143D-R	5’ GTACACCGGGTT**ATC**AGGGTGGCCGACCA 3’

Bold letters denote the codon of mutated residues.

Table 2.3 Primers used for sequencing insert CDHs

Primer name	DNA sequence
pMal-c2-F	5' TGCGTACTGCGGTGATCAAC 3’
pMal-c2-R	5’ GGATGTGCTGCAAGGCGATTAAG 3’
M13-F	5' TGTAAAACGACGGCCAGT 3'

2.2.2 Methods

2.2.2.1 General methods

Plasmid and products derived from PCR were purified by using Econo Spin™ IIa spin columns from INA OPTIKA (Nagano, Japan). PCR thermal Cycler Dice model TP 600 and model TP100 of Takara were used for PCR reactions (Takara Bio Inc., Shiga, Japan). Mupid-2X submarine electrophoresis system apparatus (Advance Co. Ltd.,

Japan) was used for agarose gel electrophoresis. PCR products were dried using ultra-small centrifugal concentrator spin dryer mini VC-15 SP (TAITEC, Co. Ltd. Koshigaya, Japan). General weight measurements were made using IB-200H electronic balance (Shimadzu corp. Kyoto, Japan) and smaller quantities measurements for the preparation of standards were made using Mettler AE240 analytical balance (Mettler, Toledo, AG, Switzerland). pH was determined using an Horiba F-22 pH meter 66 (Horiba Ltd., Kyoto, Japan). Media were autoclaved at 121 ºC for 20 minutes using BS-235 high pressure steam sterilizer (Tomy Seiko Co., Ltd., Tokyo, Japan). Filter sterilization of solutions was carried out using 0.22 μm disposable filters MILLEX-GA (Millipore, Molshiem, France). Inoculated media were incubated either in at 37 ºC with reciprocal shaker NR-1 or at 25 ºC using a NR-300 double shaker (Taitec Corporation, Tokyo, Japan) or at 30 ºC and low temperature in LTI-60ISD EYALA low temperature incubator equipped with NR-30 double shaker (EYALA, Tokyo, Japan). Cell growth was measured using the Novaspec II from Amersham Pharmachia Biotech (Piscataway, NJ, USA). Cultures and extracts were centrifuged using Hitachi Himac Compact Centrifuges RX II Series CF16RXII (rotor: 36, T16A31; 44, T15A36; 46, T15A36; and 24, T9A31) and Hitachi Himac CT15E (Hitachi Koki Company Ltd., Tokyo, Japan). Samples were vortexes using a Vortex Genie 2 (Scientific Industries, Inc., USA). Collected cells were disrupted using TOMY Ultrasonic Disruptor (UD-200). For measurement of enzyme activity, Shimadzu UV-2100S spectrophotometer (Kyoto, Japan) was used. Bio-Rad micro plate reader Model 680 (BIO-RAD Inc., Hercules, CA, USA) was used for protein assay. For shaken of 96 well plate, multi-barreled micro-plate mixer from AS ONE (Osaka, Japan) was used.

2.2.2.2 Modeling of three-dimensional structures

Swiss-Model (http://swissmodel.expasy.org/) was utilized to model the three-dimensional structure of Xt-CDH and Rs-CDH (Arnold et al., 2006). The template structure is h-HAD (PDB code: 1F0Y), which shares the highest sequence identity with that of Xt-CDH and Rs-CDH among the proteins in the Protein Data Bank (PDB) (http://www.rcsb.org/). The primary structure of Xt-CDH displayed 28% identity and 47% similarity when aligned with that of h-HAD, whereas Rs-CDH exhibited 24% identity and 42% similarity with h-HAD.

2.2.2.3 Site-directed mutagenesis

The pMal-c2 vectors harboring CDHs (Xt-CDH and Rs-CDH) were used as a template for site directed mutagenesis. Site-directed mutagenesis of both CDH genes was conducted using the forward and reverse primers listed in Table 2.1 and 2.2. PCR reactions (20 µl) were performed with 1.0 U of Pwo polymerase (Roche Diagnostics Corp.) in 1x High Fidelity buffer (which includes 1.5 mM $MgCl_2$), 0.2 mM deoxynucleotide triphosphates, 0.5 µM forward and reverse primer, and suitable amount of plasmid template with the following program: 1.0 min pre-heating step at 95 ºC; 1.0 min denaturation step at 95 ºC, 1.0 min annealing step at 55/60/63 ºC and 14 min extension step at 72 ºC for a total of 18 cycles; and 72 ºC for 5 min. Following cooling of the PCR reaction to 15 ºC, a portion of PCR product (3 µl) was loaded into 0.7% gel electrophoresis. To remain PCR product (17 µl), 1 µl (1.0 U final concentration) of restriction enzyme *Dpn*I were added, and the mix was incubated at 37 ºC overnight to digest the methylated, non-mutated parental plasmid (Rs-CDH and Xt-CDH) template. Hundred-microliters of *Escherichia coli* JM109 cells were transformed

using a portion of the digested mix (5 µl) by potassium chloride method as follows. The mixture of cells and digested mix was incubated in 1.5 ml micro-tube into water bath at 42 ºC for 45 second after the incubation for 30 min on the ice. Tubes were backed on ice for 2 min to reduce the damage to the *E. coli* cells. Next, 1.0 ml of Super Optimal Broth medium (SOC medium) were added into each tube and again incubated at 37 ºC for 1 hour under continual shaking, and plated on Luria-Bertani medium (LB) agar supplemented with 50 µg/ml ampicillin. Individual colonies were grown in 5 ml of LB broth with 50 µg/ml ampicillin, and plasmids were isolated using Econo Spin^{TM} IIa according to the manufacturer's instructions. The DNA fragments coding all twenty eight CDH mutants (twenty single mutants and four double mutants) were amplified using the primers listed in Table 2.3 and sequenced using automated BigDye Terminator Fluorescence Sequencing at faculty of medicine, Tottori University to insure that only the intended mutation was introduced. Mutants version prepared as corresponding mutants between Rs-CDH and Xt-CDH, in the current report, were Xt-G140A, Xt-F143Y, Xt-G188A, Xt-I190V/A191G, Xt-G223S/A224F, Rs-A137G, Rs-Y140F, Rs-A185G, Rs-V187I/G188A, and Rs-S220G/F221A.

2.2.2.4 Expression and purification of wild-type and mutant enzymes

The pMal-c2 vectors harboring Xt-CDH, Rs-CDH and mutant genes were transformed into the competent cell (*E. coli* JM109) supplied by Takara Inc. (Japan). Several colonies were grown for 24 h at 37 °C in 5 ml LB medium containing 50 µg/ml of Ampicillin, in a shaking incubator at 120 stroke min^{-1}. About 500 µl of the cultivated cell were inculcated into 100 ml of LB medium supplemented with 50 µg/ml of Ampicillin. These cells were cultivated at 25 °C using a reciprocal shaking (120 stroke

min^{-1}) to an optical density of 0.5 ~ 0.8 at 660 nm. Thereafter, protein expressions were induced by adding IPTG to 0.1 mM final concentration. After 12 h of protein expression, the cells were harvested by centrifugation (12000 rpm for 20 min at 4 °C). The media decanted and washed with a 0.85% potassium chloride solution followed immediately with storage at -20 °C. The cells pellet was suspended in 15 ml of 50 mM potassium phosphate buffer (KPB) (pH 7.0) containing 1.0 mM 2-mercaptoethanol (2-ME). They subsequently disrupted by ultra-sonication (TOMY Ultrasonic Disruptor, UD-200, Japan) for 5 min on ice followed by centrifugation (12000 rpm for 20 min at 4 °C). After removal of cell debris, the solution was dialyzed against 50 mM KPB (pH 7.0) containing 1.0 mM 2-ME. Expression of CDHs recombinant proteins was evaluated using a 12% SDS–PAGE under denaturing conditions (Laemmli, 1970). Gels of crude and purified proteins were stained with coomasie brilliant blue (CBB) R-250.

From the dialysate, CDHs fused with maltose binding protein (MBP) were purified using amylose resin (New England Biolabs Inc., Ipswish MA). The dialysate was loaded onto amylose column (Spin column) equilibrated with 20 mM KPB containing 200 mM NaCl, 1.0 mM ethylenediamineteteraacetic acid (EDTA), 1.0 mM 2-ME. Undesirable proteins were removed with the same buffer. Then the bound protein fused with MBP was eluted using same buffer containing 10 mM maltose. As reported previously (Arima et al., 2010), an efforts have been made to remove the MBP from CDHs with factor Xa but inactivation was observed in all the recombinant CDHs. They inferred that the inactivation of CDHs results from long-term (>6.0 h) incubation at room temperature under treatment with Factor Xa. To avoid such inactivation, in the current study, both wild-type and mutant recombinant enzymes were prepared as fused proteins with the MBP. The homogeneity of purified proteins was examined using a

12% SDS gel electrophoresis (Laemmli, 1970) under denaturing conditions and stained with CBB R-250.

2.2.2.5 Protein concentration measurements

The protein concentration was determined using the Bradford methods (Bradford, 1976) with the bovine serum albumin as standard. Specific activity was defined as units of enzyme activity per mg protein.

2.2.2.6 Enzyme assay

The spectrophotometric assay for CDHs was based on the monitoring of NADH increasing during the oxidation of L-Car by CDH at 340 nm at 30 °C. The enzyme reaction was initiated by the addition of NAD^+ at a final concentration of 2 mM to the reaction mixture (1.5 ml) containing 120 mM glycine-NaOH buffer, pH 9.5, 12 mM L-Car and an appropriate amount of enzyme (Table 2.4). The activity was calculated using an extinction coefficient of 6,200 $M^{-1} \cdot cm^{-1}$ for NADH. One unit of enzyme activity is defined as the amount of enzyme that catalyzes the formation of 1 μmol of NADH per minute under assay conditions. Specific activity was defined as units of enzyme activity per mg protein.

Table 2.4 CDH assay mixture

Glycine sodium hydroxide buffer pH 9.5 (0.9 M)	0.2 ml
L-Car (90 mM)	0.2 ml
NAD^+ (60 mM)	0.05 ml
Enzyme solution	X (0.05~0.15 ml)
Distilled water	Y (0.9~1.0 ml)
Total volume	**1.5 ml**

2.2.2.7 Kinetic parameters of CDHs

The K_m value for L-Car of CDHs was first roughly estimated using various L-Car concentrations (0.8–2000 mM) at a fixed level of the cofactor NAD^+ (2 mM). Next, the exact K_m value was ascertained from enzyme reactions using 4–5 different concentrations of L-Car around the K_m value of the specific variant. The K_m for NAD^+ was determined using different NAD^+ concentrations (0.06–2 mM) at a constant L-Car level based on the K_m of L-Car determined for CDHs. This data was fitted to the Michaelis-Menton equation using a linear regression. The values of V_{max}, K_m, k_{cat} and k_{cat}/K_m were calculated to determine how the mutations affect the enzyme functions. The V_{max} is the theoretical maximum velocity of the enzyme reaction expressed as the product formed per unit of time. K_m is the concentration of the substrate at half the maximum velocity and is expressed as a concentration. The turnover number, or the k_{cat} value, is the maximum velocity (V_{max}) divided by the concentration of the enzyme and gives information about the efficiency of the enzyme. The k_{cat}/K_m is a measure of the catalytic efficiency. By comparing these values for the mutants and wild types we will

be able to understand how these residues interact with the substrates and determine their role in catalytic function.

2.2.2.8 pH and thermal stability profile of wild-types and mutant enzymes

The thermal stability of Rs-CDH, Xt-CDH and mutant enzymes was determined by monitoring the residual enzymatic activity after 30 min incubation at different temperatures (15–55 °C) in 50 mM of KPB (pH 7.0) containing 1.0 mM of 2-ME. Residual activity was measured under standard assay conditions. The optimum pH was obtained by measuring CDH activity in a pH range of 4.5–10.5. The buffers used were acetate (pH 4.5–6.0), potassium phosphate (pH 6.0–8.0), Tris-HCl (pH 7.5–8.5), and glycine-NaOH (pH 8.5–10.5). Stability to pH was measured by assessment of residual activity after incubation of 200 μl enzyme at 30 °C for 30 min in 120 mM final concentration of different buffers (pH 4.5 ~ 10.5). The buffers used were acetate (pH 4.5–6.0), potassium phosphate (pH 6.0–8.0), Tris-HCl (pH 7.5–8.5), and glycine-NaOH (pH 8.5–10.5).

2.3 RESULTS

2.3.1 Identification of residues associated with substrate binding

The 3D structure of any CDH protein is unknown at present. Thus, the search for a structure with the closest paralog with Xt-CDH and Rs-CDH led to h-HAD (Barycki et al., 2000). Based on this evidence, the h-HAD was taken as a template for Rs-CDH and Xt-CDH homology model structures. The amino acid sequence of Xt-CDH displayed 28% identity and 47% similarity when aligned with that of h-HAD, whereas Rs-CDH exhibited 24% identity and 42% similarity with h-HAD (Fig. 2.1). In addition, all these enzymes (h-HAD, Xt-CDH and Rs-CDH) have strict NAD^+ cofactor specificity (Barycki et al., 2000; Mori et al., 1988a; Mori et al., 1994). The three-dimensional models of Rs-CDH and Xt-CDH were automatically built using SWISS-MODEL server. The structures of the enzymes belong to this family consist of two distinct domains: a large N-terminal domain in NAD^+ binding; and a small C-terminal domain, which is involved in substrate recognition and positioning. In the h-HAD structure, several residues surround the acetoacetyl moiety of the substrate (Fig. 2.1). These residues were compared to their corresponding residues in the primary structure of Xt-CDH and Rs-CDH. Seven residues namely the residues Lue157, Phe160, Gly204, Ile206, Val207, Gly239, and Ala240 were different between Xt-CDH and Rs-CDH (Fig. 2.2). These residues matched Gly140, Phe143, Gly188, Ile190, Ala191, Gly223, and Ala224 of Xt-CDH, which correspond to Ala137, Tyr140, Ala185, Val187, Gly188, Ser220, and Phe221 in Rs-CDH (Fig. 2.3).

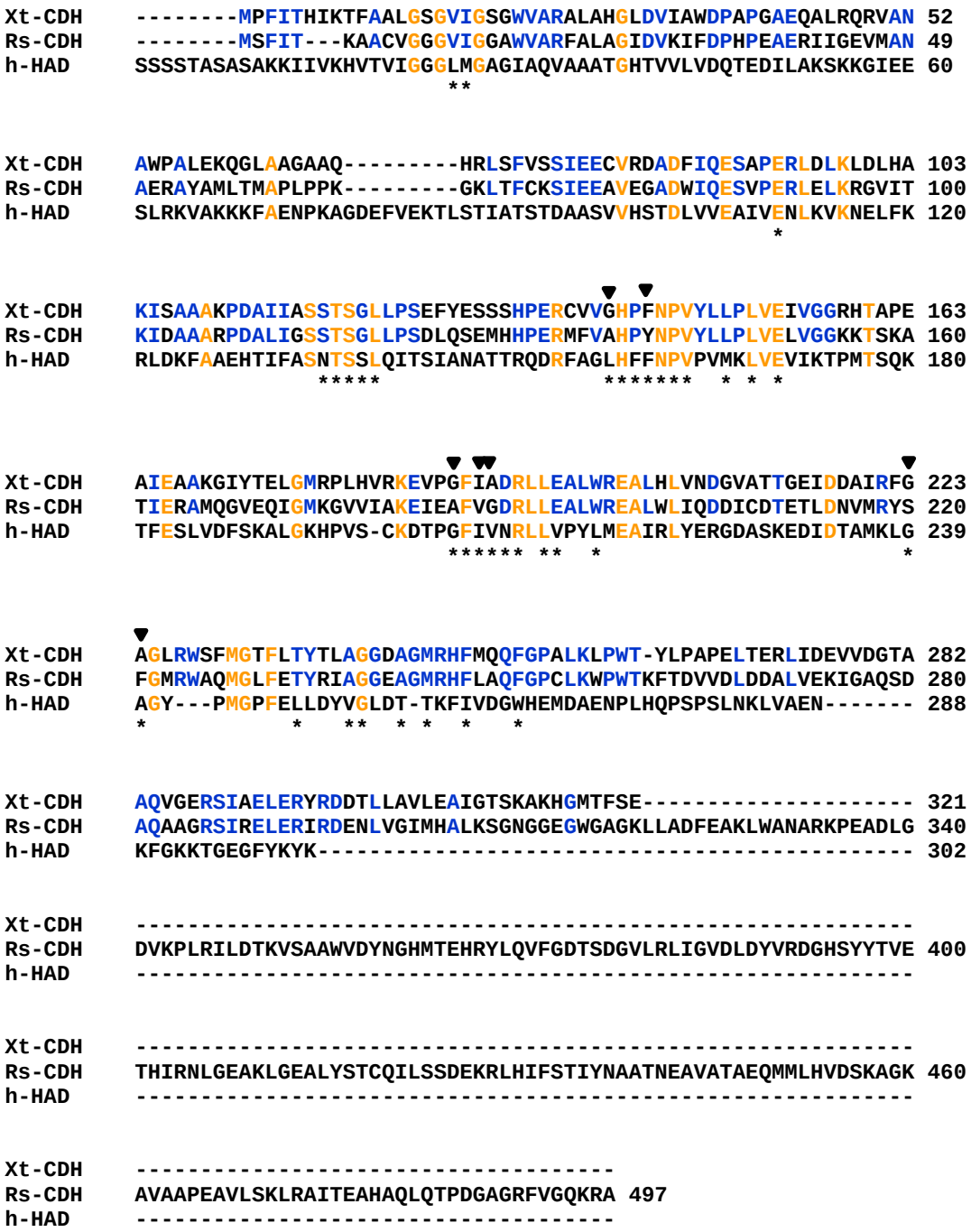

Fig. 2.1 Alignment of primary structures of Xt-CDH, Rs-CDH, and h-HAD. Multiple sequence alignments were performed using the CLUSTAL algorithm. Xt-CDH is CDH from *Xanthomonas translucens*, Rs-CDH is CDH from *Rhizobium* sp., h-HAD is human 3-hydroxyacyl-CoA dehydrogenase. The residues conserved in all sequences are indicated in orange. The residues conserved in CDHs are shown in blue. The residues placed around acetoacetyl moiety of h-HAD are denoted with an asterisk (*). The black arrowhead (▼) shows the residues involved in the mutagenesis study.

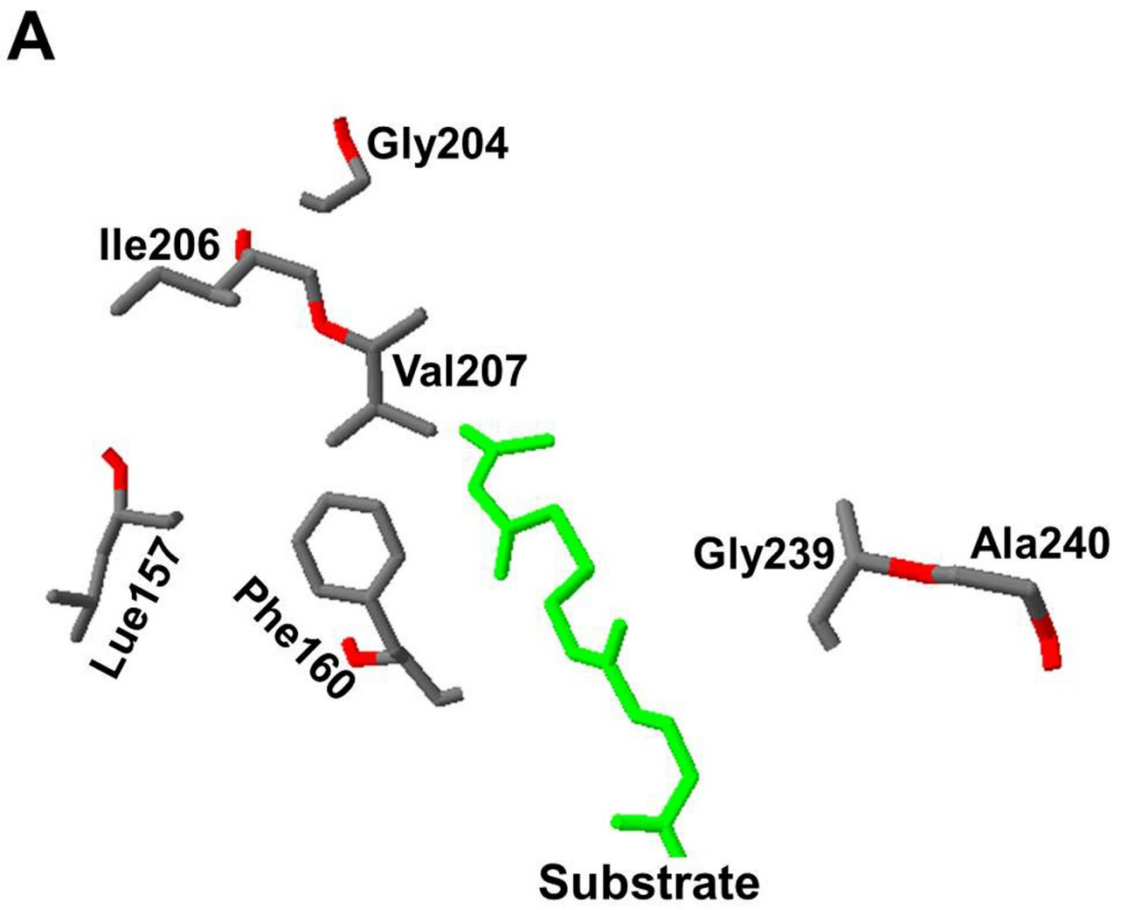

B

```
Xt-CDH   PERCVVGHPFNPVYLLPLVEIVGGRHTAPEAIEAAKGIYTELGMRP 179
Rs-CDH   PERMFVAHPYNPVYLLPLVELVGGKKTSKATIERAMQGVEQIGMKG 176
h-HAD    QDRFAGLHFFNPVPVMKLVEVIKTPMTSQKTFESLVDFSKALGKHP 196

Xt-CDH   LHVRKEVPGFIADRLLEALWREALHLVNDGVATTGEIDDAIRFGAG 225
Rs-CDH   VVIAKEIEAFVGDRLLEALWREALWLIQDDICDTETLDNVMRYSFG 222
h-HAD    VS-CKDTPGFIVNRLLVPYLMEAIRLYERGDASKEDIDTAMKLGAG 241
```

Fig. 2.2 Local structure of h-HAD around the bound substrate (acetoacetyl-CoA) and alignment of h-HAD, Rs-CDH, and Xt-CDH sequences around mutated amino acid residues. (A) Selected amino acids and the bound substrate are presented as a stick model. The amino acids are shown in gray and red. The bound substrate is shown in green. (B) The corresponding mutated amino acids in Rs-CDH and Xt-CDH are indicated by black arrowheads.

2.3.2 Substitution of the residues affects substrate affinity

To screen the residues important for catalytic activity and substrate affinity, we substituted the amino acid residues selected from Xt-CDH and its corresponding Rs-CDH using site-directed mutagenesis. Six single mutants were constructed, designated as Xt-G140A, Xt-F143Y, Xt-G188A, Rs-A137G, Rs-Y140F, and Rs-A185G. Additionally, we prepared four double mutants of neighboring residues, designated as

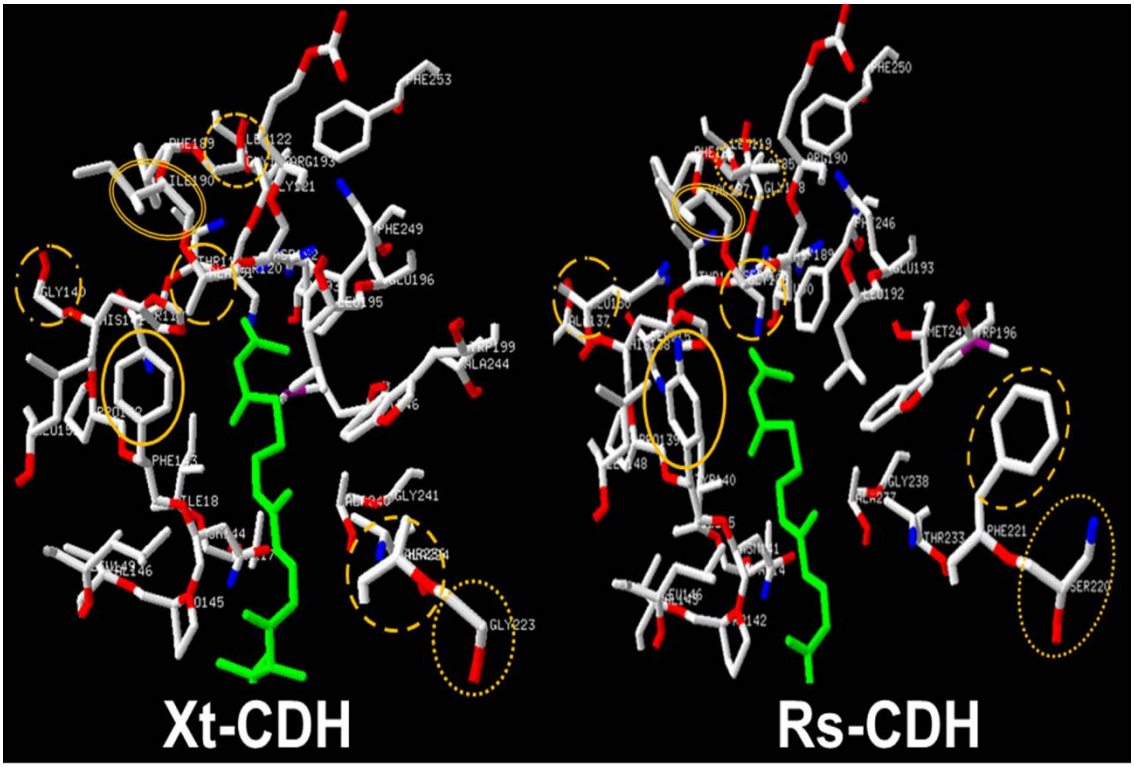

Fig. 2.3 Local structure of Xt-CDH and Rs-CDH around bound substrate. The structures were based on the homology model using h-HAD (PDB code: 1F0Y). Predicted structures were superimposed to the crystal structure of h-HAD. Selected amino acid residues and bound substrate are indicated as a stick model. Oxygen and nitrogen atoms of Rs-CDH and Xt-CDH active sites residues are depicted in red and blue, respectively. The different residues of CDHs active sites are circled with yellow circle. Each corresponding residues are indicated using same line properties.

Xt-I190V/A191G, Xt-G223S/A224F, Rs-V187I/G188A and Rs-S220G/F221A, to examine the roles of the residue sets in the catalytic ability. Wild-type and mutant recombinant enzymes were expressed in *E. coli* JM109 strains and verified using a 12% SDS-PAGE. All mutant enzymes showed a clear CDHs band comparable to that of wild-type (Rs-CDH and Xt-CDH) except that of Rs-A137G mutant (Fig. 2.4). However, evaluation o f CDH activity revealed that Rs-A137G mutant was inactive. Therefore, estimation the roles of Rs-A137G mutant and its corresponding mutant in Xt-CDH (Xt-G140A) on catalytic function and substrate binding did not pursued. Successfully expressed recombinant mutant enzymes were purified using amylose resin affinity

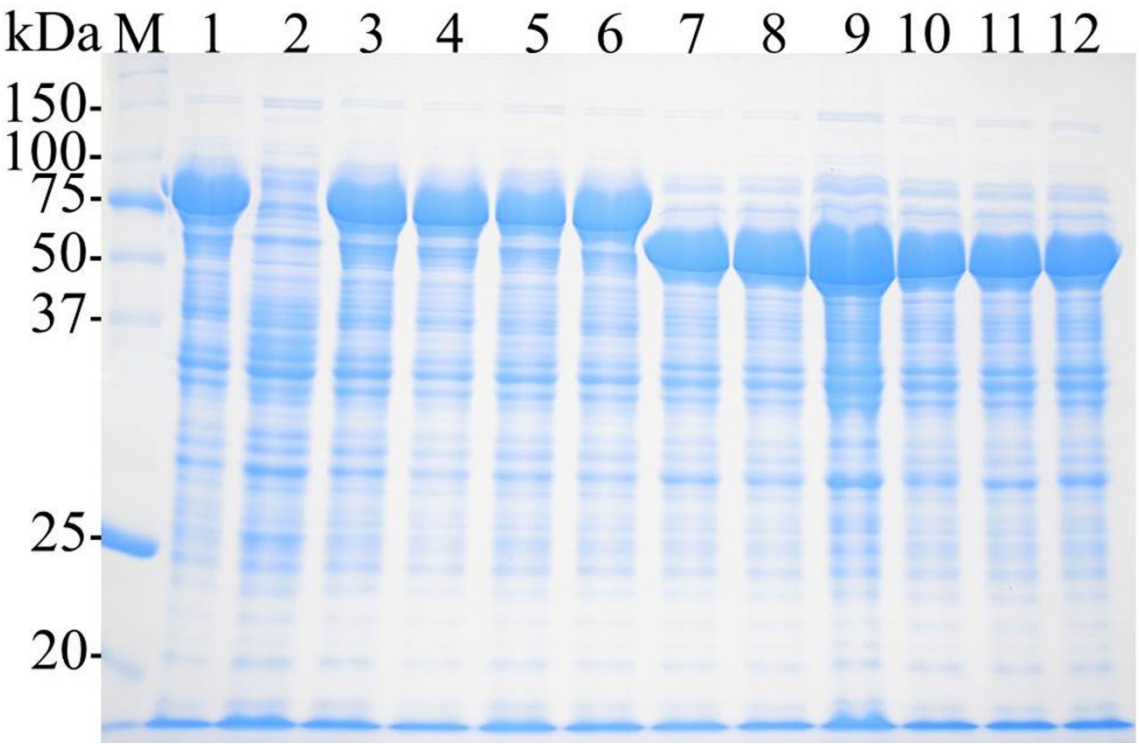

Fig.2.4 SDS-PAGE of cell free extract of Xt-CDH, Rs-CDH and their corresponding mutant enzymes. Crude enzymes were loaded into a 12% gel. M, protein molecular marker; Lane1, Rs-CDH; 2, Rs-A137G; 3, Rs-Y140F; 4, Rs-A185G; 5, Rs-V187I/G188A; 6, Rs-S220G/F221A; 7, Xt-CDH; 8, Xt-G140A; 9, Xt-F143Y; 10, Xt-G188A; 11, Xt-I191V/A191G; 12, Xt-G223S/A224F. The gel was stained with Coomassie Brilliant Blue.

chromatography (New England Biolabs Inc.).As reported previously (Arima et al., 2010), we tried to remove the fused MBP from CDHs with factor Xa, but inactivation was observed in all recombinant enzymes as a result of long incubation at room temperature (> 6 h). The presence of MBP attached to recombinant CDHs did not

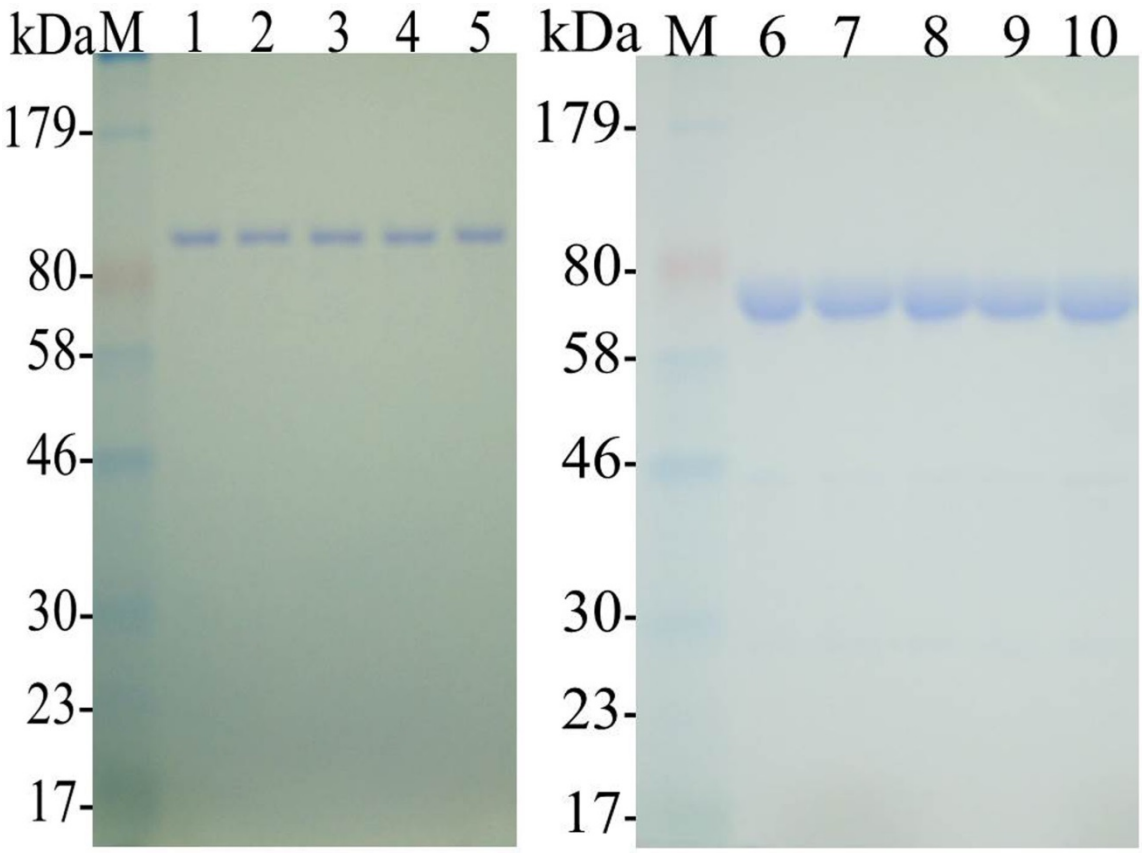

Fig.2.5 SDS-PAGE of purified Xt-CDH, Rs-CDH and their corresponding mutant enzymes. Purified enzymes were loaded into a12% gel. M, protein molecular marker; lane1, Rs-CDH; 2, Rs-Y140F; 3, Rs-A185G; 4, Rs-V187I/G188A; 5, Rs-S220G/F221A; 6, Xt-CDH; 7, Xt-F143Y; 8, Xt-G188A; 9, Xt-I191V/A191G; 10, Xt-G223S/A224F. The gels were stained with Coomassie Brilliant Blue.

influence the substrates affinity (i.e. K_m values of L-Car and cofactor NAD^+) of either enzyme (Mori et al., 1988a; Mori et al., 1994; Armia et al., 2010). Therefore, Xt-CDH, Rs-CDH and mutant enzymes were produced and characterized as fusion proteins with MBP. Purified Xt-CDH and Rs-CDH mutants showed a single protein band on SDS-PAGE (Fig. 2.5) comparable to that of apparent MW of Xt-CDH (37 kDa) and Rs-CDH (50 kDa) plus fused MBP (40 kDa).

2.3.3 Enzyme activity of Rs-CDH and Xt-CDH corresponding mutants

Catalytic activities of CDHs were determined using spectrophotometric method under optimal reaction conditions for the wild-types enzymes (Table 2.4). Specific activity of wild-types and mutant enzymes were performed and summarized in Fig. 2.6. Conversion of Tyr140 in Rs-CDH to Phe did not appreciably affect enzyme activity. This mutant enzyme (Rs-Y140F) showed 16.78 µmol min^{-1} mg^{-1} specific activity which is comparable to what was observed for Rs-CDH (17.33 µmol min^{-1} mg^{-1}). Similar approaches were observed for other two Rs-CDH mutants (Rs-A185G and Rs-S220G/F221A). However, instantaneous replacement of Val187 and G188 in Rs-CDH to Ile and Ala, respectively eliminated detectable Rs-CDH activity. In contrast to what was observed for Rs-CDH mutants, single and double mutants of Xt-CDH significantly attenuated CDH activity. Of them, the specific activities of Xt-F143Y and Xt-G223S/A224F were 1.28 and 1.76 µmol min^{-1} mg^{-1}, respectively, which are equivalent to 12.9 – 9.3 folds lower activity than that of Xt-CDH (16.48 µmol min^{-1} mg^{-1}).

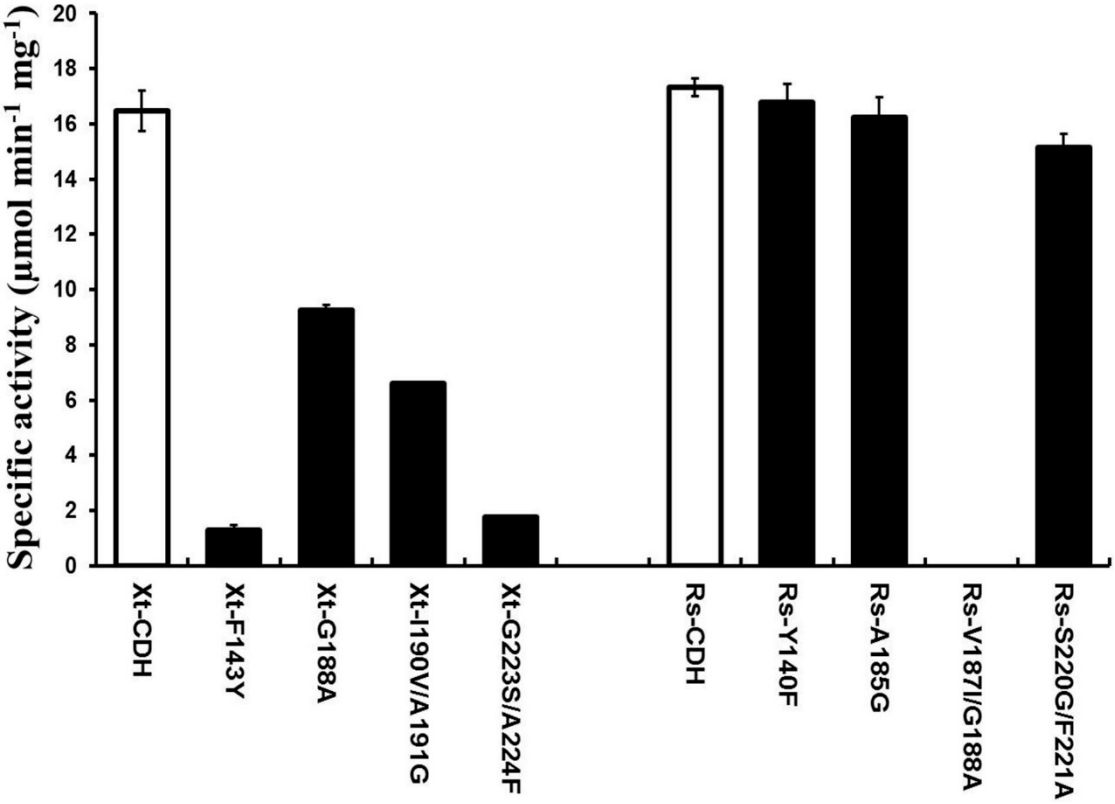

Fig.2.6 Specific activity of purified Rs-CDH, Xt-CDH, and corresponding mutants. CDH activity was measured using the standard condition described in *Material and Methods*. The values of specific activity are mean ± SD of three values.

2.3.4 Kinetic analysis of Rs-CDH and Xt-CDH corresponding mutants

The results obtained for K_m and k_{cat} for both L-Car and NAD^+ of the wild-type and mutant proteins are presented in Table 2.5, which shows that almost no variant significantly disrupted the NAD^+ affinity. In particular, the K_m values for NAD^+ of Xt-F143Y, Xt-I190V/A191G, Xt-G223S/A224F were found to be 0.32, 0.27, 0.24 mM, respectively, which is similar to that of Xt-CDH (0.32 mM). Similarly, substitution of correspond residues in Rs-CDH (Rs-Y140F, Rs-A185G and Rs-S220G/F221A) revealed proteins with K_m values for NAD^+ (0.11 – 0.15 mM) comparable to that of native enzyme. In contrast to the cofactor, these mutants showed different effects on L-Car affinity. A mutant with two simultaneous substitutions in Rs-CDH

Table 2.5 Kinetic constants of Rs-CDH, Xt-CDH and corresponding mutants

Enzyme	K_m (mM)		k_{cat} (s^{-1})	Enzyme	K_m (mM)		k_{cat} (s^{-1})
	L-Car	NAD^+			L-Car	NAD^+	
Rs-CDH	1.07 ± 0.06	0.09[a]± 0.01	11.77 ± 0.68	Xt-CDH	10.38 ± 0.36	0.32[a]± 0.01	1.97 ± 0.03
Rs-Y140F	1.61 ± 0.04	0.13[a]± 0.01	9.80 ± 0.53	Xt-F143Y	137.03 ± 1.93	0.32[b]± 0.02	0.05 ± 0.00
Rs-A185G	1.72 ± 0.02	0.15[a]± 0.02	6.03 ± 0.22	Xt-G188A	8.68 ± 0.33	0.44[a]± 0.04	1.19 ± 0.07
Rs-V187I/G188A	ND	ND	ND	Xt-I190V/A191G	87.15 ± 2.67	0.27[b]± 0.02	0.37 ± 0.01
Rs-S220G/F221A	1.21 ± 0.09	0.11[a]± 0.01	11.36 ± 0.77	Xt-G223S/A224F	96.20 ± 3.24	0.24[b]± 0.03	0.18 ± 0.01

K_m and k_{cat} were calculated from a linear regression fit to the Michaelis–Menten equation, using initial estimates from double reciprocal plots. The K_m for L-Car was evaluated at final concentration of 0.8–600 mM L-Car and 2 mM NAD^+. K_m for NAD^+ was measured at NAD^+ final concentration of 0.06–2 mM and L-Car concentration of (a) 12 mM and (b) 300 mM. The values are means ± standard deviations for three independent experiments.

ND: not detectable

(Rs-V187I/G188A) produced a protein devoid of CDH activity. Therefore, studies of its properties and kinetics parameters were not pursued. In contrast, the corresponding double mutant Xt-I190V/A191G caused 8.5-fold higher K_m relative to wild-type. For single mutants, the corresponding Rs-A185G and Xt-G188A retained K_m values of 1.72 and 8.68 mM, respectively, which are comparable to that of wild-type. Likewise, the replacement of the aromatic residue Tyr140 in Rs-CDH with Phe also produced an enzyme with kinetic properties (K_m value of 1.61 mM) similar to the native enzyme. Interesting results were obtained for its corresponding mutants Xt-F143Y, which produced the highest increase in the K_m value (137 mM) compared to that of Xt-CDH (10.4 mM). The presence of hydroxyl group on aromatic amino acid at position 143 in Xt-F143Y is responsible for the loss of affinity toward L-Car. Therefore, Phe143 of Xt-CDH and its corresponding in Rs-CDH (Tyr140) were selected for additional investigation.

2.3.5 Characterization of F143Y Xt-CDH and Y140F Rs-CDH

To probe whether addition or elimination of hydroxyl group as a result of Xt-F143Y or Rs-Y140F variants influenced catalytic environment and protein stability, we evaluated the pH activity profile and thermal stability of Xt-F143Y and Rs-Y140F. The plot of enzyme activity as a function of pH measured at 30°C showed that replacement of Phe143 in Xt-CDH with Tyr shifted the optimum pH from 9.5 to 8.0 (Fig. 2.7). In contrast, the corresponding mutant Rs-Y140F exhibits a similar pH profile of Rs-CDH. Furthermore, we evaluated the pH stability of Xt-CDH, Xt-F143Y, Rs-CDH and Rs-Y140F using different buffers (pH 4.5 – 10.5). Xt-F143Y retained about 70% of its initial activity after incubation for 30 min at pH 4.5 (Fig 2.8). This activity at lower pH contrasts with the sharp decrease in pH stability profile shown by Xt-CDH,

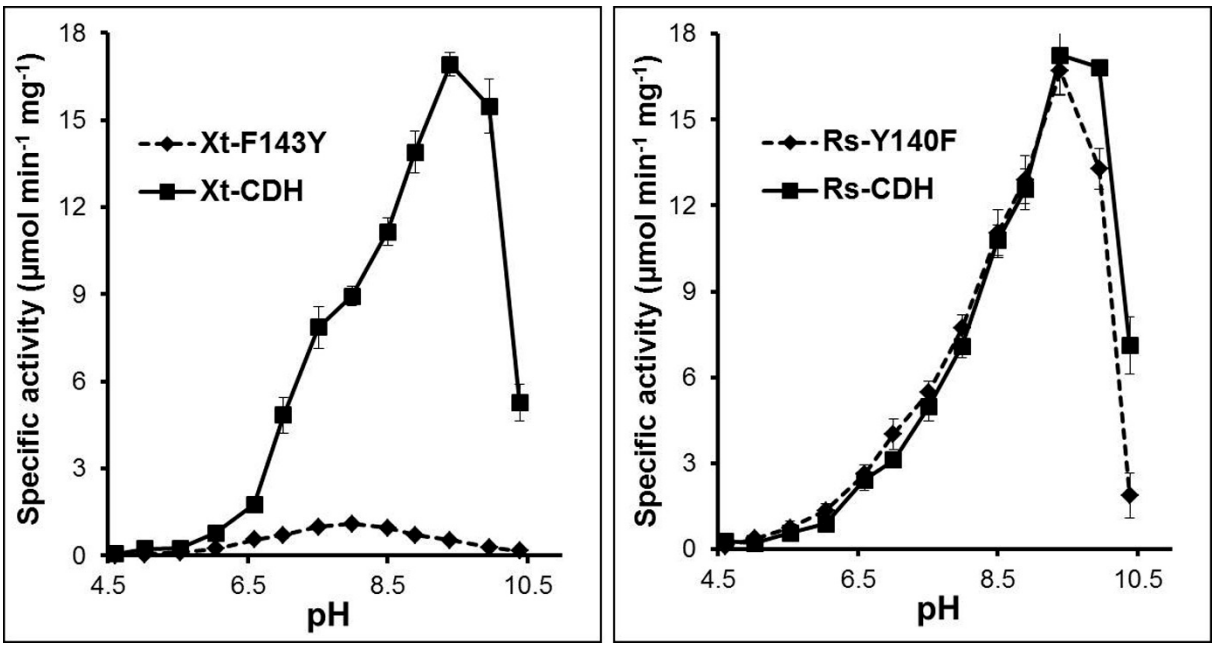

Fig. 2.7 pH profile of Xt-CDH, Rs-CDH, Xt-F143Y and Rs-Y140F enzymes. Enzyme activity was estimated under standard conditions as described in *Materials and Methods*, except that the following buffers were used in the reaction mixture at the final concentration of 120 mM (buffers: acetate (pH 4.5 – 6.0), potassium phosphate (pH 6.0 – 8.0), Tris-HCl (pH 7.5 – 8.5), glycine-NaOH (pH 8.5 – 10.5)).

which retained only 14% of the activity. However, this variation in residual activity at lower pH was not observed with Rs-Y140F mutant.

An unexpected change was also observed on the thermal stability profile when the wild-type and mutant enzymes were incubated for 30 min at different temperatures (15–55 °C). The residual activity profiles presented in Fig. 2.9 showed that Rs-Y140F was stable up to 40 °C (99%) and Rs-CDH exhibited lower thermal stability (29%) at same temperature. In contrast, heating of Xt-CDH at identical range of temperature (15–55 °C) showed constant CDH activity up to 45 °C (100%) compared to that of Xt-F143Y (3.1%).

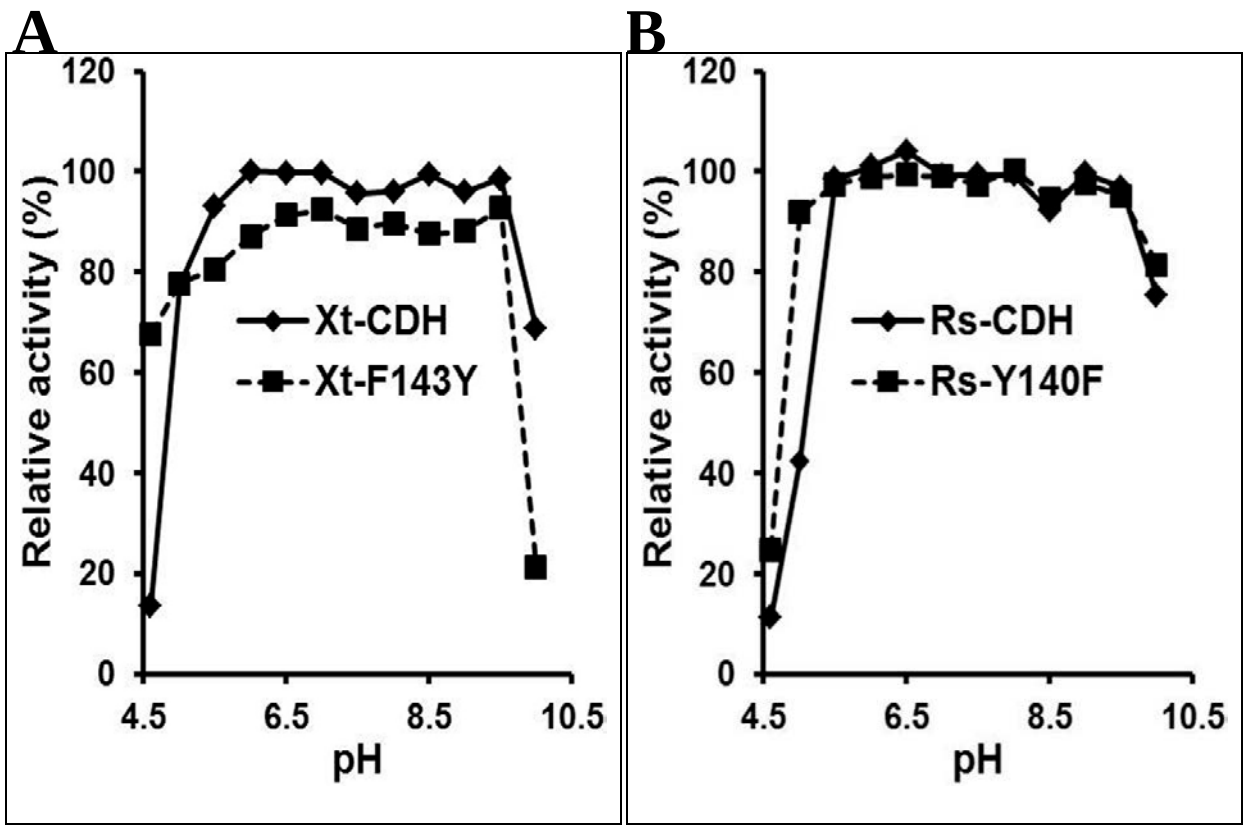

Fig. 2. 8 pH stability of wild-type forms of Xt-CDH and Rs-CDH, Xt-F143Y, and Rs-Y140F enzymes. Enzyme activity was estimated under standard conditions as described in *Materials and Methods*, after incubation of CDHs for 30 min at 30°C using the following buffers at the final concentration of 120 mM (buffers: acetate (pH 4.5 – 6.0), potassium phosphate (pH 6.0 – 8.0), Tris-HCl (pH 7.5 – 8.5), glycine-NaOH (pH 8.5 – 10.5)).

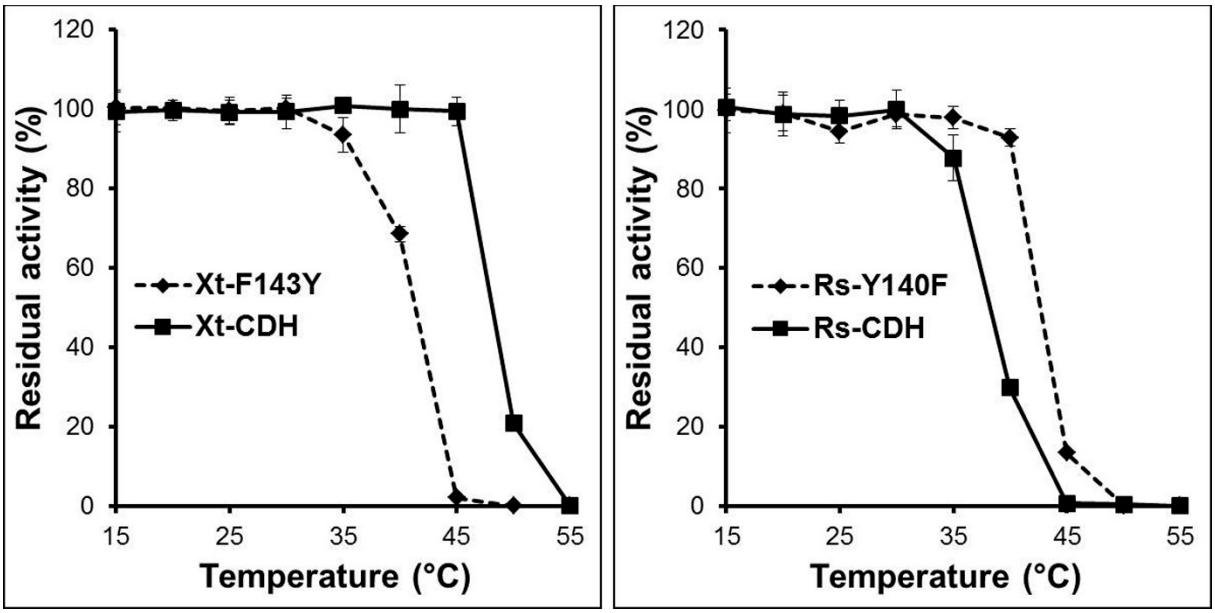

Fig. 2.9 Effect of temperature on CDH activity of wild-type forms of Xt-CDH and Rs-CDH, Xt-F143Y and Rs-Y140F. Residual activities were determined using standard conditions described in *Materials and Methods* section. Enzymes were incubated for 30 min at different temperatures (15 – 55°C). The values are means ± standard deviations for three independent experiments.

2.3.6 Phenyl ring is essential for CDH substrate recognition

To elucidate the role of Rs-Y140 and Xt-F143 aromatic ring on the activity and substrate binding of Xt-CDH and Rs-CDH, both residues were replaced with another nine amino acids having different properties (Ala, Gly, Trp, His, Lys, Asp, Asn, Ser, and Cys). The validated mutant plasmids were introduced into the *E. coli* JM109 and expressed using identical conditions to that of wild-type. A total of 18 mutants enzymes were successfully expressed after addition of IPTG. The expressions of mutant enzymes were verified using 12% SDS PAGE. After cultivation, the mutant enzymes were purified using amylose resin and showed a clear single band, which indicated that both expression and purification means are successful (Fig. 2.10). The catalytic properties of Rs-Y140 and Xt-F143 mutants are presented in Fig. 2.11 and Table 2.6.

The substitution of Phe143 residue in Xt-CDH by alanine produced a protein with a very low CDH activity (<1.5% of Xt-CDH). Its substrate affinity was 34-fold lower than that of Xt-CDH (Table 2.6). On the other hand, estimation of the specific activity of Rs-Y140A using identical substrate concentration to that of Rs-CDH (L-Car of 12 mM) was undetectable. The data underscore the importance of both residues (Rs-Y140 and Xt-F143), particularly their phenyl ring in the catalytic mechanism of Xt-CDH and Rs-CDH. Moreover, the introduction of the small sized nonpolar residue Gly at position 140 in Rs-CDH produced an inactive enzyme. Similar influence was observed with that of corresponding mutants in Xt-CDH (Xt-F143G). The specific activity of Xt-F143G was found to be 0.03 μmol min^{-1} mg^{-1}, which is equivalent to 549-fold lower activity than that of wild-type. In contrast, aromatic residue mutant Rs-Y140W, which has an indole in its side chain, retains 30% CDH activity of Rs-CDH. The k_{cat} of this mutant (0.236 s^{-1}) was dramatically lower than that of Rs-CDH (11.77 s^{-1}). Two mutants in Rs-CDH were detected to be defective in K_m and k_{cat}: Mutants Rs-Y140S and Rs-Y140C. The specific activities of Rs-Y140C and Y140S were respectively 0.11 and 0.05 μmol min^{-1} mg^{-1}. Their K_m was 292 – 308-folds higher values than that of wild-type. Furthermore, conversion of Rs-Y140 to Asp, His, Lys and Asn were also eliminated detectable CDH activity. Increasing of the substrate concentration in the assay mixture did not influence catalytic activity of these mutant enzymes. However, the specific activity data in Fig. 11a reveal that Xt-F143 mutants had different influences compared to corresponding Rs-Y140 variants in Rs-CDH. The introduction of aromatic amino acid Trp or Tyr instead of Phe143 was insufficient to retain CDH activity as it occurred in Rs-CDH. In particular, Xt-F143W mutant was inactive CDH variant. The polarity and the negative charge of an Asp residue (Xt-F143D) in this position were found to have a similar effect. Other Xt-F143 (Ser, Cys, Asn, Lys, and His) mutant enzymes exhibited much

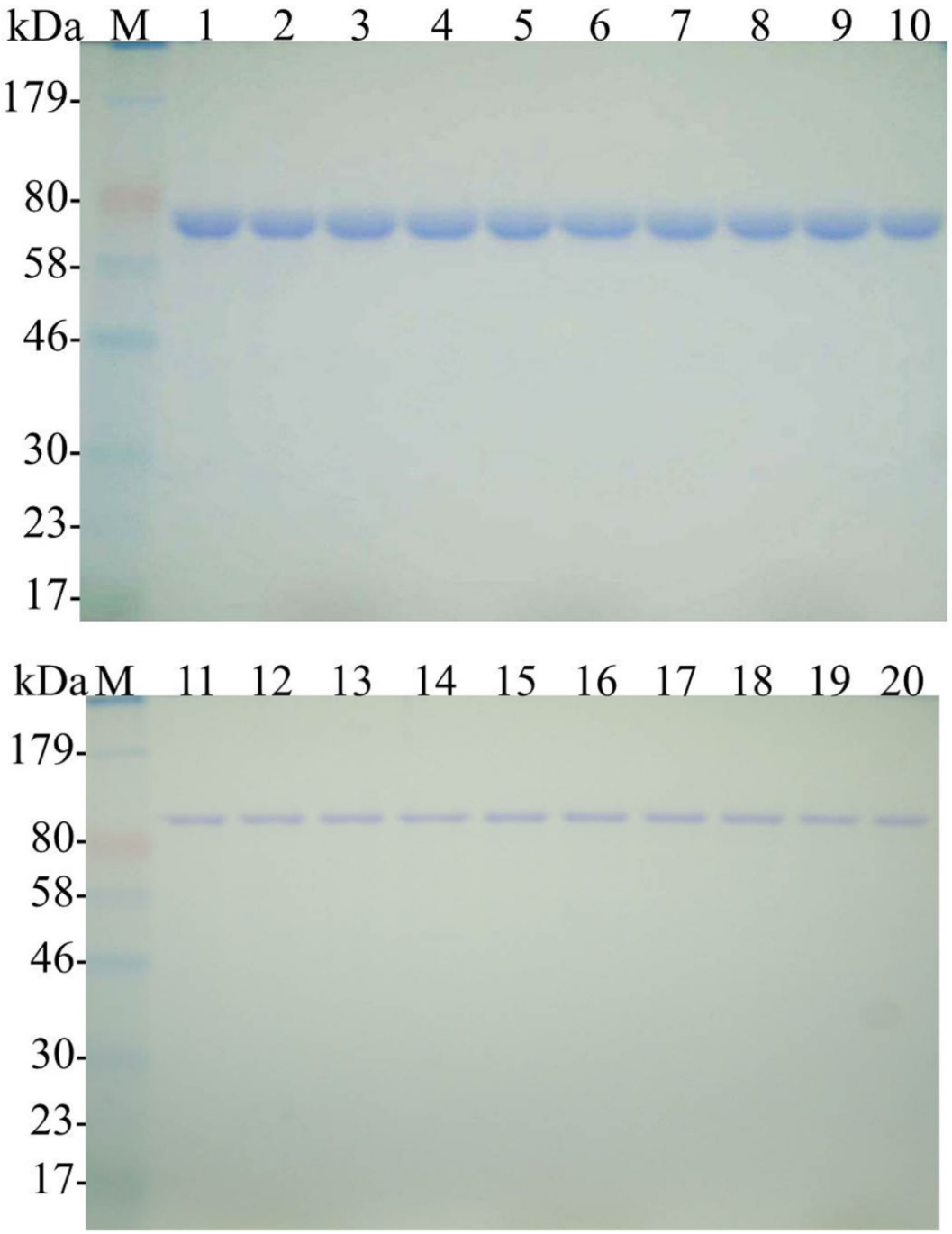

Fig. 2.10 SDS-PAGE of purified Xt-CDH, Rs-CDH, Xt-F143X and Rs-Y140X enzymes. Purified proteins were loaded into 12% gel. M, protein molecular marker; lane 1, Xt-CDH; 2, Xt-F143A; 3, Xt-F143G; 4, Xt-F143H; 5, Xt-F143C; 6, Xt-F143S; 7, Xt-F143W; 8, Xt-F143N; 9, Xt-F143K; 10, Xt-F143D; 11, Rs-CDH; 12, Rs-Y140A; 13, Rs-Y140G; 14, Rs-Y140H; 15, Rs-Y140C; 16, Rs-Y140S; 17, Xt-F143W; 18, Rs-Y140N; 19, Rs-Y140K; 20, Rs-Y140D. The gel was stained with Coomassie Brilliant Blue.

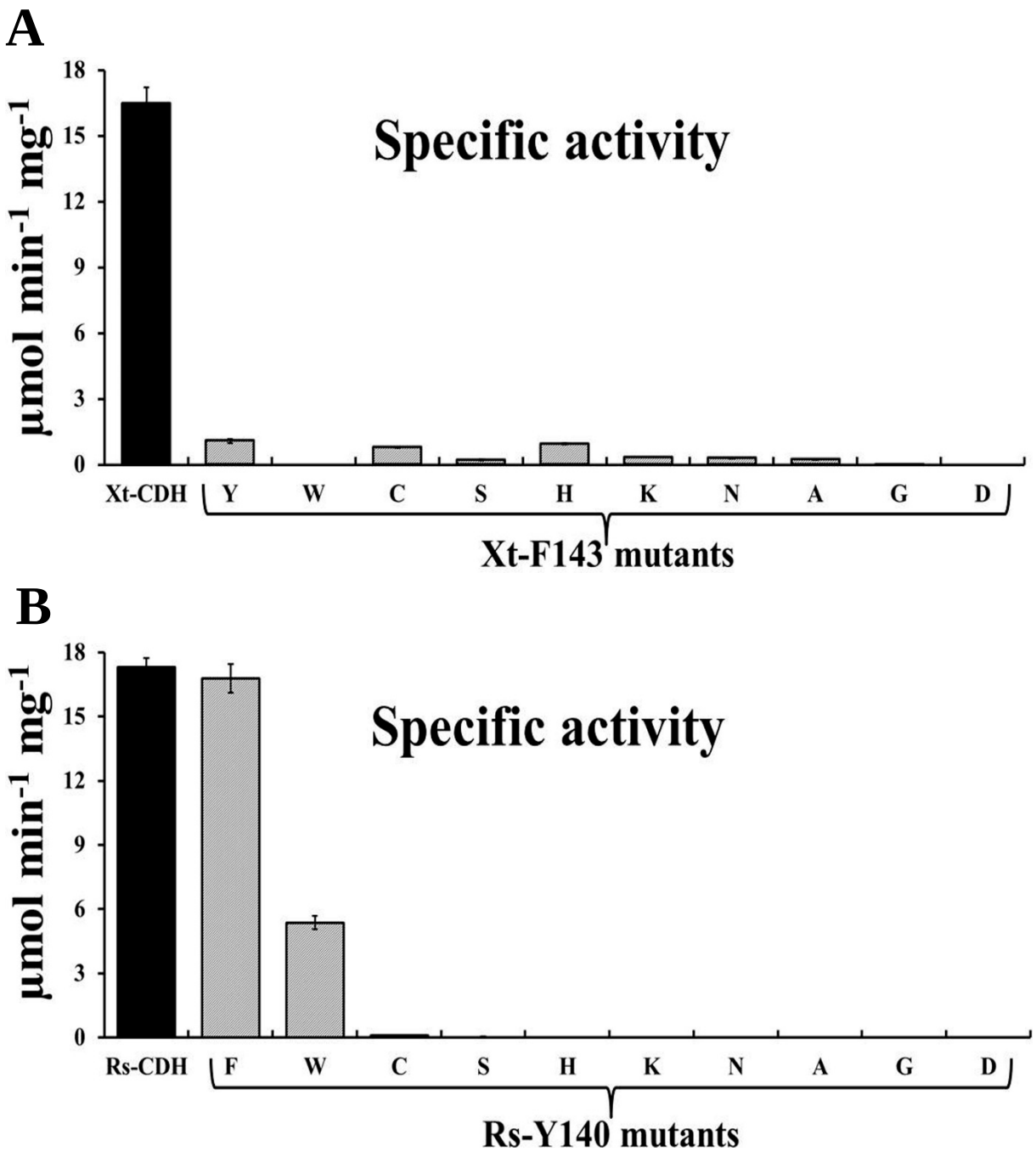

Fig 2.11 Specific activity of purified wild-type forms of Xt-CDH, Rs-CDH, Xt-F143 and Rs-Y140 mutant enzymes. (A) Specific activity of Xt-F143 mutants and (B) specific activity of Rs-Y140 mutants. Enzyme activity was measured using standard conditions described in *Materials and Methods*. The values of enzymes activity are means ± standard deviations for three independent experiments.

lower catalytic activity (0.03–1.2 μmol min^{-1} mg^{-1}) than that of Xt-CDH (16.48 μmol min^{-1} mg^{-1}). The CDH activity of Xt-F143H (0.95 μmol min^{-1} mg^{-1}), Xt-F143C (0.79 μmol min^{-1} mg^{-1}), Xt-F143K (0.34 μmol min^{-1} mg^{-1}), Xt-F143N (0.3 μmol min^{-1} mg^{-1}) and Xt-F143S (0.21 μmol min^{-1} mg^{-1}) decreased in this order. Moreover, K_m values measured for Xt-F143 mutants (Table 2.6) were drastically higher (13–284 fold) than that of Xt-CDH.

2.4 DISCUSSION

Although CDH was proposed earlier as an excellent tool for the production and measurement of the important nutrient L-Car (Schopp and Schafer, 1985), no structural information is available for this enzyme. In previous reports (Mori et al., 1988a; Mori et al., 1994), two CDHs were purified and characterized from soil isolate bacteria. They designated as Xt-CDH and Rs-CDH. They exhibited different affinity to L-Car. The K_m value of Xt-CDH (10 mM) was 10 fold higher than that of Rs-CDH (1.0 mM) (Mori et al., 1988a; Arima et al., 2010). This fact affords an excellent opportunity to elucidate the effective amino acids responsible for the affinity of CDH to L-Car. Using the alignment of Xt-CDH and Rs-CDH primary structure with the known 3D structure of h-HAD, we observed seven different residues between Xt-CDH and Rs-CDH. They are active site residues in h-HAD (Figs. 2.1 and 2.2). Therefore, we investigated the involvement of these residues in the structure–function relation of CDHs by replacing the residues of Xt-CDH (Gly140, Phe143, G188, Ile190, Ala191, Gly223, and Ala224) with the residues that occur in Rs-CDH (Ala137, Tyr140, Ala185, Val187, Gly188, Ser220, and Phe224) at the corresponding position (Fig. 2.3).

Table 2.6 Kinetic parameters of Xt-F413 and Rs-Y140 mutants

Enzyme	K_m (mM)		k_{cat} (s^{-1})	Enzyme	K_m (mM)		k_{cat} (s^{-1})
	L-Car	NAD^+			L-Car	NAD^+	
Rs-CDH	1.07 ± 0.06	0.09[a] ± 0.01	11.77 ± 0.682	Xt-CDH	10.38± 0.36	0.32[a] ± 0.01	1.97 ± 0.035
Rs-Y140F	1.61 ± 0.04	0.13[a] ± 0.01	9.796 ± 0.530	Xt-F143Y	137.03 ± 1.93	0.32[c] ± 0.02	0.051 ± 0.001
Rs-Y140W	18.66 ± 0.82	0.24[b] ± 0.01	0.236 ± 0.009	Xt-F143W	ND	ND	ND
Rs-Y140C	313.57 ± 8.16	0.25[d] ± 0.03	0.010 ± 0.001	Xt-F143C	144.91 ± 5.86	0.33[c] ± 0.03	0.051 ± 0.002
Rs-Y140S	330.08 ± 4.91	0.21[d] ± 0.02	0.003 ± 0.000	Xt-F143S	723.41 ± 23.22	0.42[e] ± 0.03	0.006 ± 0.000
Rs-Y140H	ND	ND	ND	Xt-F143H	240.26 ± 5.29	0.33[d] ± 0.01	0.039 ± 0.002
Rs-Y140K	ND	ND	ND	Xt-F143K	321.48 ± 5.35	0.88[d] ± 0.05	0.016 ± 0.002
Rs-Y140N	ND	ND	ND	Xt-F143N	477.76 ± 9.16	0.34[d] ± 0.01	0.017 ± 0.001
Rs-Y140A	ND	ND	ND	Xt-F143A	353.76 ± 22.50	0.36[d] ± 0.01	0.007 ± 0.001
Rs-Y140G	ND	ND	ND	Xt-F143G	2955.04 ± 81.35	0.37[f] ± 0.01	0.002 ± 0.000
Rs-Y140D	ND	ND	ND	Xt-F143D	ND	ND	ND

K_m and k_{cat} were calculated from a linear regression fit to the Michaelis–Menten equation, using initial estimates from double reciprocal plots. The K_m for L-Car was evaluated at final concentration of 0.8–2000 mM L-Car and 2 mM NAD^+. K_m for NAD^+ was measured at NAD^+ final concentration of 0.06–2 mM and L-Car concentration of a, 12 mM; b, 100 mM; c, 300 mM; d, 600 mM; e, 900 mM; and f, 2000 mM. The values are means ± standard deviations for three independent experiments.

ND: not detectable

Database analysis of amino acids sequences revealed that Xt-CDH and Rs-CDH are members of the family PF00725 containing two highly conserved domains: 3-hydroxyacyl-CoA N-terminal NAD^+ binding domain and 3-hydroxyacyl-CoA C-terminal domain (Birktoft et al., 1987). All amino acids analyzed in this study are regarded as placed near the substrate but distant from NAD^+. Therefore, we did not expect to have noticeable influences in NAD^+ affinity. Particularly, our findings were consistent with our earlier predictions. All constructed mutants at Xt-CDH and Rs-CDH showed K_m values for NAD^+ that were comparable to those of wild-type except the double mutant Rs-V187I/G188A (Table 2.5). This variant showed no CDH activity. Therefore, these residues appeared unambiguously to be necessary for Rs-CDH activity. The corresponding amino acids of these two residues in h-HAD are Ile206 and Val207, which are set in the active site, together with Glu170 these two amino acid residues produced a hydrogen bond interaction. The disruption of this interaction influenced the substrate binding of h-HAD (Barycki et al., 2001). Similarly, the corresponding double mutant Xt-I190V/A191G dramatically decreased catalytic activity (6.6 μmol min^{-1} mg^{-1}) and increased the K_m (87.15 mM) of Xt-CDH. This variation between the two double mutants in their reduction level was attributed to a less specific interaction between the substrate and neighboring residues as a consequence of the loss of hydrogen bond or the creation of completely different active site architecture. However, the difference in side chain length of Val187 and Gly188 in Rs-CDH compared to that of Ile190 and Ala191 in Xt-CDH might explain this variation in the catalytic activity and substrate binding. The kinetics data of Rs-S220G/F221A mutant suggested that Ser220 and Phe221 had no critical role in Rs-CDH. This effect differed from that of corresponding double mutant Xt-G223S/A224F. The aromatic character of Phe and hydroxyl group of Ser in the active site channel of Xt-CDH influenced substrate binding. This result fits

the critical role of corresponding Ala240 in h-HAD, which provides protein–substrate interaction via a bound water molecule (Barycki et al., 2001).

In terms of the enzyme kinetics for L-Car dehydrogenation, Xt-F143Y exhibited the greatest alteration compared to all other selected residues. Mutation did lead to a decrease in the catalytic and substrate affinity (~ 13 fold decrease), indicating that Phe143 does play a crucial role in catalysis and substrate binding. On the other hand, while the increase in the Michaelis constants of the Xt-F143Y suggests this residue is involved in L-Car binding, the results of its corresponding mutant in Rs-CDH (Rs-Y140F) indicated these homologies residues might play a role in catalysis. This brings us to the question what the role that these residues could play either in substrate binding and/or catalysis. Tyr and Phe are well known to have different p*K*a; the differences might be responsible for altering the pH in the catalytic environment. The change observed in the pH activity profile of Xt-F143Y (8.0) compared to that of Xt-CDH (9.5) (Fig. 2.7) is most probably attributable to a change in the catalytic environment p*K*a. This phenomenon was observed by Goldberg and co-workers (Goldberg et al., 1991) when the Tyr residue from the active site of the *E. coli* aspartate aminotransferase was mutated to Phe. The authors reported that the enzyme's preferred pH was shifted from 7.1 to 8.4. Furthermore, the introduction of the hydroxyl group in Xt-F143Y might create a new hydrogen bond between the hydroxyl group of Tyr and adjacent negatively charged residues. In such a condition, the p*K*a might also shift to the unfavorable value to allow the catalytic activity. Such interaction was observed with various enzymes when Phe was replaced with Tyr (Kanai et al., 2004). However, the steady kinetic analysis of Xt-CDH and Xt-F143Y were examined at pH 9.5, the pH at which maximum catalytic activity of wild-type was observed. In contrast, the pH profile Rs-CDH and Rs-Y140F (optimum pH of 9.5) were seen in a good agreement

with those of the native enzyme obtained from Mori and co-workers (Mori et al., 1994). The similar pH plot shape produced by Rs-Y140F and Rs-CDH indicated that the hydroxyl group of Tyr140 in Rs-CDH had no critical influence on the p*K*a value of catalytic process. The alignment of CDH proteins showed that Phe143 of Xt-CDH is conserved in all CDHs except in Rs-CDH (Mori et al., 1988b; Houriyou et al., 1993; Wargo et al., 2009; Arima et al., 2010) (Fig. 2.12). This fact might also explain the different influences produced by Xt-F143Y and Rs-Y140F on pH profile, specific activity, and substrate affinity.

Consistent with our assumption, further mutations at Tyr140 of Rs-CDH and Phe143 of Xt-CDH with various residues (Ala, Gly, His, Lys, Ser, Cys, Asn, Asp, and Trp) and the impact of the mutants on the specific activity and K_m values of Rs-CDH and Xt-CDH strongly support the hypothesis (Fig. 2.11 and Table 2.6) that the phenyl ring of aromatic residues at position 140 of Rs-CDH and 143 of Xt-CDH play a vital role in the catalytic activity and substrate binding. In Rs-CDH, only aromatic residues (Phe and Trp) instead of Tyr140 were able to retain CDH activity and substrate affinity (Fig. 2.11b). In contrast to what was observed for Rs-CDH, almost all mutants at the residue Phe143 of Xt-CDH, including Xt-F143Y and Xt-F143W, attenuated the specific activity (Fig. 2.11a) and dramatically increased the K_m value. However, Rs-Y140W mutant had 30% of Rs-CDH activity (Fig. 2.11b). The results indicate that the hydrophobicity of the aromatic ring is not the sole factor affecting substrate binding and that the size of the aromatic residue might also be considered. As shown in overall predicted structures of Rs-CDH and Xt-CDH (Fig. 2.13), Phe143 of Xt-CDH and Tyr140 of Rs-CDH are set just adjacent to the substrate. Therefore, the effects of the mutations described here (Xt-F143 and Rs-Y140 variants) indicate several roles of these residues. One possibility is that these aromatic residues are key residues

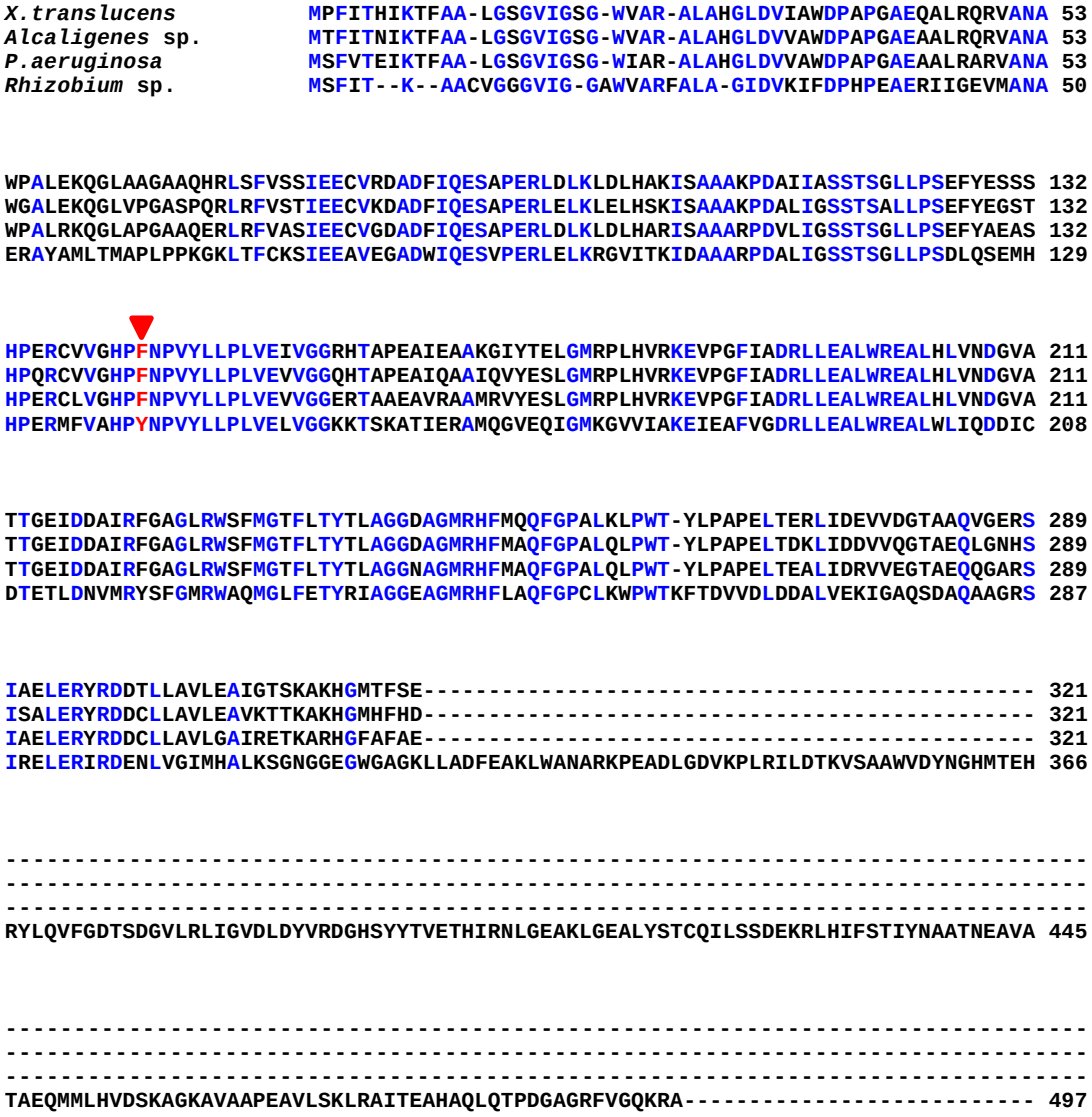

Fig. 2.12 Protein sequence alignment of L-carnitine dehydrogenases. Alignment was obtained using CLUSTALW. All protein sequences are full-length. Amino acid residues are expressed in one-letter codes and numbered in the right side of the alignment. Labels express the bacterial source of L-carnitine dehydrogenases, *X. translucens*, *Xthansomonas translucens*; *P. aeruginosa*, *Pseudomonas aeruginosa*. Residues that are conserved in all sequences are shown in blue. Phe143 of Xt-CDH and Tyr140 of Rs-CDH indicated using red arrow.

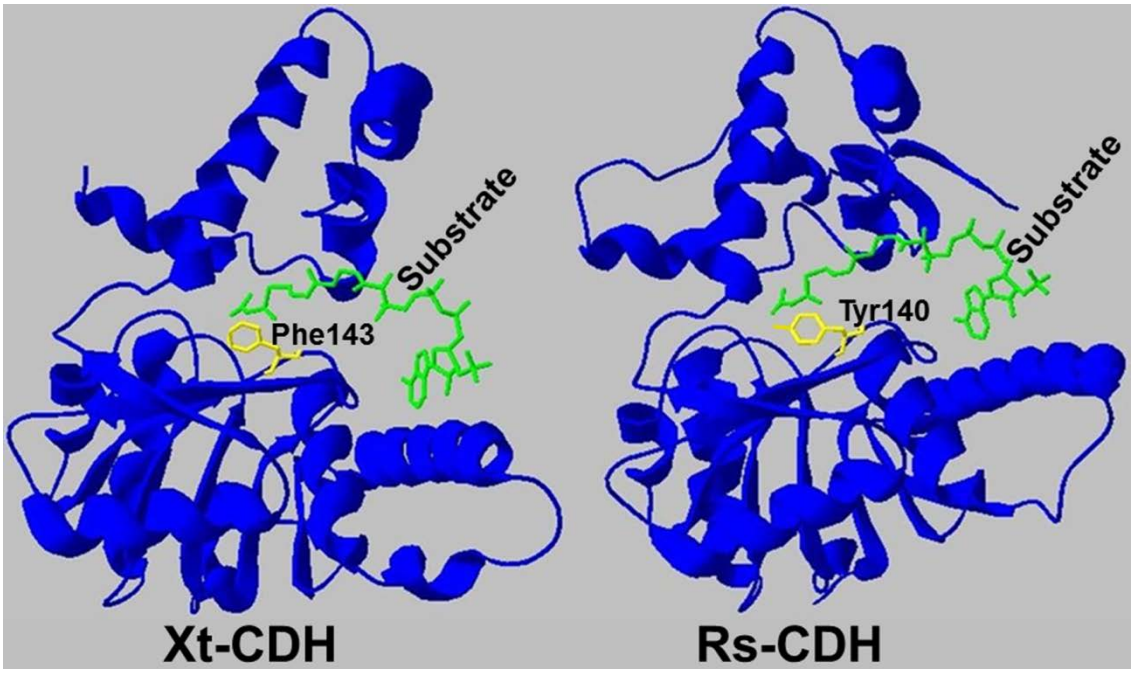

Fig. 2.13 Predicted three dimensional structure of Rs-CDH and Xt-CDH based on homology modeling using h-HAD (PDB code: 1F0Y) as template. Enzyme structures are shown as ribbon diagrams. Phe143 in Xt-CDH and Tyr140 of Rs-CDH are displayed in yellow as a stick model. The bound substrate is shown as a green stick model.

maintaining a hydrophobic environment in the active site mainly near the trimethyl moiety of the bound substrate. Replacement of Phe 143 in Xt-CDH and Tyr140 in Rs-CDH to Asp (Xt-F143D and Rs-Y140D), Lys (Xt-F143K and Rs-Y140K) explained this phenomenon. Another possibility is that the phenyl ring contributes to the active site geometry. This possibility is supported by the dramatic effects that Ala (Xt-F143A and Rs-Y140A), Ser (Xt-F143S and Rs-Y140S), and Gly (Xt-F143G and Rs-Y140G) mutants produced on K_m values. Substituting the aromatic residues with short side chain amino acids might increase the substrate channel space. This change might decrease the

interaction between the substrate and the neighboring residues in the region of the substrate recognition.

A change was also observed in thermal stability between Xt-F143Y, Rs-Y140F, and wild-type forms of these enzymes (Fig. 2.9). In Xt-CDH, when Phe143 was replaced with Tyr, a decrease in thermal stability was observed, indicating a less stable protein. In contrast, removal of this hydroxyl group as a result of Rs-Y140F mutant increased Rs-CDH stability. From such results, we infer that the hydroxyl group of the active site residue Tyr140 did not play a critical role in protein stabilization (Pace et al., 2001; Escobar et al., 1994; Guan et al., 1998), although the phenyl ring of Tyr might be important.

2.5 CONCLUSIONS

This study was designated to investigate the structure-function relation of two CDHs (Rs-CDH and Xt-CDH). The primary structure alignment of kinetically different enzymes Xt-CDH and Rs-CDH with that of h-HAD reveals several key residues that interact and/or present close to binding substrate. To investigate the roles of these different residues in the enzyme activity and substrate affinity, they were functionally and kinetically characterized. Substitution of five residues in Xt-CDH (Phe143, Ile190, Ala191, Gly223 and Ala224) with their corresponding in Rs-CDH (Tyr140, Val187, G188, S223 and F224) produced CDH mutants with altered kinetic properties that support their role in binding L-Car and Catalysis, pointed that Xt-F143Y was generated the greatest defect in the L-Car binding.

Furthermore, our results clearly clarified that the introduction of hydroxyl group of the Tyr instead of Phe in Xt-CDH changed the p*K*a of catalysis environment. This function did not observe in the Rs-CDH pH profile. Thereafter, we inferred that the hydroxyl group of the active site residue Tyr140 does not have a critical role in catalysis scenario.

Conclusively, we provided evidence related to the importance of the phenyl ring of Phe143 in Xt-CDH and its corresponding amino acid in Rs-CDH (Tyr140), although, the hydroxyl group of Tyr140 in Rs-CDH seems to be unnecessary for L-Car binding. The structural investigation provided new ideas about this poorly understood but important enzyme for L-Car measurement. To develop a suitable CDH as an excellent biocatalyst for L-Car measurement, in the absent of crystal structure conformation for any of CDHs, additional studies particularly addressing the important amino acids of CDHs using site-directed mutagenesis and other bioinformatics tool is required.

CHAPTER 3

ALANINE SCANNING MUTATION APPROACH FOR CLASIFICATION OF THE ROLES OF CONSERVED RESIDUES IN THE ACTIVITY AND SUBSTRATE AFFINITY OF L-CARNITINE DEHYDROGENASE

3.1 INTRODUCTION

It is well known that CDH has been proposed as a superior tool for assessment of biologically essential substance L-Car. CDH has been cloned from several bacterial species, including *Xanthomonas translucens, Rhizobium* sp., *Pseudomonas aeruginosa*, and *Alcaligenes* sp. (Mori et al., 1988b; Houriyou et al., 1993; Wargo and Hogan 2009; Arima et al. 2010). Comparison of the amino acids sequences reveals that there is a significant level of conservation (45%) among CDHs. Comparison of CDHs sequences among more divergent enzymes demonstrates that there is higher sequence conservation with that of HADs. The crystal structure and catalytic residues of several HADs have been well investigated (Barycki et al., 2000; 1999; Taskinen et al., 2006). This offers opportunities to study the role of conserved residues of CDHs in comparison to that of HADs.

In the first study, using homology modeling of CDHs, we demonstrated the importance of different amino acids residues for catalytic activity and substrate affinity. Particularly, we provide evidence about the importance of the phenyl ring of Phe143 in L-Car binding of CDH from Xt-CDH and its corresponding amino acid (Tyr140) in CDH from *Rhizobium* sp. Although our previous work shed light on the importance of several amino acids on the catalytic activity and substrate affinity of CDH toward L-Car, a detailed database of functional information derived from results of mutagenesis

studies and homology models must still develop a suitable CDH as an excellent biocatalyst for L-Car measurement.

The alanine scanning mutagenesis approach was developed to elucidate the importance of the amino acid side chains that most strongly modulate the interaction between a protein and its ligand or substrates (Argos, 1988; Cunningham and Wells, 1989). Ala was chosen for scanning mutagenesis because it is the most abundant amino acid in proteins and is found both internally and at surface-exposed positions in proteins. In addition, Ala does not impose extreme electrostatic or steric effects. Ala eliminates the side chain beyond the ß carbon but does not change the main chain conformation. Cunningham and Wells (1989) have demonstrated that the substitution of a single Ala for an amino acid in a protein does not substantially alter the overall fold of the protein. Thus alanine scanning has been successfully used to evaluate the functional importance of single amino acid residues within a protein.

In this Chapter, applying the alanine scanning mutagenesis approach to an analysis of the CDH has shown that Ala substitution of conserved residues within Xt-CDH with Alanine results in a set of proteins that are either catalytically inactive proteins, have marginal CDH activity, or have substantial enzymatic activity. Kinetic screening of the mutant proteins with detectable enzymatic activity demonstrated that some of these proteins had altered K_m for the donor substrate (L-Car), and one had an altered K_m for the acceptor (NAD^+) and donor substrate. Based on the kinetic data and homology model of Xt-CDH, regions and specific residues that are important for catalysis and for the recognition of the substrate in Xt-CDH are discussed.

3.2 MATERIALS AND METHODS

3.2.1 Materials

3.2.1.1 Bacterial strains, plasmids, substrates and cofactors

The cofactor NAD^+ was purchased from Oriental Yeast Co. Ltd. (Tokyo, Japan). The substrate L-Car was purchased from Hamari Chemicals, Ltd., Yonezawa, Japan. Plasmid pMal-Xt-CDH (pMal-c2 vector with the CDH genes inserted into the *BamH*I–*Hind*III gap) (Arima et al., 2010) were used for expression of the wild-type enzyme and as a template for alanine scanning mutagenesis. *Escherichia coli* JM109 which was collected from Toyobo (Japan) or Takara Bio Inc. (Shiga, Japan) was used as the host strain for general cloning procedures and for gene expression.

3.2.1.2 PCR reagents, purification and polyacrylamide gel electrophoresis

PCR primers for alanine scanning mutagenesis (Table 3.1) were synthesized at Operon Biotechnologies (Tokyo, Japan). Pwo polymerase was purchased from Roche Applied Science (USA). Agaroses used for gel-electrophoresis of DNA fragment were collected from BMA (Rockland, ME, USA) or Takara Bio Inc. (Shiga, Japan). Loading quick λ/StyI and loading quick λ/HindIII were purchased from Toyobo, Japan. Econo Spin™ IIa spin column was purchased from INA OPTIKA (Nagano, Japan). A DNA staining reagent, SYBR Gold was collected from life technologies (USA). BigDye Terminator Cycle Sequencing Ready Reaction kit ver 3.1 was from Applied Biosystems (Foster City, CA). The dye terminators, deoxynucleoside triphosphates, AmpliTaq DNA Polymerase, FS, rTth pyrophosphatase, magnesium chloride, and

Table 3.1 DNA sequences of alanine mutant primers

Primer name	DNA sequence
Xt-E93A-F	5’ AAAGCGCCCCGGCCCGCCTCGATCTGAA 3’
Xt-E93A-R	5’ TTCAGATCGAGGCGGGCCGGGGCGCTTT 3’
Xt-S117A-F	5’ CGATCATCGCCGCCAGCACGTCCGGGCT 3’
Xt-S117A-R	5’ AGCCCGGACGTGCTGGCGGCGATGATCG 3’
Xt-S118A-F	5’ ATCATCGCCAGCGCCACGTCCGGGCTGCT 3’
Xt-S118A-R	5’ AGCAGCCCGGACGTGGCGCTGGCGATGAT 3’
Xt-T119A-F	5’ ATCATCGCCAGCAGCGCGTCCGGGCT 3’
Xt-T119A-R	5’ AGCCCGGACGCGCTGCTGGCGATGAT 3’
Xt-S120A -F	5’ AGCAGCACGGCCGGGCTGCTGCCCA 3’
Xt-S120A -R	5’ TGGGCAGCAGCCCGGCCGTGCTGCT 3’
Xt-H133A-F	5’ TACGAGTCGTCCAGCGCGCCCGAGCGCTGCGT 3’
Xt-H133A-R	5’ ACGCAGCGCTCGGGCGCGCTGGACGACTCGTA 3’
Xt-R136A-F	5’ TCCAGCCACCCCGAGGCCTGCGTGGTCGGCCA 3’
Xt-R136A-R	5’ TGGCCGACCACGCAGGCCTCGGGGTGGCTGGA 3’
Xt-H141A-F	5’ TGCGTGGTCGGCGCCCCTTTCAACCCGGT 3’
Xt-H141A-R	5’ ACCGGGTTGAAAGGGGCGCCGACCACGCA 3’
Xt-N144A-F	5’ TCGGCCACCCTTTCGCCCCGGTGTACCTGCT 3’
Xt-N144A-R	5’ AGCAGGTACACCGGGGCGAAAGGGTGGCCGA 3’
Xt-Y147A-F	5’ CTTTCAACCCGGTGGCCCTGCTGCCGCTGGT 3’
Xt-Y147A-R	5’ ACCAGCGGCAGCAGGGCCACCGGGTTGAAAG 3’
Xt-E153A-F	5’ TGCTGCCGCTGGTGGCGATCGTCGGCGG 3’
Xt-E153A-R	5’ CCGCCGACGATCGCCACCAGCGGCAGCA 3’
Xt-M177A-F	5’ TACACCGAGCTGGGCGCGCGCCCGCTGCAT 3’
Xt-M177A-R	5’ ATGCAGCGGGCGCGCGCCCAGCTCGGTGTA 3’
Xt-K184A-F	5’ TGCATGTGCGCGCGGAAGTCCCCGGCTT 3’
Xt-K184A-R	5’ AAGCCGGGGACTTCCGCGCGCACATGCA 3’
Xt-E185A-F	5’ ATGTGCGCAAGGCGGTCCCCGGCTTCAT 3’
Xt-E185A-R	5’ ATGAAGCCGGGGACCGCCTTGCGCACAT 3’
Xt-F189A-F	5’ AAGGAAGTCCCCGGCGCCATCGCCGATCGTCT 3’
Xt-F189A-R	5’ AGACGATCGGCGATGGCGCCGGGGACTTCCTT 3’
Xt-D192A-F	5’ GGCTTCATCGCCGCGCGTCTGCTCGAAG 3’
Xt-D192A-R	5’ CTTCGAGCAGACGCGCGGCGATGAAGCC 3’
Xt-R193A-F	5’ TTCATCGCCGATGCGCTGCTCGAAGCGCT 3’
Xt-R193A-R	5’ AGCGCTTCGAGCAGCGCATCGGCGATGAA 3’
Xt-E196A-F	5’ CGATCGTCTGCTCGCGGCGCTCTGGCGC 3’
Xt-E196A-R	5’ GCGCCAGAGCGCCGCGAGCAGACGATCG 3’
Xt-W199A-F	5’ TGCTCGAAGCGCTCGCGCGCGAGGCGCT 3’
Xt-W199A-R	5’ AGCGCCTCGCGCGCGAGCGCTTCGAGCA 3’
Xt-R200A-F	5’ AAGCGCTCTGGGCCGAGGCGCTGCACCT 3’
Xt-R200A-R	5’ AGGTGCAGCGCCTCGGCCCAGAGCGCTT 3’
Xt-E201A-F	5’ AAGCGCTCTGGCGCGCGGCGCTGCACCT 3’
Xt-E201A-R	5’ AGGTGCAGCGCCGCGCGCCAGAGCGCTT 3’

Table 3.1 (continue)

Xt-D217A-F	5’ ACCGGTGAAATCGCCGACGCGATCCGCTT 3’
Xt-D217A-R	5’ AAGCGGATCGCGTCGGCGATTTCACCGGT 3’
Xt-R221A-F	5’ AAATCGACGACGCGATCGCCTTCGGCGCC 3’
Xt-R221A-R	5’ GGCGCCGAAGGCGATCGCGTCGTCGATTT 3’
Xt-R227A-F	5’ TTCGGCGCCGGCCTGGCCTGGTCGTTCAT 3’
Xt-R227A-R	5’ ATGAACGACCAGGCCAGGCCGGCGCCGAA 3’
Xt-W228A-F	5’ CGGCCTGCGCGCGTCGTTCATGGGCACCTT 3’
Xt-W228A-R	5’ AAGGTGCCCATGAACGACGCGCGCAGGCCG 3’
Xt-M231A-F	5’ CTGGTCGTTCGCGGGCACCTTCCTCACCTA 3’
Xt-M231A-R	5’ TAGGTGAGGAAGGTGCCCGCGAACGACCAG 3’
Xt-F234A-F	5’ TCGTTCATGGGCACCGCCCTCACCTACA 3’
Xt-F234A-R	5’ TGTAGGTGAGGGCGGTGCCCATGAACGA 3’
Xt-T236A-F	5’ ATGGGCACCTTCCTCGCCTACACCCTG 3’
Xt-T236A-R	5’ CAGGGTGTAGGCGAGGAAGGTGCCCAT 3’
Xt-Y237A-F	5’ ACCTTCCTCACCGCCACCCTGGCCGGT 3’
Xt-Y237A-R	5’ ACCGGCCAGGGTGGCGGTGAGGAAGGT 3’
Xt-N144A-F	5’ TCGGCCACCCTTTCGCCCCGGTGTACCTGCT 3’
Xt-N144A-R	5’ AGCAGGTACACCGGGGCGAAAGGGTGGCCGA 3’
Xt-M246A-F	5’ TGGCGATGCCGGCGCGCGCCATTTCATGCA 3’
Xt-M246A-R	5’ TGCATGAAATGGCGCGCGCCGGCATCGCCA 3’
Xt-R247A-F	5’ ATGCCGGCATGGCCCATTTCATGCAGCA 3’
Xt-R247A-R	5’ TGCTGCATGAAATGGGCCATGCCGGCAT 3’
Xt-H248A-F	5’ ATGCCGGCATGCGCGCGTTCATGCAGCAGTT 3’
Xt-H248A-R	5’ AACTGCTGCATGAACGCGCGCATGCCGGCAT 3’
Xt-F249A-F	5’ TGCCGGCATGCGCCATGCCATGCAGCAGTT 3’
Xt-F249A-R	5’ AACTGCTGCATGGCATGGCGCATGCCGGCA 3’
Xt-W251A-F	5’ ACTGAAGCTGCCGGCGACCTATCTGCCG 3’
Xt-W251A-R	5’ CGGCAGATAGGTCGCCGGCAGCTTCAGT 3’
Xt-Q252A-F	5’ CCATTTCATGCAGGCGTTCGGCCCGGCACT 3’
Xt-Q252A-R	5’ AGTGCCGGGCCGAACGCCTGCATGAAATGG 3’
Xt-F253A-F	5’ ATTTCATGCAGCAGGCCGGCCCGGCACT 3’
Xt-F253A-R	5’ AGTGCCGGGCCGGCCTGCTGCATGAAAT 3’
Xt-T262A-F	5’ TGAAGCTGCCGTGGGCCTATCTGCCGG 3’
Xt-T262A-R	5’ CCGGCAGATAGGCCCACGGCAGCTTCA 3’
Xt-Q284A-F	5’ TCGACGGCACCGCAGCGGCGGTGGGCGAACGCA 3’
Xt-Q284A-R	5’ TGCGTTCGCCCACCGCCGCTGCGGTGCCGTCGA 3’
Xt-S289A-F	5’ AAGTGGGCGAACGCGCCATCGCCGAGCT 3’
Xt-S289A-R	5’ AGCTCGGCGATGGCGCGTTCGCCCACTT 3’
Xt-E294A-F	5’ ATCGCCGAGCTCGCGCGCTACCGCGACGA 3’
Xt-E294A-R	5’ TCGTCGCGGTAGCGCGCGAGCTCGGCGAT 3’
Xt-R295A-F	5’ ATCGCCGAGCTCGAAGCCTACCGCGACGACA 3’
Xt-R295A-R	5’ TGTCGTCGCGGTAGGCTTCGAGCTCGGCGAT 3’
Xt-R297A-F	5’ AGCTCGAACGCTACGCCGACGACACCTT 3’
Xt-R297A-R	5’ AAGGTGTCGTCGGCGTAGCGTTCGAGCT 3’
Xt-D298A-F	5’ AACGCTACCGCGCCGACACCTTGCT 3’
Xt-D298A-R	5’ AGCAAGGTGTCGGCGCGGTAGCGTT 3’

buffer were premixed into a single tube of Ready Reaction Mix and were ready to use. Restriction enzymes, Taq polymerase and DNA sample loading dye were from New England Biolabs (Massachusetts, USA), Takara Bio Inc. (Shiga, Japan), and Toyobo (Osaka, Japan). Ampicillin was collected from Wako Pure Chemical Ind. Ltd. (Osaka, Japan). Amylose resin and Color Plus pre-stained protein marker for SDS–PAGE were from New England Biolabs Inc. (Massachusetts, USA). Enzyme samples were prepared for loading by mixing with an equal volume of 2x EzApply sample buffer (Atto, Tokyo, Japan).

3.2.1.3 Other reagents

All other chemicals and materials used in this part of the study were of the highest purity grade were supplied from Wako Pure Chemical Ind. Ltd. (Osaka, Japan) and used without further processing.

3.2.2 Methods

3.2.2.1 General methods

General weight measurements were made using IB-200H electronic balance (Shimadzu corp. Kyoto, Japan) and smaller quantities measurements for the preparation of standards were made using Shimadzu ATX84 analytical balance (Shimadzu corp. Kyoto, Japan). QSONICA Ultra Sonicator (Q125-110) (USA) was used for bacterial cell disruption. PCR thermal Cycler Dice model TP 600 and model TP100 of Takara were used for PCR reactions (Takara Bio Inc., Shiga, Japan). Plasmid and products derived from PCR were purified by using Econo Spin^{TM} IIa spin columns from INA

OPTIKA (Nagano, Japan). Agarose gel electrophoresis was performed using Mupid-2X submarine electrophoresis system apparatus (Advance Co. Ltd., Japan). PCR products were dried using ultra-small centrifugal concentrator spin dryer mini VC-15 SP (TAITEC, Co. Ltd. Koshigaya, Japan). A Horiba F-22 pH meter 66 (Horiba Ltd., Kyoto, Japan) was used for determination pH of medium, buffers. The meter was calibrated every time with pH 4.0 and 7.0 standard buffer solutions (Wako Pure Chemical Ind. Ltd., Osaka, Japan). Media were autoclaved at 121 ºC for 20 minutes using BS-245 high pressure steam sterilizer (Tomy Seiko Co., Ltd., Tokyo, Japan) or NCC 1701 (AS ONE, Osaka, Japan). Samples were vortexes using a Vortex Genie 2 (Scientific Industries, Inc., USA). A Novaspec II from Amersham Pharmachia Biotech (Piscataway, NJ, USA) was used for measurement cell growth of cultivated bacteria. Filter sterilization of solutions was carried out using 0.22 μm disposable filters MILLEX-GA (Millipore, Molshiem, France). Inoculated media were incubated either in at 37 ºC with reciprocal shaker NR-1 or at 25 ºC using a NR-300 double shaker (Taitec Corporation, Tokyo, Japan) or at 30 ºC and low temperature in LTI-60ISD EYALA low temperature incubator equipped with NR-30 double shaker (EYALA, Tokyo, Japan). Multi-barreled micro-plate mixer from AS ONE (Osaka, Japan) was used for shaking 96 well plate. For protein assay a Bio-Rad micro plate reader Model 680 (BIO-RAD Inc., Hercules, CA, USA) was used. Cultures and extracts were centrifuged using Hitachi Himac Compact Centrifuges RX II Series CF16RXII (rotor: 36, T16A31; 44, T15A36; 46, T15A36; and 24, T9A31) and Hitachi Himac CT15E (Hitachi Koki Company Ltd., Tokyo, Japan). Shimadzu UV-2100S spectrophotometer (Kyoto, Japan) was used for measurement of enzyme activity.

3.2.2.2 Site-directed mutagenesis

The pMAL-c2 plasmid with the insert of Xt-CDH (Arima et al., 2010) was used as a template of alanine mutagenesis. Site-directed mutagenesis was performed as described in Chapter 2 using the oligonucleotide primers listed in Table 3.1. Briefly, a whole range of the plasmids was amplified by Pwo polymerase (Roche Diagnostics Corp.). The PCR products were digested with *Dpn*I overnight at 37 °C. The target mutated plasmids were transferred into *E. coli* JM109. The insert CDH fragment of 42 plasmids were sequenced completely to confirm that only the intended mutations were introduced.

3.2.2.3 Protein expression and purification

Transformation, overproduction and purification of the recombinant proteins were conducted as described in Chapter 2 with minor modifications. The competent cell *E. coli* JM109 harboring Xt-CDH and mutant enzymes plasmids were cultivated for 10 h at 25 °C in 5 ml LB medium containing 50 µg/ml of Ampicillin, in a shaking incubator at 110 ~ 120 stroke min^{-1}. The protein expression was induced by addition of IPTG at a final concentration of 0.1 mM. Then cultivation was continued for another 12 h under the same conditions. After expression, the cells were harvested by centrifugation (8000 rpm for 30 min at 4 °C). The media was decanted and collected cells were washed with a 0.85% potassium chloride solution followed immediately with storage at -20 °C. The cells pellet is suspended in 2 ml of 50 mM KPB (pH 7.0) containing 1.0 mM 2-ME. They were subsequently disrupted by ultra-sonication (QSONICA Ultrasonic Sonicator, Q125-110, USA) for 5 min on ice followed by centrifugation (8000 rpm for 30 min at 4 °C). After removal of cell debris, the solution was dialyzed against 50 mM KPB (pH

7.0) containing 1.0 mM 2-ME. Expression of CDHs recombinant proteins was evaluated using a 10% SDS–PAGE under denaturing conditions (Laemmli, 1970). Gels of crude and purified proteins were stained with Coomasie brilliant blue (CBB) R-250.

From the dialysate, CDHs fused with MBP were purified using amylose resin (New England Biolabs Inc., Ipswish MA). The dialysate was loaded onto amylose column (Spin column) equilibrated with 20 mM KPB, pH 7.0, containing 200 mM NaCl, 1.0 mM EDTA, 1.0 mM 2-ME. Undesirable proteins were removed with the same buffer. Then the bound protein fused with MBP was eluted using same buffer containing 10 mM maltose. As described in Chapter 2, the presence of MBP did not influence the substrate affinity of recombinant Xt-CDH (Arima et al., 2010). Therefore, Xt-CDH and mutant enzymes fused with MBP were used for characterization. The homogeneity of purified proteins was examined using a 10% SDS gel electrophoresis under denaturing conditions (Laemmli, 1970) and stained with CBB R-250.

3.2.2.4 Enzyme assay

The enzyme activity of Xt-CDH and alanine mutant enzymes was assessed using a spectrophotometer (UV-2100 S array; Shimadzu Corp., Kyoto, Japan) by monitoring the increase in absorbance of NADH at 340 nm, as described in chapter 2. Briefly, a standard assay mixture contained 120 mM Glycine-NaOH buffer (pH 9.5), 2 mM NAD^+, 12 mM L-Car and a suitable amount of purified enzyme. To screen substrate affinity of the current version of alanine mutants, the final concentration of L-Car was excess to 300 and 900 mM. One unit of CDH activity was defined as the reduction of 1 μmol NAD^+ per minute under assay conditions. Specific activity was defined as units of enzyme activity per mg protein.

3.2.2.5 Protein concentration measurements

The protein concentration was determined using the Bradford (1976) method with the bovine serum albumin as standard. Specific activity was defined as units of enzyme activity per mg protein.

3.2.2.6 Kinetic analysis

The K_m value for L-Car of Xt-CDH and mutant enzymes was first roughly estimated using various L-Car concentrations (5 – 2000 mM) at a fixed level of NAD^+ (2 mM), except that of S117A and R200A, which were measured at a NAD^+ final concentration of 6 mM. Next, the exact K_m value was ascertained from enzyme reactions using 4–5 different concentrations of L-Car around the K_m value of the specific mutant. The K_m for NAD^+ was determined using different NAD^+ concentrations (0.03 – 6 mM) at a constant L-Car level based on the K_m of L-Car determined for mutant enzymes. This data was fitted to the Michaelis-Menton equation using a linear regression.

3.3 RESULTS

3.3.1 Site directed-mutagenesis, expression and purification of mutant enzymes

To date, four CDH protein sequences from different bacterial species were identified. They share 45% identity of protein sequence. CDHs showed high homology to that of HAD (Fig. 3.1). To test the hypothesis that the conserved residues play a role in enzyme activity and/or substrate binding, we systematically mutated 42 functional residues of conserved amino acids present in the Xt-CDH using alanine scanning mutagenesis (Fig. 3.1). Following site-directed mutagenesis of Xt-CDH gene, mutant plasmids were sequenced to confirm that desired mutations were present. Mutant Xt-CDHs were expressed in *E. coli* JM109 strain. As shown in Fig. 3.2, all introduced alanine mutants exhibit a consistent level of protein expression. The specific activities of crude mutant enzymes were analyzed, by using assay mixture described in the *Materials and Methods* section, and found that five mutant enzymes (E93A, H141A, E153A, D217A, and R227A) had no enzymatic activity. The catalytically active mutants were purified using amylose resin affinity chromatography. The purified samples showed a single protein band on SDS-PAGE (Fig. 3.3) comparable to that of apparent MW of Xt-CDH (37 kDa) plus fused MBP (40 kDa).

3.3.2 Specific activity of alanine mutants

The specific activity of each Ala mutant was compared with that of the wild type. The relative activities (i.e., specific activity of the purified mutant protein/specific activity of purified wild-type multiplied by 100 and expressed as a percentage) of

```
V. eiseniae          MTVITQLETFAAIGTGVIGSGWVARALAHGLDVVAWDPAPDAEQQLRANVANAWPA 56
B. multivorans       MAVITDIKTFAAIGTGVIGSGWIARALAHGLDVVVWDPAPGAEARLRANVANAWPA 56
P. aeruginosa        MSFVTEIKTFAALGSGVIGSGWIARALAHGLDVVAWDPAPGAEAALRARVANAWPA 56
Alcaligenes sp.      MTFITNIKTFAALGSGVIGSGWVARALAHGLDVVAWDPAPGAEAALRQRVANAWGA 56
X. translucens       MPFITHIKTFAALGSGVIGSGWVARALAHGLDVIAWDPAPGAEQALRQRVANAWPA 53
Rhizobium sp.        ---MSFITKAACVGGGVIGGAWVARFALAGIDVKIFDPHPEAERIIGEVMANAERA 53
A.radiobacter        ---MTKINKAACIGGGVIGGGWIARFLLAGIDVDVFDPHPEATRIVGEVLANAENA 53
R.etli               ---MTKISKAACIGGGVIGGGWIARFLLAGIDVDVFDPHPEAGRIVGEIIANAEKA 53

LERSGLTPGADPSRLRFVATIQACVADADFIQESAPERAALKLQLHEQISRAARPEAIIASSTSGLLPSDFYAR 130
LERVGLAAGADPARLRFESTIEACVADADFIQESAPEREALKLELHEQISRAAKPDAIIASSTSGLLPTDFYAR 130
LRKQGLAPGAAQERLRFVASIEECVGDADFIQESAPERLDLKLDLHARISAAARPDVLIGSSTSGLLPSEFYAE 130
LEKQGLVPGASPQRLRFVSTIEECVKDADFIQESAPERLELKLELHSKISAAAKPDALIGSSTSALLPSEFYEG 130
LEKQGLAAGAAQHRLSFVSSIEECVRDADFIQESAPERLDLKLDLHAKISAAAKPDAIIASSTSGLLPSEFYES 130
YAMLTMAPLPPKGKLTFCKSIEEAVEGADWIQESVPERLELKRGVITKIDAAARPDALIGSSTSGLLPSDLQSE 130
YAMLTGAPLPARGKLTFRETLEEAVAGADWIQESVPERLDLKRKVLTQIDTAARPDALIGSSTSGLLPTDLQRD 130
YAMLTGAPLPPRGKLTFCETLAEAVADADWIQESVPERLDLKRGVLTEIDAAARPEALIGSSTSGLLPTDLQRN 130

ATHPQRCVVGHPFNPVYLLPLVEVLGGTRSAAETLDAAMQVYAGLGMRPLRVRKEVPGFIADRLLEALWREALH 204
ATHPERCVVGHPFNPVYLLPLVEVLGGARTSPEAVEAAMAIYRKLGMRPLHVRKEVPGFIADRLLEALWREALH 204
ASHPERCLVGHPFNPVYLLPLVEVVGGERTAAEAVRAAMRVYESLGMRPLHVRKEVPGFIADRLLEALWREALH 204
STHPQRCVVGHPFNPVYLLPLVEVVGGQHTAPEAIQAAIQVYESLGMRPLHVRKEVPGFIADRLLEALWREALH 204
SSHPERCVVGHPFNPVYLLPLVEIVGGRHTAPEAIEAAKGIYTELGMRPLHVRKEVPGFIADRLLEALWREALH 201
MHHPERMFVAHPYNPVYLLPLVELVGGKKTSKATIERAMQGVEQIGMKGVVIAKEIEAFVGDRLLEALWREALW 201
MRHPERLFVAHPYNPVYLLPLVEIVGGEKTSKETIQAAMDRLPPIGMKGVHIAKEIEAFVGDRLLEALWREALW 201
MTHPERLFVAHPYNPVYLLPLVEIVGGEKTSAGTIRAAIERLAPIGMKGVHIAKEIEAFVGDRLLEALWREALW 201

LVNEGVATTGEIDDAIRFGAGIRWSFMGTFLTYTLAGQDAGMRHFMQQFGPALELPWTKLVA-PELTEALIERV 277
LVNEGVATTGEIDDAIRFGAGIRWSFMGTFLTYTLAGGDAGMRHFMQQFGPALELPWTKLAA-PTLTDELIDRV 277
LVNDGVATTGEIDDAIRFGAGLRWSFMGTFLTYTLAGGNAGMRHFMAQFGPALQLPWTYLPA-PELTEALIDRV 277
LVNDGVATTGEIDDAIRFGAGLRWSFMGTFLTYTLAGGDAGMRHFMAQFGPALQLPWTYLPA-PELTDKLIDDV 277
LVNDGVATTGEIDDAIRFGAGLRWSFMGTFLTYTLAGGDAGMRHFMQQFGPALKLPWTYLPA-PELTERLIDEV 277
LIQDDICDTETLDNVMRYSFGMRWAQMGLFETYRIAGGEAGMRHFLAQFGPCLKWPWTKFTDVVDLDDALVEKI 273
LIKDDICTVETLDDVIRYSFGLRWAQMGLFQTYRIAGGEAGMRHFLAQFGPALQWNWTKLMDVVDLDDALVEKI 273
LIHDDICTVETLDDVIRYSFGLRWAQMGLFQTYRIAGGEAGMRHFLAQFGPCLAWPWTKLTDVVDLDDALIEKI 273

VEGTTEQLGRRSIKELERYRDECITEVLGAIAAVKARHGMRAED------------------------------ 321
VDGTSEQQGKRSIKELERYRDECITEVLKAIAAVKARHGMRFED------------------------------ 321
VEGTAEQQGARSIAELERYRDDCLLAVLGAIRETKARHGFAFAE------------------------------ 321
VQGTAEQLGNHSISALERYRDDCLLAVLEAVKTTKAKHGMHFHD------------------------------ 321
VDGTAAQVGERSIAELERYRDDTLLAVLEAIGTSKAKHGMTFSE------------------------------ 321
GAQSDAQAAGRSIRELERIRDENLVGIMHALKSGNGGEGWGAGKLLADFEAKLWANARKPEADLGDVKPLRILD 351
GQQSDEQAAGLSIRELERIRDENLVGILQTLKGSHGGKGWGAGKLLKDFEQNLWATGGGERKLYDLARPLRLIE 351
GRQSDEQAAGLSIRALERIRDENLVGILQALKGGDNGKGWGAGKLLKDFEQTLWARGGDAAASADPSKPLRLVE 351
```

Fig. 3.1 Protein sequence alignment of CDHs and bacterial 3-hydroxyacyl-CoA dehydrogenases. Alignment was obtained using ClustalW. CDHs were from *Alcaligenes* sp., *P. aeruginosa* (*Pseudomonas aeruginosa*), *X. translucens* (*Xanthomonas translucens*), and *Rhizobium* sp. The 3-hydroxyacyl-CoA dehydrogenases were from *V. eiseniae* (*Verminephrobacter eiseniae*), *B. multivorans* (*Burkholderia multivorans*), *A. radiobacter* (*Agrobacterium radiobacter*), and *R. etli* (*Rhizobium etli*). Residues that are conserved in all sequences are shown in blue or red color. Residues conserved in CDHs are highlighted in gray. Residues involved in the mutagenesis study are shown in red color.

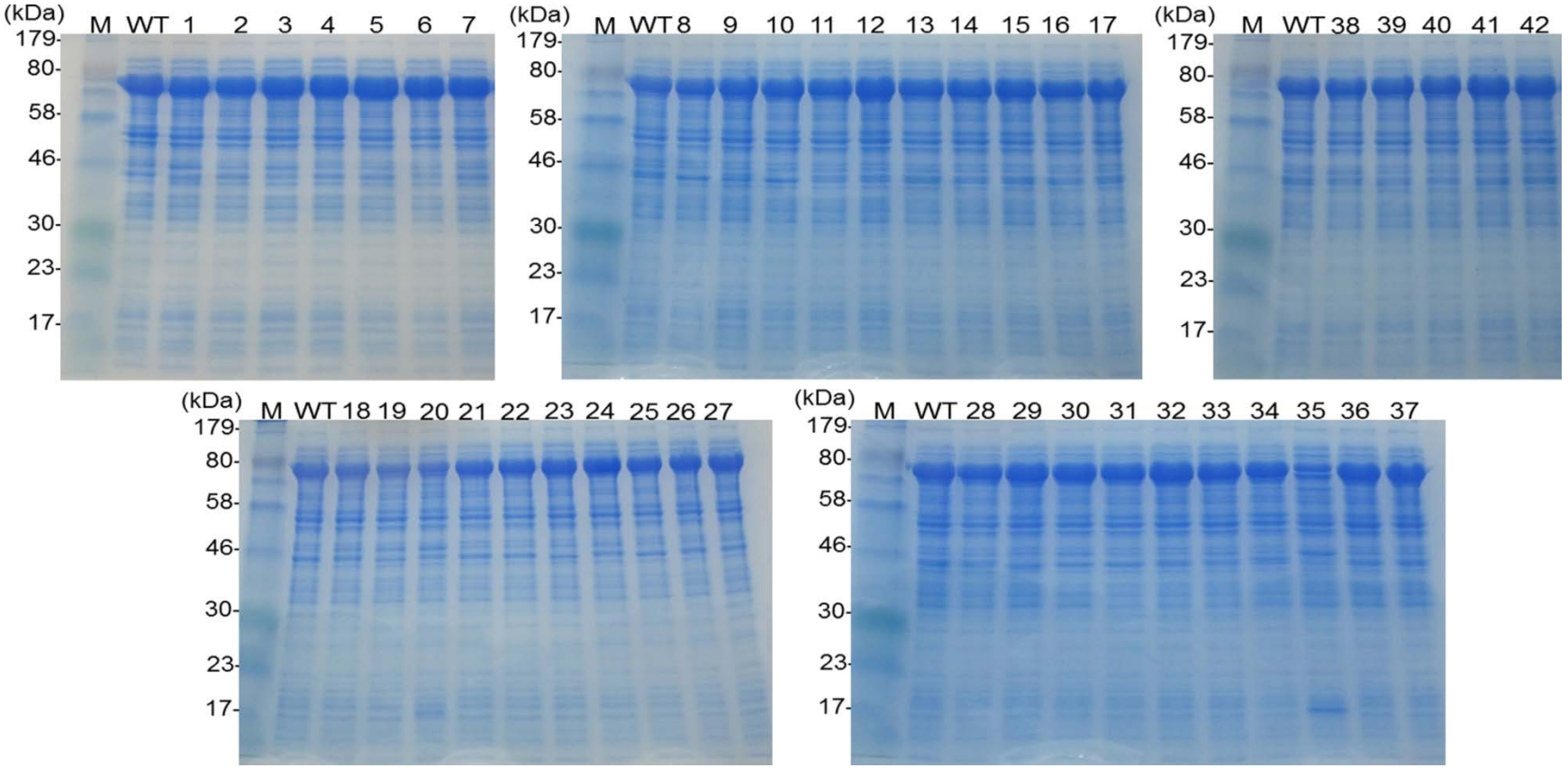

Fig. 3.2 SDS-PAGE of cell free extract of wild-type (Xt-CDH) and alanine mutant enzymes. M, protein molecular marker; WT, wild-type; lane 1, E93A; 2, S117A; 3, T119A; 4, S120A; 5, H133A; 6, R136A; 7, H141A; 8, N144A; 9, Y147A; 10, E153A; 11, M177A; 12, K184A; 13, E185A; 14, F189A; 15, D192A; 16, R193A; 17, E196A; 18, W199A; 19, R200A; 20, E201A; 21, D217A; 22, R221A; 23, R227A; 24, W228A; 25, M231A; 26, F234A; 27,T236A; 28, Y237A; 29, M246A; 30, R247A; 31, H248A; 32, F249A; 33, Q252A; 34, F253A; 35, W261A; 36, T262A; 37, Q284A; 38, S289A; 39, E294A; 40, R295A; 41, R297A; 42, D298A. The gel was stained with Coomassie Brilliant Blue.

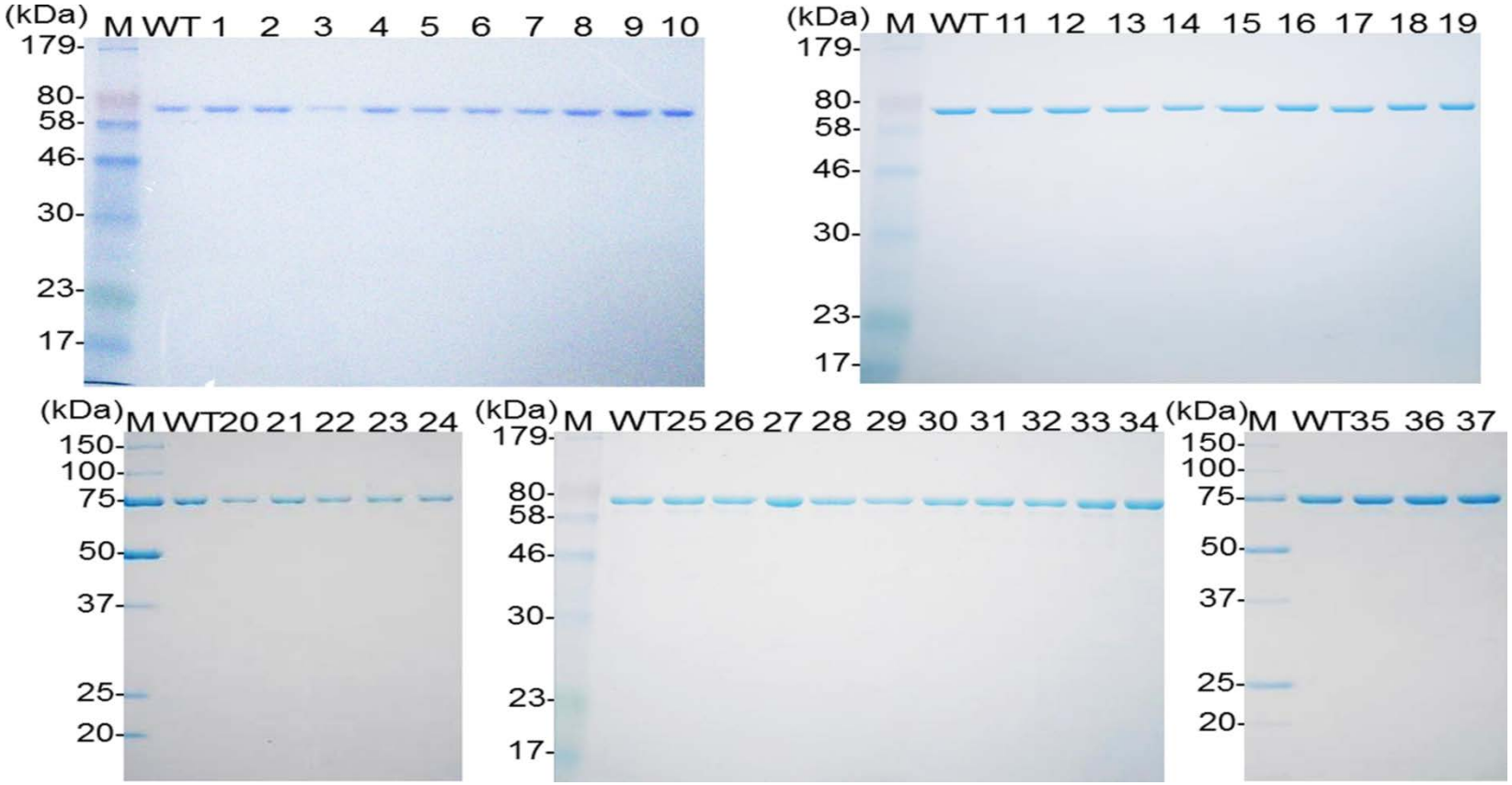

Fig. 3.3 SDS-PAGE of purified wild-type (Xt-CDH) and mutant enzymes. Samples were loaded on a 10% gel. M, protein molecular marker; WT, wild-type; lane 1, S117A; 2, S120A; 3, N144A; 4, Y147A; 5, F189A; 6, R193A; 7, E196A; 8, W199A; 9, R200A; 10, E201A; 11, W228A; 12, M231A; 13, F234A; 14, Y237A; 15, M246A; 16, F249A; 17, Q252A; 18, F253A; 19, W261A; 20, E185; 21, R221A; 22, R136A; 23, D192A; 24, Q284A; 25, T119A; 26, H133A; 27, M177A; 28, K184A; 29, T236A; 30, R247A; 31, H248A; 32, S289A; 33, E294A; 34,R295A; 35, T262A; 36, R297A; 37, D298A. The gel was stained with Coomassie Brilliant Blue.

purified mutant enzymes are presented in Fig. 3.4. Twenty three mutant enzymes (S117A, S120A, R136A, Y147A, F189A, D192A, R193A, E196A, W199A, R200A, E201A, R221A, W228A, M231A, F234A, Y237, M246A, F249A, F253A, W261A, Q284A, R297, and D298A) had less than 8% enzyme activity. They include 10 mutated proteins, which retained less than 1% of Xt-CDH catalytic activity (S120A, R193A, E196A, W199A, E201A, W228A, F234A, F253A, W261A, and D298A). In addition, four mutant enzymes (N144A, E185A, Q252A, and T262A) had enzymatic activity that was 15–45% of Xt-CDH. Ten mutants (T119A, H133A, M177A, K184A, T236A, R247A, H248A, S289A, E294A, and R295A) retained more than 70% of Xt-CDH activity. Of those H133A and K184A were retained enzymatic activities slightly higher than that of Xt-CDH.

3.3.3 Alanine mutants exhibit alteration of the substrate affinity of CDH

To evaluate the influence of mutation on the K_m of CDH for L-Car, the catalytically active mutants were screened for L-Car affinity using assay mixtures of different L-Car concentrations (12, 300, and 900 mM). The specific activity of cell free extracts at excess L-Car concentration was analyzed (Fig. 3.5), and then compared to what was observed for standard assay mixture (i.e. specific activity for CDH at different L-Car concentration (300 and 900 mM) / specific activity of standard assay condition (12 mM)). Figure 3.5a shows that the specific activity of some mutants (N144A, E185A, M246A, Q252A, K184A, T236A, H248A, and E294A) was enhanced by the addition of excess L-Car. As can be seen in the data presented in Fig. 3.5b, 23 mutant enzymes (S117A, S120A, N144A, Y147A, E185A, F189A, R193A, E196A, W199A, R200A, E201A,

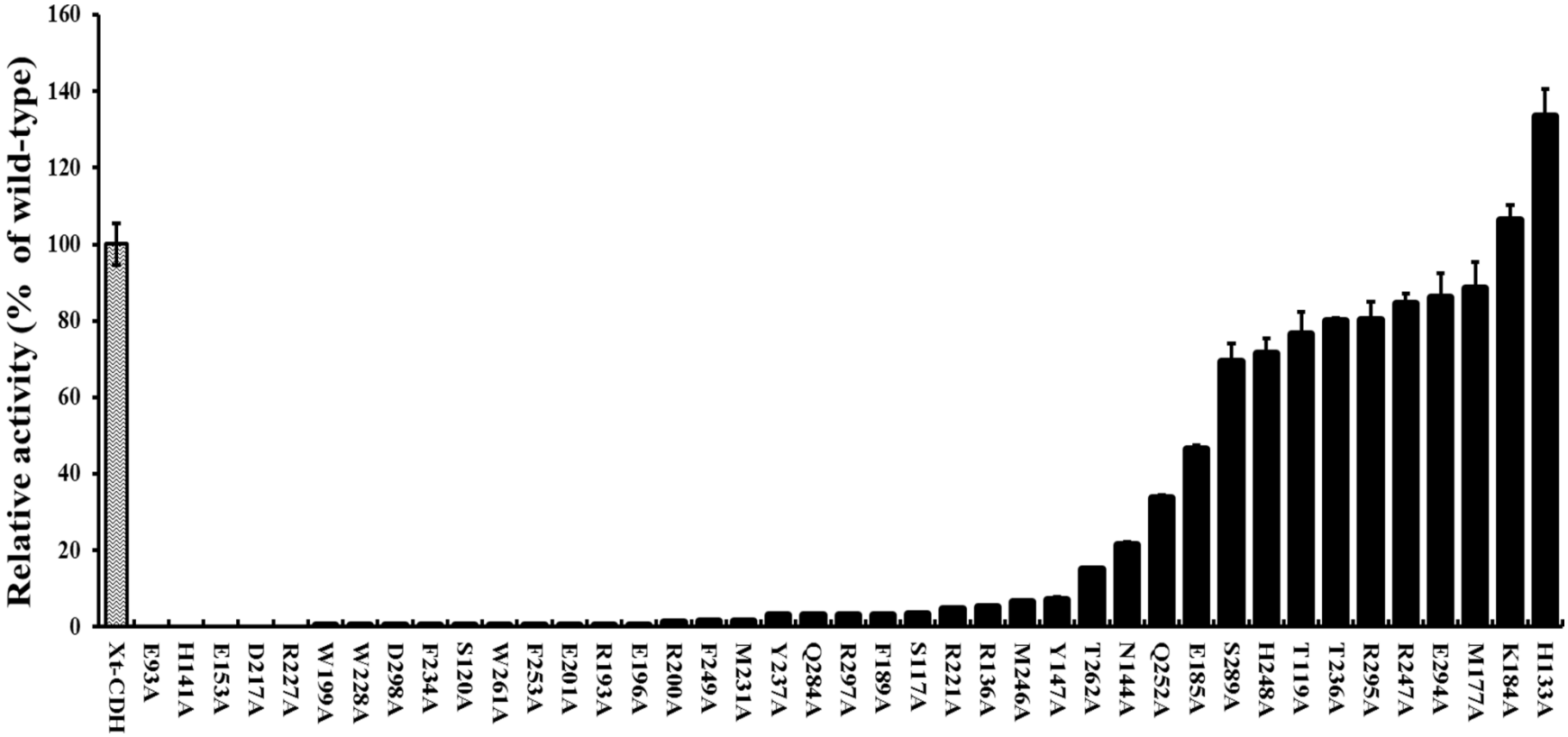

Fig. 3.4 Specific activity of purified Xt-CDH and mutant enzymes. Activity of alanine mutant enzymes were expressed as a percentage of Xt-CDH (specific activity of purified Xt-CDH = 12.96 µmol min^{-1} mg^{-1}). Enzyme activity was measured using standard conditions as described in *Materials and Methods*. The values of enzyme activity are means ± standard deviations for three independent experiments

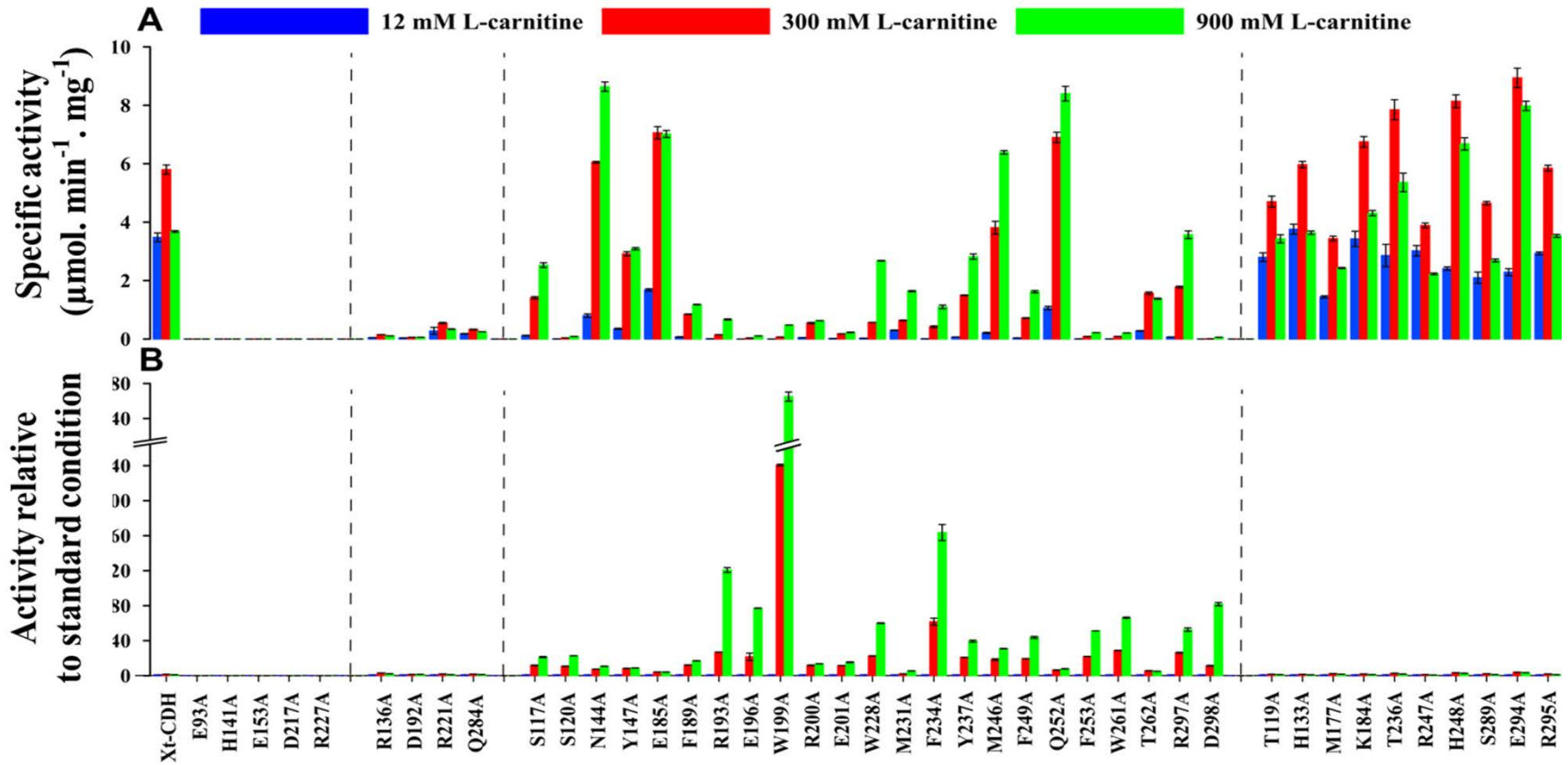

Fig. 3.5 Substrate affinity screening of alanine mutant enzymes **A** specific activity of mutants cell free extract at different L-Car concentrations (12, 300, and 900 mM), and **B** activity relative to standard condition of mutant enzymes (i.e. specific activity for CDH at different L-Car concentrations (12, 300, and 900 mM)/ specific activity of standard assay condition (12 mM)). Except for the L-Car concentration, enzyme activity was measured using standard conditions as described in *Materials and Methods*. The values of enzyme activity are means ± standard deviations for three independent experiments

D298A) showed marked reduction of L-Car affinity, indicating high K_m values. Consequently, these mutant enzymes were subjected to further characterization.

3.3.4 Kinetic analysis

The kinetic parameters K_m and k_{cat} for L-Car and NAD^+ of purified mutant enzymes were performed and are summarized in Table 3.2. Data obtained inferred that all analyzed alanine mutant caused significant increment in the K_m value compared to that of Xt-CDH. The K_m values for E185A, Q252A, and T262A were 40.4, 101.4, and 89.1 mM, respectively, which are equivalent to 4 – 10 fold greater values than that of Xt-CDH. In contrast, these mutant proteins caused 5.8 – 8 fold lower k_{cat}. Therefore, the mutations at positions 185, 252, and 262 were inferred to have a minor effect on the catalytic efficiency compared to other alanine mutant enzymes. The greatest effect was observed with seven other mutant enzymes (R193A, E196A, W199A, F249A, F253A, W261A, and D298A). Their K_m was extremely high, and could not be measured precisely. Therefore, their K_m values for L-Car were assumed to be >2000 mM, the maximum concentration of L-Car used for the measurement of kinetic constants. However, a modest influence on the K_m value was observed from 13 mutant proteins (S117A, S120A, N144A, Y147A, F189A, R200A, E201A, W228A, M231A, F234A, Y237A, M246, and R297A). These enzymes generated a varied alteration in CDH affinity toward L-Car. Their K_m values were 164 – 1056 mM, which was equivalent to 16–105-fold higher values than that of Xt-CDH. In contrast to L-Car affinity, the impacts of introduced Ala mutants on CDH affinity to the cofactor NAD^+ fluctuated (Table 3.2). The mutants S117A, F189A, and R200A were, respectively, increased K_m of NAD^+ to 3.76, 1.04, and 2.25 mM. However, only four mutants (Y147A, W228A,

Table 3.2 Kinetic parameters of Xt-CDH and mutant enzymes

Enzyme	K_m (mM)		k_{cat} (s^{-1})	Enzyme	K_m (mM)		k_{cat} (s^{-1})
	L-Car	NAD^+			L-Car	NAD^+	
Xt-CDH	10.2[a] ± 0.1	0.31[c] ± 0.01	1.279 ± 0.022	**W228A**	1009.5[a] ± 48.4	0.07[h] ± 0.01	0.008 ± 0.001
S117A	307.6[b] ± 13.5	3.76[f] ± 0.07	0.019 ± 0.001	**M231A**	308.8[a] ± 18.4	0.09[f] ± 0.01	0.010 ± 0.001
S120A	667.0[a] ± 20.7	0.66[g] ± 0.08	0.001 ± 0.000	**F234A**	1056.2[a] ± 59	0.09[h] ± 0.02	0.001 ± 0.000
N144A	164.0[a] ± 1.3	0.35[e] ± 0.02	0.079 ± 0.002	**Y237A**	799.7[a] ± 52.2	0.39[g] ± 0.00	0.013 ± 0.001
Y147A	284.0[a] ± 9.1	0.08[f] ± 0.01	0.007 ± 0.001	**M246A**	336.2[a] ± 12.3	0.39[f] ± 0.04	0.044 ± 0.001
E185A	40.4[a] ± 2.1	0.36[d] ± 0.03	0.220 ± 0.009	**F249A**	>2000	n.d.	n.d.
F189A	205.7[a] ± 7.9	1.04[f] ± 0.02	0.009 ± 0.001	**Q252A**	101.4[a] ± 8.1	0.40[e] ± 0.03	0.157 ± 0.016
R193A	>2000	n.d.	n.d.	**F253A**	>2000	n.d.	n.d.
E196A	>2000	n.d.	n.d.	**W261A**	>2000	n.d.	n.d.
W199A	>2000	n.d.	n.d.	**T262A**	89.1[a] ± 2.5	0.53[e] ± 0.04	0.068 ± 0.003
R200A	767.1[b] ± 1.5	2.25[h] ± 0.08	0.001 ± 0.000	**R297A**	830.7[a] ± 49.1	0.26[g] ± 0.01	0.016 ± 0.004
E201A	331.9[a] ± 7.2	0.35[f] ± 0.02	0.003 ± 0.001	**D298A**	>2000	n.d.	n.d.

[a] K_m and k_{cat} were calculated from a linear regression fit to the Michaelis–Menten equation using initial estimates from double reciprocal plots. The K_m for L-Car was evaluated at the final concentration of 5–2000 mM L-Car and NAD^+ concentration of (a) 2 mM and (b) 6 mM. K_m for NAD^+ was measured at NAD^+ final concentration of 0.03–6 mM and L-Car concentration of [c] 12 mM; [d] 100 mM; [e] 300 mM; [f] 600 mM; [g] 1500 mM; and [h] 2000 mM.

[b] n.d.: not detectable

M231A, and F234A) slightly decreased NAD^+ K_m. Their K_m values were ranged from 0.07 – 0.09 mM. Other Ala mutant enzymes (N144A, E185A, E201A, Y237A, M246A, T262A, and R297A) retained K_m values comparable to that of Xt-CDH (0.31 mM).

3.4 DISCUSSION

Both CDHs and HADs belong to the oxidoreductases family. All these enzymes share common features: they are homodimers that require NAD^+/$NADP^+$ as the acceptor substrate. Furthermore, their protein sequences are subdivided into two domains: N-terminal-NAD^+ binding domain and C-terminal catalytic domain. The 3D structures of several HADs have been solved experimentally, but none has been obtained for CDHs. Although, we used homology modeling of CDH to identify the essential residues for catalytic function, in the absence of the experimental information on the tertiary structure confirmation of CDH, it is difficult to select all the important residues for specific functions. These residues are identifiable by the site-directed mutagenesis of functional residues along the entire length of the specific domain. Once identified, these residues can be further modified either to analyze the functional properties of specific residues or to improve the catalytic performance of CDHs for better estimation of L-Car. In this study, the contributions to enzyme activity and substrate affinity of 42 conserved functional residues present in Xt-CDH were analyzed using alanine scanning mutagenesis. The obtained results were discussed in comparison to the reported predicted structure for Xt-CDH.

The results depicted in Fig. 3.4 demonstrated that substitution of different conserved amino acids within Xt-CDH elicited proteins with widely varying dehydrogenation ability. The lowest enzymatic activity observed was less than 1% of

Xt-CDH (S120A, R193A, E196A, W199A, E01A, W228A, F234A, F253A, W261A, and D298A) compared to other mutants such as H133A and K184A, which retained more than 100% of Xt-CDH. It is well known that Ala does not impose extreme electrostatic or steric effects. Actually, Ala eliminates the side chain but does not change the main chain conformation. Furthermore, many researchers demonstrated that the substitution of a single Ala for an amino acid in a protein does not substantially alter the overall fold of the protein (Cunningham and Wells 1989). Consequently, for those mutants with low activity, it was necessary to alter substrate affinity. This assumption is consistent with the screening results of all active mutants toward L-Car affinity using assay mixtures of different L-Car concentrations (12, 300, and 900 mM) (Fig. 3.5). Following the results of catalysis activity and substrate affinity presented in Fig. 3.4, 3.5a, c and Table 3.2, Ala mutant enzymes could be placed into four categories: mutants showing no activity, mutants defective in k_{cat} and substrate affinity, mutants defective in k_{cat} only, and mutants having a similar approach to that of Xt-CDH.

The results for five inactive mutants (E93A, H141A, E153A, D217A, and R227A) implied their crucial roles in the catalytic function of CDH. Of those, equivalent residues of E93 and H141 were observed as catalytic residues in several enzymes of this family (Barycki et al., 2000; 1999), considering that the mutation of homology residue H143 of bacterial diketoreductase to Ala and Lys caused a complete loss of catalytic activity. The mutant enzymes did not influence substrate affinity (Huang et al., 2012). Therefore, we anticipated a similar effect: the complete loss of activity by H141A suggests that imidazole group of H141 is essential for electronic transfer during catalysis. On the other hand, the homology residue of E93 in h-HAD been found to be E110. This residue serves one of six hydrogen bonds present around NAD^+ (Barycki et al., 2000). In our model (Fig. 3.6), E153 served two hydrogen bonds with H141.

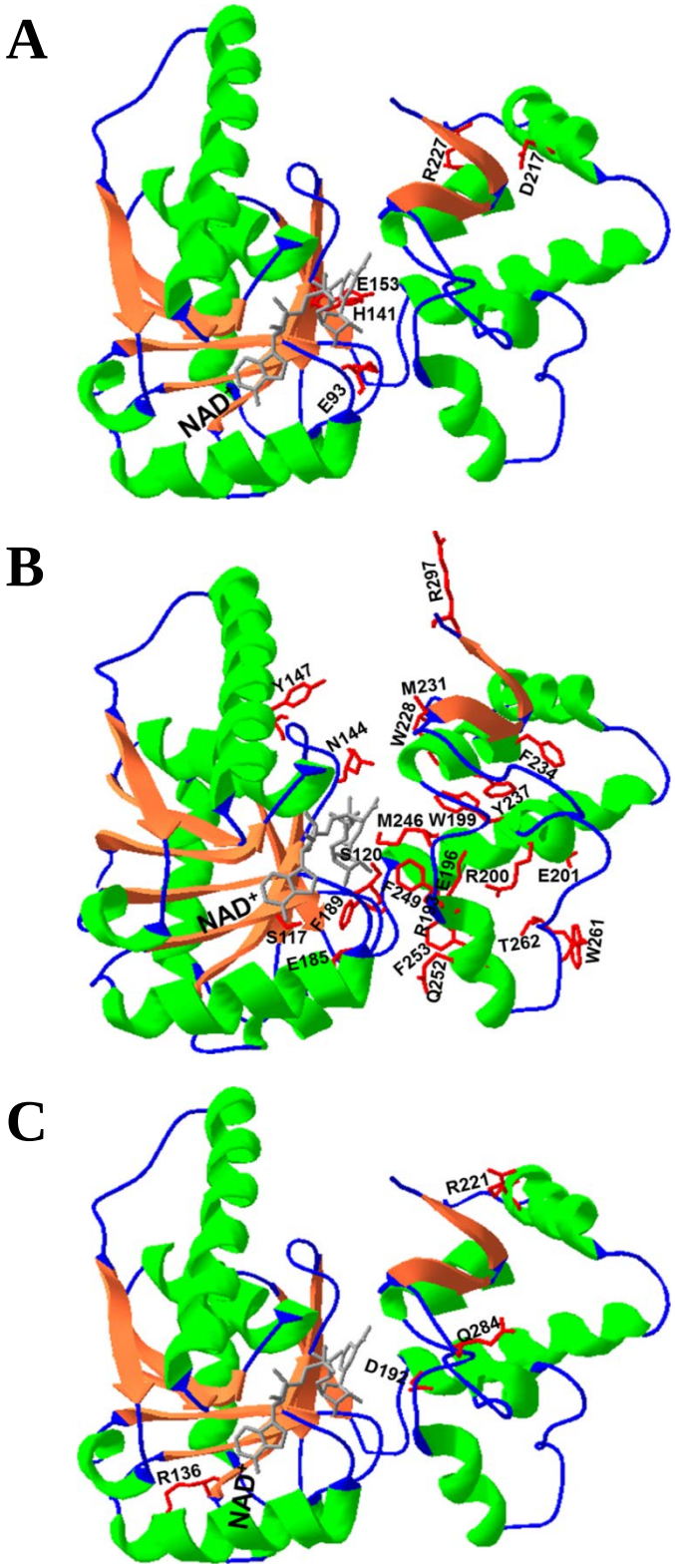

Fig. 3.6 Position of mutated amino acids in the predicted three-dimensional structure of Xt-CDH based on homology modeling using h-HAD (PDB code: 1F0Y) as template Enzyme structures are shown as ribbon diagrams. The mutant residues are displayed in red as a stick model. The bound NAD^+ is shown as a gray stick model. **A** Mutants showing no enzymatic activity. **B** Mutants altered K_m and k_{cat} of Xt-CDH. **C** Mutants defective in k_{cat}

Therefore, abolishing the activity resulting from Ala mutation suggests that this residue is necessary for the proper orientation of catalytically important H141. This phenomenon was observed with an experimentally resolved 3D structure of Human HAD (h-HAD) (Barycki et al., 2001).

Among mutant versions characterized in this study, 23 variants were observed to alter the K_m and k_{cat} of Xt-CDH. These residues scattered through the hypothetical active site channel towards the putative catalytic site of Xt-CDH (Fig. 3.6b). Of those, five residues (R193, E196, W199, F249, and F253) occurred near L-Car (Fig. 3.6b). They were strongly defective in L-Car binding (K_m >200-folds of Xt-CDH) (Table 3.2). Based on the homology model of Xt-CDH, the catalytic domain composed of five alpha-helixes and two beta sheets (Fig. 3.6). These residues clustered in helixes I and IV. These helixes and helix III were predicted to form an L-Car binding moiety. This assumption was based on the proper orientation of the bound substrate to the NAD^+ coenzyme. Therefore, despite the potential inaccuracy of our model, we were able to predict that the side-chains of these residues are near the trimethyl moiety of L-Car. This prediction fits the binding mechanism of different L-Car analogs, which were considered as substrates of enzymes with resolved 3D structures. In such enzymes, the trimethyl group plays a crucial role in substrate binding (Kim et al., 1994; Gadda et al., 2004).

The kinetic data of W261A and D298A mutants were identified as having similar influences on the K_m. The residue D298, which did not appear in our model, is expected to be present near the active site entrance. Therefore, a mutant of this residue might change the overall nature of the active site entrance. In a previous report (Arima et al.,

2010), deletion of the last five C-terminal amino acids of Xt-CDH leads to produce an inactive CDH. Consequently, we assume that additional C-terminal residues might be important either for enzyme activity and/or substrate affinity. However, the properties of W261A variant differ to an extreme degree from what one would have expected based on the structural model. This mutant is expected to have a minimum effect on the substrate binding because it is present far from the substrate. However, W261A exhibited a K_m value more than 200-fold higher than that of Xt-CDH. If our model is correct, the data presented herein are insufficient to explain the effect of this residue. Therefore, we believe that the question surrounding its role is still unresolved. Additional mutants (S117A, S120A, N144A, Y147A, F189A, R200A, E201A, W228A, M231A, F234A, Y237A, M246A, and R297A) were identified as being important for L-Car binding (approximately 16 – 105-fold higher K_m value). Of those, 4 residues are located in helix I (R200 and E201) and III (F234 and Y237), which were predicted to be a part of the active site (Fig. 3.6b). Furthermore, a residue equivalent to S120 in h-HAD (S137) has been implicated in the catalysis site of that enzyme. This is mediated the hydrogen bond of 3-hydroxyl group. Therefore, removal of the catalytically important hydroxyl group might be responsible for the alteration of the substrate affinity.

For mutants defective in k_{cat} only (R136A, D192A, R221A, and Q284A), the homology model (Fig. 3.6c) clearly showed that D192 is essential for CDH activity. The location of D192 near the L-Car is analogous to the catalysis residues N208 in h-HAD and N208 in pig heart HAD (Barycki et al., 2001; 1999). Although R221 and Q284 are located in the catalytic domain, their roles in protein functions remain unclear. An additional analysis is required to completely explain their roles in the catalytic function of Xt-CDH. However, mutant R136A was inferred to be an important residue.

Based on our data, the charged residue R136 appears to take part in the network around NAD^+. In contrast to what was observed for L-Car affinity, the alteration of S117, F189, and R200 in Xt-CDH changed NAD^+ affinity. The homology model suggests close contact between S117 and F189 with the NAD^+ coenzyme, considering that the shorter carbon side chain of the Ala might disrupt the hydrogen bonds that are present in the NAD^+ moiety.

3.5 CONCLUSIONS

In conclusion, comparison of CDHs amino acid sequencing with related proteins of oxidoreductase super family revealed higher homology among CDHs and HADs. Consequently, the present study was designated to test the hypothesis that the conserved residues of CDHs are involved in catalytic function and substrate affinity depending on their position in the predicted structure of Xt-CDH. As expected, 32 mutant enzymes were found to exhibit a substantial decreased in the catalytic activity of Xt-CDH. In particular, alteration of E93, H141, E153, D217, and R227 indicated their crucial roles for proper function of Xt-CDH. The data presented here suggest that key residues and catalytic mechanism of Xt-CDH might be similar to that of h-HAD regardless their differences on the substrate specificity. Furthermore, the results of kinetic parameters for 23 alanine mutants (S117A, S120A, N144A, Y147A, E185A, F189A, R193A, E196A, W199A, R200A, E201A, W228A, M231A, F234A, Y237, M246A, F249A, Q252A, F253A, W261A, T262A, R297, and D298A), were shown to be involved in binding L-Car. The results of these residues confirmed their vital roles to orient L-Car in the correct conformation that allows for optimal catalysis, whereas

R136, D192, and R221, surrounding the bound substrates, are important mainly for catalysis rate of CDH.

In the absence of a crystal structure confirmation for any of the CDHs, the information on the structure-function relation presented in this study will be valuable for additional modification in order to better understand the catalytic mechanism of CDHs. Nevertheless, mutant residues with important functional effects identified in this study required further analysis using more intensive mutagenesis to complete the interpretation of their functional roles.

CHAPTER 4

GENERAL CONCLUSIONS AND FUTURE PROSPECTIVE

4.1 SUMMARY

Naturally occurring quaternary ammonium compound 3-hydroxy-4-trimethylamin-obutyrate (L-Carnitine) has been found in all eukaryotes and several prokaryotes. In mammals, it is an essential nutrient for energy production and fat metabolism in skeletal muscle and heart tissues. The main function of L-carnitine (L-Car) is associated with the transport of fatty acids across the mitochondrial inner membrane. Besides, it accelerates the entry of fatty acids in the form of acyl-carnitine derivatives, thereby resulting in increased β oxidation rate, L-Car assists in maintaining cell pool free of toxic acyl group. In addition, many researchers have found that L-Car has potentially beneficial effects on athletic performance, obesity, ergogenic aid, diabetes, liver healthy, hemodialysis, male infertility, insulin sensitivity, and protein catabolism. Moreover, L-Car deficiency is associated with various conditions, including genetic disorders in the metabolism of fatty acids, branched-chain amino acids, and organic acidurais. Such symptoms are well known to decrease with L-Car supplementation, which raises its concentration in the body, and thereby overcomes these deficiency problems. Consequently, accurate measurement of L-Car in a nutrient survey of foods and in clinical diagnosis is necessary to avoid such health problems.

Several methods have been proven for L-Car assessment such as radioenzymatic, HPLC, and tandem mass spectrophotometry, in addition to enzymatic method. Many of these methods are often not available in clinical laboratories. Therefore, a spectrophotometric method using L-carnitine dehydrogenase (CCDH) has been proposed as the most convenient method for rapid and low-cost assessment of L-Car.

Two CDHs have been detected from soil isolates bacteria identified as *Xanthomonas translucens* (Xt-CDH) and *Rhizobium* sp. (Rs-CDH) in the Faculty of Agriculture, Tottori University, Tottori, Japan. Past works have focused on the purification and characterization of CDHs as well as to decrypt their protein sequences which lead to better understand of CDH properties.

Based on the substrate affinity variation of Xt-CDH (10 mM) and Rs-CDH (1.1 mM), in the first study, we inspect the hypothesis that different residues among the active sites of Xt-CDH and Rs-CDH are important for catalytic activity and/or substrate binding. Database analysis of CDHs primary structures revealed high homology with that of h-HAD. Consequently, we compared the amino acid sequence of Xt-CDH and Rs-CDH with the recognized 3D structure of h-HAD (PDB code: 1F0Y). In the structure of h-HAD, several residues surround the acetoacetyl moiety of the substrate. Of them, seven residues namely Lue157, Phe160, Gly204, Ile206, Val207, Gly239, and Ala240 were selected. These residues matched Gly140, Phe143, Gly188, Ile190, Ala191, Gly223, and Ala224 of Xt-CDH, which correspond to Ala137, Tyr140, Ala185, Val187, Gly188, Ser220, and Phe221 in Rs-CDH. The residues of Xt-CDH were replaced with that of Rs-CDH at the corresponding position and *vice versa*. As expected, Xt-CDH mutants (Xt-F143Y, Xt-I190V/A191G, and Xt-G223S/A224F) significantly elevated the K_m value, these residues implicating in the L-Car binding. In contrast, Rs-CDH mutants were exhibited slight effects on substrate affinity, except for Rs-V187I/G188A, which was devoid of enzyme activity. Among the current mutants version, Xt-F143Y caused a higher increase in the K_m value. Consequently, mutant Xt-F143Y and its corresponding in Rs-CDH (Rs-Y140F) were further characterized. Examination of the optimum pH revealed that the preferred pH of Xt-F143Y was shifted from 9.5 to 8.0 compared to that of corresponding mutant (Rs-Y140F).

Moreover, the kinetic parameters of additional mutants at Xt-F143 and Rs-Y140 (replaced with residues Ala, Gly, Lys, Cys, Ser, Asn, His, Asp, Trp, and Phe) were scrutinized. All Rs-Y140 mutants, except aromatic residues (Rs-Y140F and Rs-Y140W), produced proteins that were almost entirely devoid of enzyme activity and with disrupted affinity to L-Car. Additionally, all Xt-F143 variants, event that of Xt-F143Y and Xt-F143W, exhibit consistent reduction in enzyme activity and substrate affinity. Analysis of these mutants provides a better understanding of the structural and functional relationships between CDHs and its ligand L-Car. The effects of residues Xt-F143 and Rs-Y140 on catalytic activity and substrate affinity were unexpected. As the aromatic property of these residues does not the sole factor, results emphasize the important role for physical properties of these residues, such as size, on the substrate recognition.

Second site-directed mutagenesis study was attempted to examine the roles of functional conserved residues. A total of 42 residues have been selected based on their strict homology among the CDHs and bacterial 3-hydroxyacyl-CoA dehydrogenase. Alanine scanning mutagenesis approach has been applied by substitution of residues with alanine residues. The resultant mutants were analyzed for catalytic activity. Five of the mutant enzymes were inactive (E93A, H141A, E153A, D217A, and R227A). Active mutants were evaluated for their influence on L-Car affinity using assay mixtures of different L-Car concentration (12, 300, and 900 mM). Based on the obtained results, mutants could be categorized into three groups; mutants influenced k_{cat} only (R136A, D192A, R221A, and Q284A), mutants altered k_{cat} and K_m for L-Car (S117A, S120A, N144A, Y147A, E185A, F189A, R193A, E196A, W199A, R200A, E201A, W228A, M231A, F234A, Y237, M246A, F249A, Q252A, F253A, W261A, T262A, R297, and D298A), and mutants had similar approach to that of Xt-CDH

(T119A, H133A, M177A, K184A, T236A, R247A, H248A, S289A, E294A, and R295A). The mutant enzymes affected the K_m values were subjected for steady kinetics analysis. The analytical data implied that all mutants had increased K_m value. Of those, R193A, E196A, W199A, R200A, F249A, and F253A that produced the greatest L-Car affinity disruption (K_m >200-folds of Xt-CDH) clustered near the putative active site. According to the reported data of this part of the study, we are able to underscore the important conserved residues for substrate affinity of the entire catalytic domain, which could be considered as blueprint for the rational of further intensive mutagenesis studies.

Overall, the uses of the site-directed mutagenesis and homology model in the two studies of this dissertation have contributed significantly to our understanding of the catalytic mechanism and substrate binding of CDH. In both studies, the data obtained from the predicted structures and kinetic study of CDH was shown to be applicable to improve the catalytic function and substrate affinity of CDH as a superior tool for L-Car assessment.

4.2 FUTURE PROSPECTIVE

The current dissertation lays the framework for future investigations that could be include the following set of experiments:

First, further mutational studies of the residues influenced substrate affinity (K_m) and *catalytic activity* (k_{cat}). In chapter 3 of current project, alanine substitution of 23 amino acids drastically influenced both K_m and k_{cat} of Xt-CDH. Of them, 15 residues were closed to the bound substrates or in the entrance of the active site channel. Works have

been initiated to scrutinize effects of site-directed random mutagenesis on the catalytic activity and substrate affinity. The library of mutant enzymes have been constructed (not discussed in the current dissertation), but not characterized yet. With the efficient screening of mutant protein library in hand, a number of opportunities could be pursued. A novel CDH with high substrate affinity or enzymatic activity could be obtained from any of the mutation and then would be characterized with further kinetics parameters

Second, investigation effects of the current version of alanine mutation on the CDH stability. The study in Chapter 3 investigates effect of alanine mutation of conserved residues on catalytic activity and substrate affinity but did not illustrate the effects of mutation on CDH thermal stability. Examination of this factor for alanine mutants will help to understand the impact of alanine mutation on substrate affinity especially for residues that are distant from the active site such as Trp261. In general, we would expect to find that mutations to any of such residues would influence CDHs thermal stability. Consequently, further studies should induce a mutation to improve stability of CDH.

Third, further investigation of resides varied in the active site of Xt-CDH and Rs-CDH. Chapter 2 screened the roles of several residues of CDHs active sites on substrate affinity. Xt-F143Y, Xt-I190V/A191G, Xt-G223S/A224F, Rs-V187I/G188A were found to be important for catalytic activity and substrate affinity. The detailed analysis clarified the possible roles of Xt-F143Y but did not answer the question around the function of other mutants. Future studies should include single point mutation followed with collection of steady kinetic parameters. Modification of these residues particularly in Xt-CDH will reveal narrowest active site. We could hypothesize that mutation to larger residues near the active site instead of smaller one could effectively influenced

interaction with substrate.

REFERENCES

Abdenur, J. E., Chamoles, N. A., Guinle, A. E., Schenone, A.B., Fuertes, A. N. J. (1998). Diagnosis of isovaleric acidaemia by tandem mass spectrometry: False positive result due to pivaloylcarnitine in a newborn screening programme. *Journal of Inherited Metabolic Disease*, 21: 624–630.

Agarwal, A., Said, T. M. (2004). Carnitines and male infertility. Review Article. *Reproductive Biomedicine Online*, 8: 376–384.

Argos, P. (1988). An investigation of protein subunit and domain interfaces. *Protein Engineering*, 2: 101–113.

Armia, J., Uesumi, A., Mitsuzumi, H., and Mori, N. (2010). Biochemical characterization of L-carnitine dehydrogenases from *Rhizobium* sp. and *Xanthomonas translucens*. *Bioscience, Biotechnology, and Biochemistry*, 74: 1237–1242.

Arnold, K., Bordoli, L., Kopp, J., and Schwede, T. (2006). The SWISSMODEL workspace: a web-based environment for protein structure homology modelling. *Bioinformatics*, 22: 195–201.

Aurich, H., and Kleber, H. P. (1968). Reiningung und Eigenschaften der Carnitindehydrogenase aus Pseudomonas aeruginosa. *European Journal of Biochemistry*, 6: 196–201.

Aurich, H., Kleber, H. P., Sorger, H., and Tauchert, H. (1968). Purification and properties of carnitine dehydrogenase from *Pseudomonas aeruginosa*. *European Journal of Biochemistry*, 6: 196–201.

Barycki, J. J, O'Brien K. L., Birktoft, J. J., Strauss, A. W., Banaszak, L. J. (1999). Pig heart short chain L-3-hydroxyacyl-CoA dehydrogenase revisited: Sequence analysis and crystal structure determination. *Protein Science*, 8: 2010–2018.

Barycki, J. J., O'Brien, K. L., Strauss, A. W., and Banaszak, L. J. (2000). Sequestration of the active site by interdomain shifting (Crystallographic and spectroscopic evidence for distinct conformations of L-3-hydroxyacyl-CoA dehydrogenase). *Journal of Biological Chemistry*, 275: 27186–27196.

Barycki, J. J., O'Brien, L. K., Strauss, A. W., Banaszak, L. J. (2001). Glutamate 170 of human L-3-hydroxyacyl-CoA dehydrogenase is required for proper orientation of

the catalytic histidine and structural integrity of the enzyme. *Journal of Biological Chemistry*, 276: 36718–36726.

Bieber, L. L. (1988). Carnitine. *Annual Review of Biochemistry*, 57: 261–283.

Birktoft, J. J., Holden, H. M., Hamlin, R., Xuong, N. H., and Banaszak, L. J. (1987). Structure of L-3-hydroxyacyl-coenzyme A dehydrogenase: preliminary chain tracing at 2.8 Å resolution. *Proceedings of the National Academy of Sciences of the United State of America*, 84: 8262–8266.

Bradford, M. M. (1976). A rapid and sensitive method for the quantitation of microgram quantities of protein utilizing the principle of protein-dye binding. *Analytical Biochemistry*, 72: 248–256.

Bremen, R. H., Vienna, E. K. (1990). Carnitine: biochemical, analytical, experimental and clinical aspects [Review]. *Journal of Clinical Chemistry and Clinical Biochemistry*, 28: 289–36.

Bremer, J. (1983). Carnitine-metabolism and functions. *Physiological Reviews,* 63: 1420–1480.

Calo, L. A., Vertolli, U., Davis, P. A., Savica, V. (2012). L-carnitine in hemodialysis patients. *Hemodialysis International*, 16: 428 –434.

Casillas, E. R. (1973). Accumulation of carnitine by bovine spermatozoa during maturation in the epididymis. *Journal of Biological chemistry*, 248: 8227–32.

Cederblad, G., and Lindstedt, S. (1972). A method for the determination of carnitine in the picomole range. *Clinica Chimica Acta*, 37: 235–43.

Cerretelli, P., and Marconi, C. (1990). L-carnitine supplementation in humans. The effects on physical performance. *International Journal of Sports Medicine*, 11: 1–14.

Chace, D. H., DiPerna, J. C., Kalas, T. A., Johnson, R. W., and Naylor, E. W. (2001). Rapid Diagnosis of Methylmalonic and Propionic Acidemias: Quantitative Tandem Mass Spectrometric Analysis of Propionylcarnitine in Filter-Paper Blood Specimens Obtained from Newborns. *Clinical Chemistry*, 47: 2040–2044.

Chiu Ming, N. G., Blackman M. R., Wang, C., and Swerdloff, S. (2004). The role of carnitine in the male reproductive system. *Annals of the New York Academy of Sciences*, 1033: 177–188.

Christianson, D. D., Wall, J. S., Cavins, J. F., and Dimler, R. J. (1963). Chromatography of quaternary nitrogen compounds on buffered cation-exchange resins. *Journal of Chromatography A*, 10: 432–438.

Cunningham, B. C., Wells, J. A. (1989). High-resolution epitope mapping of hGH-receptor interactions by alanine-scanning mutagenesis. *Science*, 244: 1081–1085.

David, L., Michae, N., and Cox, M. (2005). Lehninger Principles of Biochemistry. *W.H. Freeman and Company, New York.*

Dayanand, C.D., Krishnamurthy, N., Ashakiran, S., and Shashidhar, K.N., (2011). Carnitine: A novel health factor-An overview. *International Journal of Pharmaceutical and Biomedical Research*, 2: 79–89.

de Sousa, C., English, N.R., Stacey, T. E., and Chalmers, R. A. (1990). Measurement of L-carnitine and acylcarnitines in body fluids and tissues in children and in adults. *Clinica Chimica Acta*, 187: 317– 28.

Demarquoy, J., Georges, B., Rigault, C., Royer, M-C., Clairet, A., Soty, M., Lekounoungou, S., and Borgne, F. L. (2004). Radioisotopic determination of L-carnitine content in foods commonly eaten in Western countries. *Food Chemistry*, 86: 137–142.

Duran, M., Loof, N. E., Ketting, D., and Dorland, L. (1990). Secondary carnitine deficiency. *Journal of Clinical Chemistry and Clinical Biochemistry*, 28: 359–363.

Eichler, K., Bourgis, F., Buchet, A., Kleber, H. P., and Mandrand-Berthelot, M. A. (1994). Molecular characterization of the cai operon necessary for carnitine metabolism in *Escherichia coli*. *Molecular Microbiology*, 13: 775–786.

Elssner, T., Engemann, C., Baumgart, K., and Kleber, H-P. (2001). Involvement of Coenzyme A Esters and Two New Enzymes, an Enoyl-CoA Hydratase and a CoA-Transferase, in the Hydration of Crotonobetaine tol-Carnitine by Escherichia coli. *Biochemistry*, 40: 11140–11148.

Englard, S. (1979). Hydroxylation of γ-butyrobetaine to carnitine in human and monkey tissues. *FEBS Letters*, 102: 297–300.

Escobar, W. A., Miller, J., and Fink, A. L. (1994). Effects of site-specific mutagenesis of tyrosine 105 in a Class A f-lactamase. *Biochemical Journal, 303*, 555–558.

Fiona, F., Clark, G. C., and Victor, A. Z. (1997). Topology of carnitine palmitoyl-transferase I in the mitochondrial outer membrane. *Biochemical Journal*, 323: 711–718.

Fraenkel, G. (1954). The distribution of vitamin BT (carnitine) throughout the animal kingdom. *Archives of Biochemistry and Biophysics*, 50: 486–495.

Fraenkel, G., and Friedman, S. (1957). Carnitine. Vitamins and Hormones, 15: 73–118.

Fraenkel, G., Blewett, M., and Coles, M. (1948). BT, a new vitamin of the group and its relation to the folic acid group, and other anti-anaemia factors. *Nature*, 161: 981–983.

Friedman, S. (1958). Determination of carnitine in biological materials. *Archives of Biochemistry and Biophysics*, 75: 24–30.

Gadda, G., Powell, N. L., Monon, P. (2004). The trimethyl-ammonium head group of choline is a major determinant for substrate binding and specificity in choline oxidase. *Arch Biochem Biophys*, 430: 264–273.

Goldberg, J. M., Swanson, R. V., Goodman, H. S., and Kirsch, J. F. (1991). The Tyrosine-225 to Phenylalanine mutation of *Escherichia coli* aspartate aminotransferase results in an alkaline transition in the spectrophotometric and kinetic p*K*a values and reduced values of both k_{cat} and K_m. *Biochemistry*, 30: 305–312.

Goldmann, A., Boivin, C., Fleury, V., Message, B., Lecoeur, L., Maille, M., and Tepfer, D. (1991). Betaine Use by Rhizosphere Bacteria: Genes Essential for Trigonelline, Stachydrine, and Carnitine Catabolism in Rhizobium meliloti Are Located on pSym in the Symbiotic Region. *Molecular Plant- microbe Interactions*, 4: 571–578.

Golper, T. A., Goral, S., Becker, B. N., and Langman, C. B. (2003). Lcarnitine treatment of anemia. *American Journal of Kidney Diseases*, 41: 27–34.

Goulas, P. (1988). Purification and properties of carnitine dehydrogenase from *Pseudomonas putida*. *BBA - Protein Structure and Molecular Enzymology*, 957: 335–339.

Grimont, P. A. D., Vancanneyt, M., Lefevre, M., Vandemeulebroecke, K., Vauterin, L., Brosch, R., Kersters, K., Grimont, F. (1996). Ability of Biolog and Biotype-100 Systems to Reveal the Taxonomic Diversity of the Pseudomonads. *Systematic and Applied Microbiology*, 19: 510–527.

Guan, Y., Hickey, M. J., Borgstahl, G. E. O., Hallewell, R. A., Lepock, J. R., O'Connor, D., Hsieh, O. Y., Nick, H. S., Silverman, D. N., and Tainer, J. A. (1998). Crystal

structure of Y34F mutant human mitochondrial manganese superoxide dismutase and the functional role of tyrosine 34. *Biochemistry*, 37: 4722–4730.

Gulewitch, V. S., Krimberg, R. (1905). Zur Kenntnis der Extraktionsstoffe der Muskeln. 2.Mitteilung über das Carnitin. *Hoppe-Seyler's Zeitschrift fur physiologische Chemie*, 45: 326–330.

Hanschmann, H., and Kleber, H. P. (1997). Purification and characterization of D(+)-carnitine dehydrogenase from Agrobacterium sp.-a new enzyme of carnitine metabolism. *Biochimica Biophysica Acta*, 1337: 133−142.

Hanschmann, H., Doss, A., and Kleber, H.P. (1994). Occurrence of carnitine dehydrogenases with different steriospecificity in Agrobacterium sp. *FEMS Microbiology Letters*, 119: 371–376.

Hanschmann, H., Ehricht, R., and Kleber, H. P. (1996). Purification and properties of L(−)-carnitine dehydrogenase from Agrobacterium sp. *Biochimica Biophysica Acta- General Subjects*, 1290: 177–183.

Horne, D. W. and Broquist, H. P. (1973). Role of lysine and e-N-trimethyllysine in carnitine biosynthesis. Studies in Neurospora crassa. *Journal of biological chemistry*, 248: 2170–2175.

Houriyou, K., Takahashi, M., Mizoguchi, J., and Imamura, S. (1993). Essentially pure microorganism capable of producing carnitine dehydrogenase. *Japan patent*, 161492–A/1.

Huang, H., Lu, Z., Liu, N., Chen, Y. (2012). Identification of important residues in diketoreductase from *Acinetobacter baylyi* by molecular modeling and site-directed mutagenesis. *Biochimie*, 94: 471–478.

Jakobs, B. S., and Wanders, R.J.A. (1995). Fatty acid beta-oxidation in peroxisomes and mitochondria: the first, unequivocal evidence for the involvement of carnitine in shuttling propionyl-CoA from peroxisomes to mitochondria. Biochemical and *Biophysical Research Communication*, 213: 1035–1041.

Jung, H., Jung, K., Kleber, H. P., and Sorger, H. (1990). Reinigung und eigenschaften der carnitindehydrogenase aus Pseudomonas aeruginosa. *European Journal of Biochemistry*, 6: 196–201.

Jung, H., Buchholz, M., Clausen, J., Nietschke, M. Revermann, A., Schmid, R., and Jung, K. (2002). CaiT of *Escherichia coli*, a New Transporter Catalyzing L-

Carnitine/γ-Butyrobetaine Exchange. *The Journal of Biological Chemistry*, 277: 39251–39258.

Kanai, R., Haga, K., Akiba, T., Yamane, K., and Harata, K. (2004). Role of Phe283 in enzymatic reaction of cyclodextrin glycosyltransferase from alkalophilic *Bacillus* sp.1011: Substrate binding and arrangement of the catalytic site. *Protein Science*, 13: 457–465.

Kendler, B.S. (1986). Carnitine: an overview of its role in preventive medicine. *Preventive Medicine*, 15: 373–390.

Kim, K. S., Lee, J. Y., Lee, S. J., Ha, T. K., Kim, D. H. (1994). On binding forces between aromatic ring and quaternary ammonium compound. *Journal of American Chemistry Society*, 116: 7399–7400.

Kleber, H. P. (1997). Bacterial carnitine metabolism. *FEMS Microbiology Letters*, 147: 1–9.

Kleber, H. P., Seim, H., Aurich, H., and Strack, E. (1977). Verwertung von Trimethylammoniumverbindungen durch Acenetobacter calcoaceticus. *Archive of Microbiology*, 112: 201−206.

Lever, M., Bason, L., Leaver, C., Hayman, C. M., and Chambers, S. T. (1992). Same day batch measurement of glycine betaine, carnitine, and other betaines in biological material. *Analytical Biochemistry*, 205: 14–21.

Lindstedt, G., Lindstedt, S., Midtvedt, T., and Toft, M. (1967). The formation and degradation of carnitine in Pseudomonas. *Biochemistry*, 6: 1262–1270.

Magoulas, P. L., and El-Hattab, A. W. (2012). Systemic primary carnitine deficiency: an overview of clinical manifestations, diagnosis, and management. *Orphanet Journal of Rare Diseases*, 7: 68 –73.

Marquis, N. E., Frizt, B. (1964). Enzymological determination of free carnitine concentration in rat tissues. *Journal Lipid Research*, 5:184–7.

Matsumoto, K., Yamada, Y., and Takahashi, M. (1990). Fluorometric determination of carnitine in serum with immobilized camitine dehydrogenase and diaphorase. *Clinica Chimica Acta*, 36: 2072–2076.

Matsumoto, Y., Amano, I., Hirose, S., Tsuruta, Y., Hara, S., Murata, M., and Imai, T. (2001). Effects of L-carnitine supplementation on renal anemia in poor responders to erythropoietin. *Blood Purification*, 19: 24-32.

McEntyre, C. J., Lever, M., and Storer, M. K. (2004). A high performance liquid chromatographic method for the measurement of total carnitine in human plasma and urine. *Clinica Chimica Acta*, 344: 123–130.

Mcgan-j, J. D., and Daniel, W.F. (1976). An improved and simplified radioisotopic assay for the determination of free and esterifled carnitine. *Journal of Lipid Research*, 17: 277–281.

McGarry, J. D., and Brown, N. F. (1997). The mitochondrial carnitine palmitoyl-transferase system. From concept to molecular analysis. *European Journal of Biochemistry*, 244: 1–14.

Mehlman, M. A., and Wolf, G. (1962). Studies on the distribution of free carnitine and the occurrence and nature of bound carnitine. *Archives of Biochemistry and Biophysics*, 98: 146–153.

Meier, P. J. (1987). D-Carnitin, harmlos? Gitzelmann R, Baerlocher K, Steinmann B. (Eds.) Carnitin in der Medizin. Schattauer Verlag, Stuttgart, New York, 101-104.

Minkler, P. E., and Hoppel, C.L. (1993). Quantification of Free Carnitine, Individual Short- and Medium-Chain Acylcarnitines, and Total Carnitine in Plasma by High-Performance Liquid Chromatography. *Analytical Biochemistry*, 212: 510–518.

Minkler, P. E., Brass, E. P., Hiatt, W. R., Ingalls, S. T., and Hoppel, C.L. (1995). Quantification of carnitine, acetylcarnitine, and total carnitine in tissues by high-performance liquid chromatography. *Analytical Biochemistr*, 231: 315–22.

Minkler, P. E., Ingalls, S. T., and Hoppel, C. L. (1987). Determination of total carnitine in human urine by high performance liquid chromatography. *Journal of Chromatography B: Biomedical Sciences and Applications*, 420: 385–393.

Mitchell, M. E. (1978). Carnitine metabolism in human subjects. I. Normal metabolism. *American Journal of Clinical Nutrition*, 31: 293–306.

Miura-Fraboni, J., and Englard, S. (1983). Quantitative aspects of γ-butyrobetaine and D- and L-carnitine utilization by growing cell culture of *Acenetobacter calcoaceticus* and *Pseudomonas putida*. *FEMS Microbilogy Letters*, 18: 113–116.

Mori, N., Kasugai, T., Kitamoto, Y., and Ichikawa, Y. (1988a). Purification and Some Properties of Carnitine Dehydrogenase from Xanthomonas translucens. *Agricultural and Biological Chemistry*, 52: 249–250.

Mori, N., Mitsuzumi, H., and Kitamoto, Y. (1994). Purification and properties of carnitine dehydrogenase from *Pseudomonas* sp. YS-240. *Journal of Fermentation and Bioengineering,* 78: 337–340.

Mori, N., Shirota, K., Kitamoto, Y., and Ichikawa, Y. (1988b). Cloning and expression in *Escherichia coli* of the carnitine dehydrogenase gene from *Xanthomonas translucens. Agricultural and Biological Chemistry,* 52: 851–852.

Murthy, M. S., and Pande, S. V. (1987). Malonyl-CoA binding site and the overt palmitoyltransferase activity reside on the opposite sides of the outer mitochondrial membrane. *Proceedings of the National Academy of Science,* 84: 378–382.

Nelson, P. J., Pruitt, R. E., Henderson, L. R. L., Jenness, R., Henderson, L. M. (1981). Effect of ascorbic acid deficiency on the in vivo synthesis of carnitine. *Biochimca. Biophysica. Acta*, 672: 123–127.

Nikolaos, S., George, A., Telemachos, T., Maria, S., Yannis, M., and Konstantinos, M. (2000) Effect of L-carnitine supplementation on red blood cells deformability in hemodialysis patients. *Renal Failure,* 22: 73–80.

Ogier de Baulny, H., Saudubray, J. M. (2002). Branched-chain organic acidurias. *Semin Neonatol,* 7: 65-74.

Olson, J.A. (1966). Lipid metabolism. *Annual Review of Biochemistry,* 35: 559–558.

Pace, C. N., Horn, G., Hebert, E. J., Bechert, J., Shaw, K., Urbanikova, L., Martin, J. S., and Sevcik, J. (2001). Tyrosine hydrogen bonds make a large contribution to protein stability. *Journal of Molecular Biology,* 312: 393–404.

Palmieri L, Ronca, F., Malengo, S., and Bertelli, A. (1994) Protection of beta-thalassaemic erythrocytes from oxidative stress by propionyl carnitine. *International journal of tissue reactions,* 16: 121–129.

Panter, R. A., and Mudd, J. B. (1969). Carnitine levels in some higher plants. *FEBS Letters,* 5: 169–170.

Parvin, R., and Pande, S. V. (1977). Microdetermination of (-) Carnitine and Carnitine Acetyltransferase Activity. *Analytical Biochemistry,* 79: 190–201.

Paul, H. S., Sekas, G., Siamak A., and Adibi, S. A. (1992). Carnitine biosynthesis in hepatic peroxisomes. Demonstration of γ-butyrobetaine hydroxylase activity. *European Journal of Biochemistry,* 203: 599–605.

Paulson, D. J. and Shug, A. L. (1981). Tissue specific depletion of L-carnitine in rat heart and skeletal muscle by D-carnitine. *Life Sciences*, 28: 2931–2938.

Pearson, N., Chase, J. F. A., and Tubbs, P. K. (1974). (-)-Carnitine by DTNB method. In: Bergmeyer, H. U., ed. Methods of enzymatic analysis. New York Academic Press, 1762–1764.

Peter, L., Douglas, L. J., Eric, M. Y., and Sandra, S. (2012). Carnitine deficiency presenting with encephalopathy and hyperammonemia in a patient receiving chronic enteral tube feeding: a case report. *Journal of Medical Case Reports*, 6: 227–230.

Pons, R., and De Vivo, D. C. (1995). Primary and secondary carnitine deficiency syndromes. *Journal of Child Neurology*, 10: 2S8–2S24.

Preusser, A., Wagner, U., Elssner, T., and Kleber, H. P. (1999). Crotonobetaine reductase from Escherichia coli consists of two proteins. *Biochimica Biophysica Acta-Protein Structure and Molecular Enzymology*, 1431: 166–178.

Price, N., Van der Leij, F., Jackson, V., Corstorphine, C., Thomson, R., Sorensen, A., and Zammit, V. (2002). A novel brain-expressed protein related to carnitine palmitoyl-transferase I. *Genomics*, 80: 433–442.

Ramsay, R. R., and Arduini, A. (1993). The carnitine acyltransferases and their role in modulating acyl-CoA pools. *Archives of Biochemistry and Biophysics*, 302: 307–314.

Ramsay, R. R., Gandour, R. D., Van der Leij, F. R. (2001). Molecular enzymology of carnitine transfer and transport. *Biochemica Biophysica Acta, Protein Structure and Molecular Enzymology*, 1546: 21–43.

Rebouche, C. J. (1992). Camitine function and requirements during the life cycle. *The Federation of American Societies for Experimental Biology Journal*, 6*:* 3379–386.

Rebouche, C. J. (1996). Role of carnitine biosynthesis and renal conservation of carnitine in genetic and acquired disorders of carnitine metabolism. In Carnitine : Pathobiochemical Basics and Clinical Applications (Seim, H. and Loster, H., eds.), pp. 111–121, Ponte Press, Bochum

Rebouche, C.J. and Engel, A.G. (1980). Tissue distribution of carnitine biosynthetic enzymes in man. *Biochimica Biophysica Acta*, 630: 22–29.

Regitz, V., Shug, A. L., and Fleck, E. (1990). Defective Myocardial Carnitine Metabolism in Congestive Heart Failure Secondary to Dilated Cardiomyopathy and to Coronary, Hypertensive and Valvular Heart Diseases. *The American Journal of Cardiology*, 65: 755 –760.

Rinaldo, P., Matern, D., and Bennett, M. J. (2002). Fatty acid oxidation disorders. *Annual reviewers-Physiology*, 64: 477–502.

Rizzon, P., Biasco, G., Dibiase, M., Boscia, F., Rizzo, U., Minafra, F., Bortone, A., Siliprandi, N., Procopio, A., Bagiella, E., and Corsi, M. (1989). High doses of L-carnitine in acute myocardial infarction: metabolic and antiarrhythmic effects. *European Heart Journal*, 10: 502–508.

Robbert, H., Le Marrec, C., Blanco, C., and Jabbar, M. (2000). Glycine betaine, carnitine, and choline enhance salinity tolerance and prevent the accumulation of sodium to a level inhibiting growth of *Tetragenococcus halophila*. *Applied and Environmental Microbiology*, 66: 509–517.

Ronca, F., Palmieri, L., Malengo, S., and Bertelli, A. (1994). Effect of L-propionyl carnitine on in-vitro membrane alteration of sickle-cell anaemia erythrocytes. *International journal of tissue reactions*, 16: 187–194.

Sachan, D. S. and Hoppel, C. L. (1980). Carnitine biosynthesis: Hydroxylation of N6-trimethyl-lysine to 3-hydroxy-N6-trimethyl-lysine. *Biochemical Journal*, 188: 529–534.

Sanchez-Hernandez, L., Garcia-Ruiza, C., Cregoa, A. L., Marina, M. L. (2010). Sensitive determination of d-carnitine as enantiomeric impurity of levo-carnitine in pharmaceutical formulations by capillary electrophoresis–tandem mass spectrometry. *Journal of Pharmaceutical and Biomedical Analysis*, 53: 1217–1223.

Santer, R., Fingerhut, R., Lässker, U., Wightman, P. J., Fitzpatrick, D. R., Olgemöller, B., and Roscher, A. A. (2003). Tandem Mass Spectrometric Determination of Malonylcarnitine: Diagnosis and Neonatal Screening of Malonyl-CoA Decarboxylase Deficiency. *Clinical Chemistry*, 49: 660–662.

Schopp, W., Schafer, A. (1985). Quantitative Bestimmung von L-carnitine mit Hi]fe von carnitindehydrogenase aus *Pseudomonas putida*. *Fresenius' Zeitschrift für Analytische Chemie*, 320: 285–289.

Schwabedissen-Gerbling, H., Gerhardt, B. (1995). Purification and characterization of carnitine acyltransferase from higher plant mitochondria. *Phytochemistry*, 39: 36–43.

Seim, H., Loster, H., Claus, R., Kleber, H. P., and Strack, E. (1982). Formation of γbutyrobetaine and trimethylamine from quaternary ammonium compounds structure-related to L-carnitine and choline by Proteus vulgaris. *FEMS Microbiology Letters*, 13: 201–205.

Setyahadi, S., Ueyama, T., Arimoto, T., Mori, N., and Kitamoto, Y. (1997). Purification and properties of a new enzyme, D-carnitine dehydrogenase from *Agrobacterium* sp. 525a. *Bioscience, Biotechnology and Biochemistry,* 61: 1055–1058.

Setyahadi. S., Harada, E., Mori, N., Kitamoto, Y. (1998). Production of L-carnitine from D-carnitine by partially purified D- and L-carnitine dehydrogenase of *Agrobacterium* sp. 525a. *Journal of Molecular Catalysis B: Enzymatic*, 4: 205–209.

Shimizu, N., Yamaguchi, S., Orii, T. (1994). A study of urinary metabolites in patients with dicarboxylic aciduria for differential diagnosis. *Pediatrics International*, 36: 139–145.

Shug, A. L., Thomsen, J. H., Folts, J. D., Bittar, N., Klein, M. I., Koke, J. R., and Huth, P.J. (1978). Changes in tissue levels of carnitine and other metabolites during myocardial ischemia and anoxia. *Archives of Biochemistry and Biophysics,* 187: 25–33.

Spagnoli, L. G., Corsi, M., Villaschi, S., Palmieri, G., and Maccari, F. (1982). Myocardial carnitine deficiency in acute myocardial infarction. *The Lancet*, 1: 1419–1420.

Staney, C. A. (2004). Carnitine Deficiency Disorders in Children. *Annals of the New York Academy of Sciences*, 1033: 42–51.

Steiber, A., Kerner, J., and Hoppel, C. L. (2004). Carnitine: a nutritional, biosynthetic, and functional perspective. *Molecular Aspects of Medicine,* 25: 455–473.

Stenmark, P., Gurmu, D., Nordlund, P. (2004). Crystal Structure of CaiB, a Type-III CoA Transferase in Carnitine Metabolism. *Biochemistry,* 43: 13996–14003.

Strack, E., Lorenz, I., and Rotzsch, W. In Protides of the Biological Fluids, 7th Colloquium, edited by H. Peeters. Elsevier, Amsterdam, 1960: 248–251.

Suzuki, Y., Masumura, Y., Kobayashi, A., Yamazaki, N., Harada, Y., Osawa, M. (1982). Myocardial carnitine deficiency in chronic heart failure. *The lancet*, 319: 116–119.

Takahashi, M., Ueda, S., Misaki, H., Sugiyama, N., Matsumoto, K., Matsuo, N., and Murao, S. (1994). Carnitine determination by an enzymatic cycling method with carnitine dehydrogenase. *Clinical Chemistry*, 40: 817–821.

Taskinen, J. P., Kiema, R. T., Hiltunen, J. K., and Wierenga, R. K. (2006). Structural Studies of MFE-1: the 1.9 Å Crystal Structure of the Dehydrogenase Part of Rat Peroxisomal MFE-1. *Journal of Molecular Biology*, 355: 734–746.

Tein, I. (2003). Carnitine transport: pathophysiology and metabolism of known molecular defects. *Journal of Inherited Metabolic D.isease*, 26: 147-169.

Tein, I., DiMauro, S., Xie, Z. W., and De Vivo, D. C. (1996). Valproic acid impairs carnitine uptake in cultured human skin fibroblasts. An in vitro model for the pathogenesis of valproic acid-associated camitine deficiency. *Pediatric Research*, 34: 281–287.

Tomita, M., and Sendju, Y. (1927). Über die Oxyaminverbindungen welche die Biuret Reaktionen zeigen. III. Spaltung der γ-amino-ß-oxybuttersäure in die optisch-aktiven Komponente. *Physiological Chemistry*, 169: 263–277.

Uanschou, C., Frieht, R., and Pittner, F. (2005). What to Learn from a Comparative Genomic Sequence Analysis of L-Carnitine Dehydrogenase. *Monatshefte für Chemie*, 136: 1365–1381.

Van der Leij, F. R., Kram, A. M., Bartelds, B., Roelofsen, H., Smid, G. B., Takens, J., Zammit, V. A., and Kuipers, J. R. (1999). Cytological evidence that the Cterminus of carnitine palmitoyltransferaseI is on the cytosolic face of the mitochondrial outer membrane. *Biochemical Journal*, 341: 777–784.

Vaz, F. M. Ofman, R., Westinga, K. Back, J. W., and Wanders, R.J. (2001). Molecular and biochemical characterization of rat ε-N-trimethyllysine hydroxylase, the first enzyme of carnitine biosynthesis. *Journal of Biological Chemistry*, 276: 33512–33517.

Vazi, F. M., and Wanders, R. J. A. (2002). Carnitine biosynthesis in mammals. *Biochemical Journal*, 361: 417–429.

Verhoeven, N. M., Roe, D. S., Kok, R. M., Wanders, R. J. A., Jakobs, C., and Roe, C. (1998). Phytanic acid and pristanic acid are oxidized by sequential peroxisomal

and mitochondrial reactions in cultured fibroblasts. *Journal of Lipid Research*, 39: 66–74.

Vernez, L., Hopfgartner, G., Wenk, M., and Krahenbuhl, S. (2003). Determination of carnitine and acylcarnitines in urine by high-performance liquid chromatography – electrospray ionization ion trap tandem mass spectrometry. *Journal Chromatography A*, 984: 203–213.

Veselá, E., Racek, J., Trefil, L., Jankovy'ch, V., and Pojer, M. (2001). Effect of L-carnitine supplementation in hemodialysis patients. *Nephron*, 88: 218–223.

Wargo, M. J., and Hogan, D. A. (2009). Identification of genes required for *Pseudomonas aeruginosa* carnitine catabolism. *Microbiology, 155*, 2411–2419.

Watkins, P. A. (1997). Fatty acid activation. *Progress in Lipid Research*, 36: 55-83.

Williams, M. H. (1994). The use of nutritional ergogenic aids in sports: is it an ethical issue? *International Journal of Sport Nutrition*, 4: 120–131.

Youn, S. C. (2008). Effects of L-carnitine on obesity, diabetes, and as an ergogenic aid. *Asia Pacific Journal of Clinical Nutrition*, 17: 306–308.

Zhou, X., and Liu, F., and Zhai, S. (2007). Effect of L-carnitine and/or L-acetyl-carnitine in nutrition treatment for male infertility: a systematic review. *Asia Pacific Journal of Clinical Nutrition*, 16: 383–390.

ABSTRACT

Naturally occurring quaternary ammonium compound L-carnitine (L-Car), as an essential biological nutrient, has been well investigated. Thereafter, several approaches have been established for measurement the concentration of L-Car in the clinical diagnosis and nutrient analysis. Of them, a spectrophotometric assay method using L-carnitine dehydrogenase (CDH) has been proposed as a superior tool (easy, rapid and low-cost) for L-Car measurement. While several CDHs have been purified and characterized from different soil isolate bacteria, no study has been conducted in the structure function relationship for any of CDHs. Therefore, the current study was conducted to investigate the role of several amino acid residues in the catalytic activity and substrate affinity that could provide new and useful information insight into the catalytic mechanism for improvement the properties of two recombinant CDHs isolated from *Xanthomonas translucens* (Xt-CDH) and *Rhizobium* sp. (Rs-CDH).

Chapter 1 outlines the rationale and aims of the current dissertation, summarizes relative studies of L-Car properties, in vivo biosynthesis, biological functions, deficiency and assessment and also provides a brief note on CDH research progress.

In Chapter 2, the study was conducted to identify residues important for affinity to the substrate of CDHs. Based on the substrate affinity variation of Xt-CDH (10 mM) and Rs-CDH (1.1 mM), we compared the primary structure of Xt-CDH and Rs-CDH with the recognized 3D structure of human 3-hydroxyacyl-CoA dehydrogenase (h-HAD) (PDB code: 1F0Y). In the h-HAD structure, several residues surround the acetoacetyl moiety of the substrate namely the residues Lue157, Phe160, Gly204, Ile206, Val207, Gly239, and Ala240. These residues matched Gly140, Phe143, Gly188,

Ile190, Ala191, Gly223, and Ala224 of Xt-CDH, which correspond to Ala137, Tyr140, Ala185, Val187, Gly188, Ser220, and Phe221 in Rs-CDH. The residues of Xt-CDH were replaced with that of Rs-CDH at the corresponding position and vice versa. The resulting mutant enzymes were purified and subjected to kinetic characterization. All Rs-CDH mutants exhibited slight effects on substrate affinity, except for the double mutants Rs-V187I/G188A, which was devoid of enzyme activity. For Xt-CDH mutants, Xt-F143Y, Xt-I190V/A191G, and Xt-G223S/A224F significantly elevated the K_m value, implicating the residues in L-Car binding. Of them, mutation of Phe143 with Tyr caused a higher increase in the K_m value. Therefore, mutant Xt-F143Y and its corresponding in Rs-CDH (Rs-Y140F) were further characterized. The preferred pH of Xt-F143Y was shifted from 9.5 to 8.0 compared to that of corresponding mutant (Rs-Y140F). Moreover, the kinetic parameters of additional mutants at Xt-F143 and Rs-Y140 (replaced with residues Ala, Gly, Lys, Cys, Ser, Asn, His, Asp, Trp, and Phe) were scrutinized. All Rs-Y140 mutants, except aromatic residues (Rs-Y140F and Rs-Y140W), produced proteins that were almost entirely devoid of enzyme activity and with disrupted affinity to L-Car. Additionally, all Xt-F143 variants, event that of Xt-F143Y and Xt-F143W, exhibit consistent reduction in enzyme activity and substrate affinity. Analysis of these mutants provides a better understanding of the structural and functional relationships between CDHs and its ligand L-Car. The effects of residues Xt-F143 and Rs-Y140 on catalytic activity and substrate affinity were unforeseen. As the aromatic property of these residues does not the sole factor, results emphasize the important role for physical properties, such as volume, of residues might play essential role in substrate recognition.

The study in Chapter 3 was carried out to explore functionally important residues in Xt-CDH. A total of 42 residues were selected for site-directed mutagenesis based on

their strict homology among the CDHs and bacterial 3-hydroxyacyl-CoA dehydrogenase. All residues were substituted with alanine (alanine scanning mutagenesis). The resultant mutants were analyzed for catalytic activity. Five of the mutant enzymes were inactive (E93A, H141A, E153A, D217A, and R227A). Active mutants were evaluated for their influence on L-Car affinity using assay mixtures of different L-Car concentration (12, 300, and 900 mM). Based on the obtained results, mutants could be categorized into three groups; mutants influenced k_{cat} only (R136A, D192A, R221A, and Q284A), mutants altered k_{cat} and K_m for L-Car (S117A, S120A, N144A, Y147A, E185A, F189A, R193A, E196A, W199A, R200A, E201A, W228A, M231A, F234A, Y237, M246A, F249A, Q252A, F253A, W261A, T262A, R297, and D298A), and mutants had similar approach to that of Xt-CDH (T119A, H133A, M177A, K184A, T236A, R247A, H248A, S289A, E294A, and R295A). The mutant enzymes affected the K_m values were subjected for steady kinetics analysis. The analytical data implied that all mutants had increased K_m value. Of those, R193A, E196A, W199A, R200A, F249A, and F253A that produced the greatest L-Car affinity disruption (K_m >200-folds of Xt-CDH) clustered near the putative active site. Overall, the reported data of this section underscores the important conserved residues for substrate affinity of the entire catalytic domain, which could be considered as blueprint for the rational of further intensive mutagenesis studies to improve the catalytic function and substrate affinity of CDH.

摘要

第 4 級アンモニウム化合物の一つである L-カルニチン（L-Car）は、脂肪代謝において脂肪酸をミトコンドリアに運ぶ担体の役割を果たし、脂肪酸の β 酸化に必須とされる化合物である。先天性有機酸代謝異常の患者では、蓄積した脂肪酸が L-Car と結合して排出されると共に、L-Car 不足が心臓血管疾患や高コレステロール血症といった様々な欠乏症を引き起こす原因となるため、L-Car 含量の測定は、診断や食品分析に利用される。L-Car 脱水素酵素（CDH）は特異的に L-Car を酸化する酵素であり、これを利用した比色的な L-Car 含量の測定の実現は、医療や食品分野における飛躍的な L-Car 分析の簡便化に繋がる。これまでにいくつかの微生物から CDH が単離され、その性質が明らかとされているが、その機能と構造の関係に関する知見は未だ乏しい。そこで本研究では、*Xanthomonas translucens* 及び *Rhizobium* sp.由来の CDH（Xt-CDH 及び Rs-CDH）の実用化と高機能化を目指し、L-Car への親和性や触媒活性に関わるアミノ酸残基を対象とした構造－機能相関についての詳細な知見を得ることを目的とした。

第一章では、本研究の研究意義と目的、そして、L-Car の生合成と生理機能、欠乏による生体への影響と血中 L-Car 値評価を踏まえた近年の研究動向について述べる。

第二章では、CDH の基質認識における重要な残基の同定を行った。これまで明らかとなっている酵素、Xt-CDH と Rs-CDH の L-Car に対する K_m 値は、それぞれ 10 mM 及び 1 mM であり、その性質の違いがどの構造に起因しているのかが不明であった。そこで、1 次構造上類似性を示すヒトの 3-hydroxyacyl-CoA dehydrogenase（h-HAD）の立体構造（PDB code: 1F0Y）を参考に、基質アセトアチル領域を取り巻く残基の中で、両酵素で異なる残基（Xt-CDH：Gly140、Phe143、Gly188、Ile190、Ala191、Gly223、Ala224；Rs-CDH：Ala137、Tyr140、Ala185、Val187、Gly188、Ser220、Phe221）をピックアップした。続いて、それぞれの対応する残基を入れ替えた交互変異の酵素を作成し、精製し

た後に酵素反応速度論的解析を行った（下線部の残基は、下線部分を 1 セットにした 2 重変異酵素を作成）。Rs-CDH では、全て変異で基質親和性にわずかな変化しか見られず、2 重変異酵素である Rs-V187I/G188A では、完全に活性が失われた。一方で Xt-CDH の変異酵素では、Xt-F143Y、Xt-I190V/A191G そして Xt-G223S/A224F において、顕著な K_m 値の上昇が確認された。これら中で、Xt-F143Y が最も K_m 値が上昇していたため、Xt-F143Y 及び Rs-CDH の相当する変異酵素 Rs-Y140F を、研究対象として取り上げた。Xt-F143 及び Rs-Y140 を上記とは別の残基（Ala、Gly、Lys、Cys、Ser、Asn、His、Asp、Trp、Phe）に置換し、それぞれの精製酵素を調整した。Rs-Y140 の変異酵素では、芳香族アミノ酸以外のアミノ酸に置換した全ての変異酵素において、完全に活性が失われ、同様に Xt-F143 の変異酵素は全て一律に、基質親和性と活性に低下が見られた。本研究結果は、CDH の特定の構造が L-Car 結合に大きく関わることを証明したものであり、構造と機能の関連性に迫る新たな知見を導き出した。Xt-F143 及び Rs-Y140 が基質認識や活性強度に関わる重要な残基である一方、唯一のファクターではないことに加え、その機序は謎が多く、どのような基質認識メカニズムの解明が今後の課題である。

第三章では、全体的な構造に着目し、Xt-CDH の酵素触媒機能に重要な残基を探索した。部位特異的変異のターゲットとして、CDH や細菌由来の 3-hydroxyacyl-CoA dehydrogenase の間で強く保存される 42 残基を選択し、全ての残基を Ala に置換した。活性を調べた結果、5 つの変異酵素（E93A、H141A、E153A、D217A 及び R227A）以外は活性を保持していたため、続いて極端に異なる L-Car 濃度条件で活性測定を行い、各変異酵素の L-Car に対する親和性を分析した。その結果、変異による影響を基に、変異部位は次の 3 つのグループ化された；①k_{cat} のみ変化した変異（R136、D192、R221、Q284）、②k_{cat} 及び K_m 共に変化した変異（S117、S120、N144、Y147、E185、F189、R193、E196、W199、R200、E201、W228、M231A、F234、Y237、M246、F249、Q252、F253、W261、T262、R297、D298）、③性質に変化が見られなかった変異酵素（T119、H133、M177、K184、T236、R247、H248、S289、E294、R295）。これらの中で、K_m 値が低下した変異酵素は一つもなく、K_m 値が上昇した変異部

位の中でも、R193、E196、W199、R200、F249、F253 の 6 つの部位は、活性中心に近く、L-Car に対する親和性は野生型酵素と比べて 200 倍以上も低下した。本章のデータは、触媒部位全体の基質親和性に関わる重要な残基は酵素間で保存されていることが示されたものであり、CDH の触媒機能と基質親和性を向上に向けた研究において、合理的かつ集約的な変異の設計図となり得ると考えられる。

LIST OF PUBLICATIONS

(1) Mohamed M. Eltayeb, Isam A. Mohamed Ahmed, Jiro Arima, Nobuhiro Mori. Identification of residues essential for the activity and substrate affinity of L-carnitine dehydrogenase. *Molecular Biotechnology*, 55 (3), 268–276 (2013).

This paper covers **Chapter 2** in the thesis.

(2) Mohamed M. Eltayeb, Jiro Arima, Nobuhiro Mori. Alanine-scanning mutation approach for classification of the roles of conserved residues in the activity and substrate affinity of L-carnitine dehydrogenase. *Biotechnology Letters*, 36(2), 309–17 (2014).

This paper covers **Chapter 3** in the thesis.